Root Quantity, Activity and Below-Ground Competition in *Grevillea robusta* Agroforestry Systems

Research Project R6363

Final Technical Report to the Forestry Research Programme,
Department for International Development

Reporting Period: 1 July 1995 to 31 March 1998

D.M. Smith*, N.A. Jackson*, J.M. Roberts* & C.K. Ong†

This publication is an output from a research project funded by the Department for International Development of the United Kingdom. However, the Department for International Development can accept no responsibility for any information provided or views expressed. Project R6363, Forestry Research Programme.

* Institute of Hydrology
Crowmarsh Gifford
Wallingford, Oxfordshire
OX10 8BB
UNITED KINGDOM

Tel: 01491 838800
Fax: 01491 692424
E-mail: M.Smith@ioh.ac.uk

† ICRAF
P.O. Box 30677
Nairobi
KENYA

IH/DFID Report No. 98/7

TABLE OF CONTENTS

EXECUTIVE SUMMARY iii

1. BACKGROUND
1..1 The Researchable Constraint 1
1.2 Relevant Previous Research 1
1.2.1 *Competition and complementarity in agroforestry* 1
1.2.2 *Distribution of tree and crop roots in agroforestry* 2
1.2.3 *Use of* Grevillea robusta *in agroforestry* 3
1.2.4 *Investigation of below-ground interactions in agroforestry* 3
1.3 Identification of Demand for the Project 4

2. PROJECT PURPOSE
2.1 The Purpose of the Project 6

3. RESEARCH ACTIVITIES
3.1 Location and Climate 7
3.2 Experimental Design and Site Management 7
3.3 Determination of Root Length Distributions 7
3.3.1 *Collection of root samples* 7
3.3.2 *Measurement of root length* 11
3.3.3 *Analysis of root length data* 11
3.4 Observation of Root Growth Using Minirhizotrons 12
3.4.1 *Minirhizotron design* 12
3.4.2 *Placement of minirhizotrons and capture of images* 14
3.4.3 *Analysis of images* 14
3.5 Estimation of Tree Root Length Using Fractal Branching Models 14
3.5.1 *Sampling of roots* 14
3.5.2 *Assessment of branching characteristics* 16
3.5.3 *Recursive branching algorithm for estimation of root lengths* 16
3.6 Measurement of Sap Flow in Tree Roots 17
3.6.1 *Use of sap flow gauges on roots* 17
3.6.2 *Collection of sap flow data* 17
3.6.3 *Determination of soil and leaf water potentials* 19
3.7 Measurement of the Hydraulic Conductances of Roots 20
3.7.1 *Determination of the hydraulic conductivity of roots of* G. robusta 21
3.7.2 *Determination of the hydraulic conductivity of maize roots* 21
3.8 Model of Water Uptake by Tree and Crop Roots in Agroforestry 23
3.8.1 *2-dimensional soil water model* 23
3.8.2 *Uptake of water by trees* 24
3.8.3 *Uptake of water by a mixture of trees and crops* 27

4. OUTPUTS: RESEARCH RESULTS
4.1 Rainfall During the Project 28
4.2 Tree and Crop Root Lengths 29
4.2.1 *Root lengths per tree* 29
4.2.2 *Root length distributions* 33

4.2.3 *Root lengths and competition* 33
4.3 Observation of Root Growth Using Minirhizotrons 42
4.4 Branching Characteristics of Tree Roots and Estimates of Root Length 45
4.4.1 *Branching characteristics of roots of* Grevillea robusta 45
4.4.2 *Parameterisation of the recursive branching algorithm* 48
4.4.3 *Results from the recursive branching algorithm* 48
4.4.4 *Comparison of estimated and measured root length* 49
4.5 Sap Flow in Roots of *Grevillea robusta* 52
4.5.1 *Measurement of flow reversal* 52
4.5.2 *Sap flow in roots after a poor rainy season* 52
4.5.3 *Sap flow in roots at the onset of the rainy season* 55
4.5.4 *Uptake of water from soil with a uniform water potential* 57
4.5.5 *Sap flow in roots after irrigation of the soil surface* 58
4.5.6 *Effects of downward siphoning on the soil water balance* 58
4.5.7 *Implications of downward siphoning for agroforestry* 60
4.5.8 *Competition and complementarity for water between* G. robusta *and crops* 60
4.6 Hydraulic Conductivities of *Grevillea robusta* and maize roots 61
4.7 Performance of Model of Water Uptake in Agroforestry 63
4.7.1 *Parameterisation of the uptake model* 63
4.7.2 *Model output* 63
4.7.3 *Simulation of competition, complementarity and reverse flow phenomena* 72
4.7.4 *Testing of the model* 72
4.7.5 *Assumptions and simplifications in the model* 72
4.7.6 *Future development of the model* 73

5. CONTRIBUTION OF THE OUTPUTS TO DEVELOPMENT
5.1 Progress Towards Development Goals 74
5.2 Dissemination of Results and Plans for Dissemination 75
5.2.1 *Publications* 75
5.2.2 *Internal reports* 75
5.2.3 *Other dissemination of results* 76

6. REFERENCES 77

ACKNOWLEDGEMENTS 80

APPENDIX A: CODING FOR RECURSIVE BRANCHING ALGORITHM 81
APPENDIX B: INPUT DATA REQUIRED FOR USE OF WATER UPTAKE MODEL 83
APPENDIX C: CODING FOR MODEL OF WATER UPTAKE BY ROOTS IN AGROFORESTRY 87

EXECUTIVE SUMMARY

Below-ground physical and plant physiological processes controlling the partitioning of water between trees and crops in agroforestry systems are poorly understood. In the semi-arid tropics, where the availability of water is usually the most important environmental constraint on agricultural or forest productivity, competition for water between trees and crops has consequently constrained the development of sustainable systems of land use based on agroforestry. To enable agroforesters to optimise the use of trees on farms in the semi-arid tropics, a goal of DFID's Forestry Research Strategy, more information on below-ground interactions between the root systems of trees and crops was therefore required. To address this need, root distributions, uptake of water by roots and the processes controlling abstraction of water by trees and crops were studied in an East African agroforestry system combining *Grevillea robusta* and maize (*Zea mays*).

Field work for the project was located at Machakos, in a semi-arid region of Kenya, at a site with no water table and soil <2 m in depth. Studies of root quantity and activity at the site were carried out between October 1995 and July 1997.

Profiles of root length densities for *G. robusta* and maize were determined from root samples collected by soil coring. Maximum root length densities for the trees and maize coincided in the top layer of soil, with *G. robusta* dominating the population of roots at all times and all depths. When mixed with trees, growth of maize roots into deeper soil was suppressed. Thus, despite previous assertions that *G. robusta* had few roots at the surface, severe competition for water between *G. robusta* and maize should be expected unless there is a spatially distinct source of water available to the trees, but not the crop. The extent of complementarity for water between trees and crop is thus more likely to be dependent on the distribution of below-ground resources than the root distributions of trees.

The dynamics of water uptake by vertical and lateral roots of *G. robusta* were compared by measurement of sap flow. While uptake from all depths was found, use of water from the wettest soil layers always predominated. As the subsoil layers were not recharged during the project, the trees therefore competed strongly with the maize. Furthermore, our measurements showed, for the first time, that water can be transported by tree roots from wet soil at the surface to dry subsoil, a process termed 'downward siphoning'. This process, and the inverse process, 'hydraulic lift', may have far-reaching implications for the design and management of agroforestry in the semi-arid tropics. Knowledge of their role in tree-crop interactions will consequently be a crucial step in progress towards achieving optimal use of trees on farms.

Measurements of the hydraulic conductances of the root systems of *G. robusta* and maize were made in the field and used in the development of a physically-based model of the partitioning of water resources between trees and crops in agroforestry. This model can be used to predict quantitatively the spatial extent of competition and complementarity for water in agroforestry. The model thus promises to become a valuable tool for use by researchers in designing and evaluating strategies for optimising the use of trees in agriculture in regions where competition for water currently constrains the development of agroforestry.

1. BACKGROUND

1.1 The Researchable Constraint

As populations in the developing world expand, pressures on natural resources to provide for the needs of people are increasing. Land-use systems employed in these regions must consequently meet rising demands for food and fuel, but without causing degradation of resources and losses in productivity. Agroforestry systems exhibit many attributes that contribute to sustainability, while producing both food and wood, and so they are often promoted as a solution to land-use problems in tropical regions. However, successful use of agroforestry requires that utilisation of water, light and nutrients by trees and crops in the system is complementary; to as large an extent as possible, component species in agroforestry mixtures should utilise resources at separate times or from separate sources. Without such spatial or temporal complementarity, competition for resources is liable to limit the productivity of either the trees or crop, or both, and thus reduce acceptance of the system by local land users, so that environmental resources remain vulnerable to degradation.

Where plants compete, advantage is gained if one plant is able to acquire more of a resource in limited supply than a neighbour (Grime, 1979). Hence, plants that are more successful at capturing resources thrive while less successful plants experience stress as resources are depleted, causing impaired growth and productivity (Nambiar and Sands, 1993). A key to developing successful agroforestry technologies in which complementarity among species is maximised is therefore understanding the processes controlling the capture and partitioning of resources by trees and crops. Knowledge of these processes and the ability to predict the impact of competition in agroforestry systems will enable generic strategies for managing agroforestry to be developed. These strategies will be designed to enhance complementarity in resource use and thus improve the chances of successfully implementing agroforestry. Research into resource capture by trees and crops will consequently contribute to the development of sustainable systems of land use in tropical regions where environmental degradation would otherwise threaten the economic security of rural communities.

The most important environmental constraint on agroforestry in semi-arid regions is usually below-ground competition for water. However, few detailed studies have been made of the processes governing uptake of water by competing root systems in agroforestry. Evaluation of strategies for managing water in agroforestry and development of models of water uptake in mixtures has thus been limited by a lack of data concerning the quantity and activity of tree and crop roots. To address this need, root distributions and the processes controlling abstraction of water by tree and crop roots were studied in an East African agroforestry system combining *Grevillea robusta* and maize (*Zea mays*).

1.2 Relevant Previous Research

1.2.1 *Competition and complementarity in agroforestry*

One of the goals of combining trees and crops in agroforestry systems is to make better use of the environmental resources - light, CO_2, nutrients and water - required by plants for growth. This can be accomplished by either making use of resources that would otherwise be lost from the system or by increasing the efficiency of resource utilisation (Ong *et al*., 1996). Examples of the latter include changes in the photosynthetic efficiency

of crop plants in the sheltered microclimate of windbreaks (Brenner *et al*., 1995), while productive utilisation of a higher proportion of available resources can be achieved when, for example, deep networks of tree roots take up water or nutrients draining or leaching through the rooting zone of the crop (van Noordwijk *et al*., 1996). Where such enhancements to resource utilisation are realised in land-use systems, real gains in productivity can be achieved (Ong and Black, 1994). In addition, as trees and shrubs play a vital role in the mitigation of land degradation (Cooper *et al*., 1996), gains in productivity achieved by adoption of agroforestry are likely to be sustainable in the long term.

A danger of introducing trees into systems of crop production, however, is that the trees and crop may compete for resources. Competition between trees and crops results, for example, when exploitation of a resource by trees reduces its availability to levels that limit growth and productivity of the crop (Anderson and Sinclair, 1993). If the crop is more valuable to farmers than the products from the trees, such competition will result in failure of the agroforestry system, because it will not be adopted by farmers. Competition for light results from shading of crops by trees, but where nutrients or water are the resources most limiting production, below-ground competition is most important.

In semi-arid regions, water is often the most limiting resource and competition for water can impair the effectiveness of agroforestry systems. Govindarajan *et al*. (1996) and McIntyre *et al*. (1997) identified competition for water as the major reason for the poor performance of hedgerow intercropping systems in semi-arid zones of East Africa. Both found that where seasonal rains were not sufficient to cause recharge of soil below the rooting zone of the crop, uptake of water by the hedges reduced the availability of water to adjacent maize or cowpea (*Vigna unguiculata*) crops, causing losses in yield.

A key to successfully using agroforestry to increase the productive use of resources is to ensure that the trees and crop exploit different resource pools, particularly at times when the availability of a resource is potentially limiting (Ong *et al*., 1996). In systems where such niche differentiation occurs between trees and crops, capture of a limiting resource by trees does not reduce its availability to the crop; productive utilisation of resources can then increase without impaired crop performance because of competition. Where trees and crops exploit spatially or temporally distinct resource pools, they are complementary in their use of resources and are said to exhibit ‘complementarity’ in resource use (Ong *et al*., 1996; van Noordwijk *et al*., 1996).

Because of the adverse effects of competition for water in agroforestry in semi-arid areas (Onyewotu *et al*., 1994; McIntyre *et al*., 1997), complementarity for water is a critical feature of agroforestry systems suitable for adoption in these regions. Smith *et al*. (1997) were able to demonstrate complementarity for water between windbreak trees and adjacent millet (*Pennisetum glaucum*) in the Sahel, but only where the trees were able to exploit groundwater resources during dry spells. If such a spatially distinct source of water was not present at a location, complementary use of water could not occur and competition thus reduced crop growth near the trees.

1.2.2 *Distribution of tree and crop roots in agroforestry*

The extent of competition and complementarity for water in agroforestry systems is dependent, in part at least, on the relative distributions of the roots of the trees and crop.

Maximum root length densities for most crops occur near the soil surface and decline exponentially with depth (van Noordwijk *et al*., 1996). Ideally, trees used in agroforestry should have a different root distribution, preferably with substantial root length densities below the rooting zone of the crop. Thus, it is widely held that tree species used in agroforestry should be deep-rooted, as complementarity for below-ground resources should then be more probable and competition avoided. However, Jonsson *et al*. (1988) called for clarification of what is meant by "deep-rooted", as like Toky and Bisht (1992), they found that root distributions for crops and many trees commonly used in agroforestry were very similar. As a consequence, Jonsson *et al*. contended that there was little support for the suggestion that some trees have few roots in the topsoil, because trees described as deep-rooted were most likely to have the bulk of their roots near the surface, with only a small proportion of roots reaching much deeper levels in the soil.

Thus, it is not sufficient to characterise the likelihood of competition or complementarity simply on the basis of the distributions of tree and crop roots. The locations of below-ground resource pools exploited by trees and crops are likely to be important , as are the mechanisms controlling uptake of resources by roots. To make advances in our understanding of competition and complementarity for water in agroforestry, it was therefore necessary to investigate both root length distributions and the plant physiological processes controlling uptake of water.

1.2.3 *Use of* Grevillea robusta *in agroforestry*

G. robusta has been used, for at least the last century, as a shade tree in tea plantations in South Asia and East Africa (van Noordwijk *et al*., 1996). It was observed to have few superficial lateral roots and to therefore have a high potential for complementarity when used in agroforestry (Lott *et al*., 1996). It is now widely used in agroforestry in East Africa and is a common sight among the fields of the Kenyan highlands. It is grown primarily for the production of straight poles for use in construction.

Previous studies of the rooting characteristics of *G. robusta* have supported the view that it has a deeply-penetrating root system with few laterals (Howard *et al*., 1997). However, Huxley *et al*. (1994) found from root counts on trench faces that the root distribution of the species overlapped that of maize near the surface, but extended into the subsoil, past the deepest crop roots. Although unable to quantify the effects of competition, they concluded that competition between *G. robusta* and maize for below-ground resources could be substantial.

1.2.4 *Investigation of below-ground interactions in agroforestry*

The mechanisms controlling below-ground interactions between trees and crops have not been studied as intensively as above-ground processes. The primary reason for this has been the difficulty of working with root systems, especially in the field. In recent years, however, there have been important technical and methodological advances that have enabled new insights to be gained into the properties of root systems. We have applied some of these new methods to the study of roots and water uptake in agroforestry.

Measurement of root length distributions has always been labour-intensive and continues to be so, but newly developed systems for measuring the lengths of root samples using digital image analysis have enabled faster processing of samples and taken the subjectivity out of the task (Cunningham *et al*., 1989; Kaspar and Ewing, 1997). Minirhizotrons can

also be used in the field to observe root growth *in situ* (Brown and Upchurch, 1991; Gijsman *et al*., 1991). Additionally, van Noordwijk *et al*. (1994) and Spek and van Noordwijk (1994) developed a numerical method of estimating root lengths from the diameters of tree roots, on the basis of the fractal properties of root branching, that may be especially useful in quickly assessing the rooting patterns of trees used in agroforestry (van Noordwijk and Purnomosidhi, 1995).

The application of methods for measuring sap flow in plants (Smith and Allen, 1996) to root systems has enabled the activity of different portions of tree root systems to be assessed (Ong and Khan, 1993; Green and Clothier, 1995). Lott *et al*. (1996) used measurements of sap flow in roots to investigate the potential for complementary use of water by *G. robusta* in agroforestry. Investigation of the hydraulic properties of root systems, and the control they exert over uptake of water, has become possible on a routine basis in the field because of the development of the a new instrument, the high pressure flow meter, by Tyree *et al*. (1995).

Use of these new techniques in this project has enabled us to gather information on below-ground interactions in agroforestry that would have been unobtainable in even the recent past. This information should contribute to efforts by agroforesters to utilise knowledge of physiological and environmental processes to achieve real increases in the productivity of tropical agriculture. The ability to predict the extent of competition or complementarity for water between trees and crops in semi-arid environments has been a key challenge in meeting this goal. The approach to modelling the partitioning of water resources between trees and crops developed on the basis of the measurements carried out for this project thus represents an important step forward for the development of agroforestry.

1.3 Identification of Demand for the Project

The need for research in the area of resource utilisation and partitioning was identified and established as a priority in ICRAF's strategic programme at a planning workshop held in Nairobi in January 1992 attended by independent consultants with a wide range of expertise. The Institute of Hydrology and Nottingham University were identified as joint international collaborators in ICRAF's resource utilisation programme. The three institutes subsequently developed a co-ordinated programme to improve understanding of tree-crop interactions in established agroforestry periods over a five year period. This became the CIRUS (for Complementarity in Resource Use on Sloping land) programme, for which research activities in the field began in 1993. It was recognised later that information on below-ground interactions between trees and crops would be required to complement information on the soil water balance and above-ground interactions. To fulfil this need, this project became part of the CIRUS programme in 1995.

In the longer term, research undertaken for the CIRUS programme was intended to improve productivity and sustainability and increase the opportunities for resource-poor farmers, particularly those working marginal lands on hillslopes. The comprehensive database obtained describing resource capture, tree and crop growth and hydrology over an extended period was also to be made available to members of the DFID Agroforestry Modelling Group to support development of effective process-based agroforestry models, the testing of underlying assumptions and validation of model output. An important benefit of the close link with ICRAF is that results from the CIRUS experiments will be

incorporated into their strategic programme to develop sustainable agroforestry systems and disseminated through the Agroforestry Research Network for Africa (AFRENA) and the CGIAR system.

2. PROJECT PURPOSE

2.1 The Purpose of the Project

The constraint on development addressed by this study was our poor understanding of the below-ground physical and biological processes controlling the partitioning of water resources between trees and crops in agroforestry systems. To address this constraint, root growth and water uptake by tree and crop roots were investigated and a model of water uptake by tree and crop mixtures was developed.

The specific objectives of the project were:

1. To define the spatial distribution and seasonal dynamics of roots in a *G. robusta*-crop agroforestry system;

2. To describe the patterns and seasonal changes in water uptake of the components of this agroforestry system, and;

3. To develop a root model for integration into water balance and growth models for agroforestry.

In the context of the Forestry Research Strategy, the project addressed the purpose level objective of improving knowledge of tree/crop interactions in the below and above ground environment and incorporating this knowledge into management strategies. At the goal level, this project addressed the objective of optimising the use of trees within farming systems.

The project fell under the umbrella of the CIRUS experiment, which was a collaborative research programme hosted by ICRAF and involving scientists from ICRAF, the Institute of Hydrology and the University of Nottingham. The CIRUS programme included studies of other important processes controlling resource use in agroforestry, such as the impact of combining trees and crops on the soil water balance, modification of crop microclimate by the tree overstorey and crop growth and physiology. Projects R4853, R5810 and R6364 of the Forestry Research Programme funded these other aspects of the CIRUS experiment.

3. RESEARCH ACTIVITIES

3.1 Location and Climate

Field work for the project was conducted at ICRAF's Machakos Research Station (1°33′S, 37°8′E; 1560 m above mean sea level), in the uplands south-east of Nairobi, Kenya. The experimental plots were located on a south-facing, ~20 % slope with an alfisol (Khandic Rhodustalf), sandy clay loam in texture, overlying hard gneiss bedrock. The depth of the bedrock varied considerably, ranging from 0.2 m or less in places to 2 m (Wallace *et al*., 1995). A water table was not observed at the site and excavations revealed that the bedrock was free of deep cracks and that roots of the trees did not penetrate more than 2 to 3 mm into the weathered surface of the rock.

The climate of the surrounding region is semi-arid, with a bimodal distribution of rainfall. Mean annual rainfall is 782 mm, with 345 mm in the long rains, from March to June, and 265 mm in the short rains, from October to December.

3.2 Experimental Design and Site Management

The plots for the CIRUS experiment comprised a number of combinations of *G. robusta* and maize, as shown in Fig. 3.1. Work on roots was confined to the crop-only (designated C_g) treatment and the tree-only (T_d) and tree + crop (CT_d) treatments, which contained trees planted in a grid pattern with spacings of 3 x 4 m. Each plot measured 20 x 20 m and there were four replications of each treatment in randomised blocks. In addition to the trees and crop, each plot contained a strip of vetiver grass (*Vetiveria zizanoides*) planted along the contour across the centre of each plot as an erosion-control measure; these were clipped at 14 day intervals to minimise their competitive impact on nearby trees or crop plants.

The trees were planted at the site in October, 1991, using three-month old seedlings of local Embu provenance, and pruned annually by lopping branches from the lowest 1 m of the crowns. In September-October, 1996, prior to the 1996 short rains, the trees were severely pruned, leaving only the uppermost ~15 % of the volume of each tree crown.

If not dry-sown prior to the first rain of each growing season, maize (local Katumani composite) was planted in relevant plots once at least 20 mm of rain was received within a period of 7-10 d. Rows of maize ran along the contours of the slope and were spaced 1 m apart. Approximately 12 d after emergence, the maize was thinned to leave a spacing between plants in the same row of 0.3 m.

Additional measurements were made at times in an adjacent area of complementary plots containing *G. robusta* trees planted in the same arrangement. These plots were established in 1992 and pruned annually, although the severe pruning carried out in 1996 in the main plots was not done in the complementary plots.

3.3 Determination of Root Length Distributions

3.3.1 *Collection of root samples*

The vertical and horizontal distribution of tree and crop roots in the C_g, T_d and CT_d plots was assessed using the soil coring method (Böhm, 1979). Cores were collected twice in each growing season between the short rains of 1995 and the 1997 long rains, a period covering four growing seasons. The initial set of samples was collected after the first

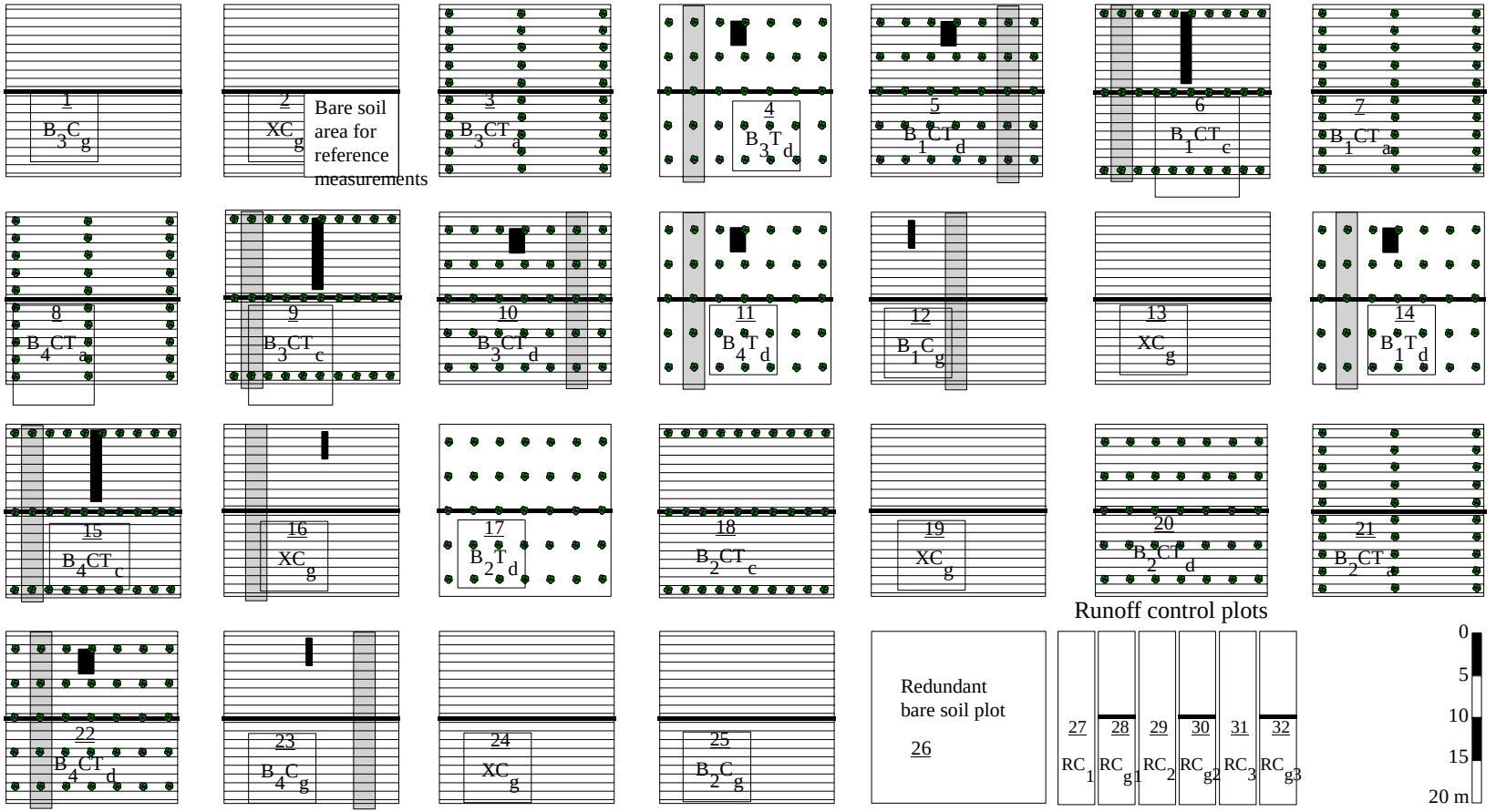

Figure 3.1: Layout of plots in the CIRUS experiment at Machakos, Kenya. Treatments combining maize and *Grevillea robusta* trees are designated: C_g, for crop only (without trees); T_d, for trees (without crop) dispersed in a 3 x 4 m arrangement; CT_d, for crop with dispersed trees; CT_c, for crop with trees planted along contours in a 9 x 2 m arrangement; and CT_a, for crop with trees planted across contours (9 x 2 m). Work on roots in CIRUS was confined to the C_g, T_d and CT_d treatments, using four replications of each. Shaded rectangles in the plots mark the locations of installations deployed in the companion project, R6364, to determine water balances.

Table 3.1: Growth stage of maize and timing of root sampling for each season of the project, with the number of root samples (*n*) collected in each season.

Year	Season*	Coring	Growth stage**	Dates of coring	Timing of coring (DAE†)	*n*
95	SR	A	5-7 leaves	13-17 Nov.	15-19	980
		B	tasselling/anthesis	13-18 Dec.	45-50	1464
96	LR	A	7-8 leaves	23-27 Apr.	20-24	841
		B	anthesis	29 May - 4 Jun.	56-62	864
	SR	A	7-9 leaves	9-13 Dec.	22-26	1334
		B	anthesis	13-15 Jan.	57-59	1159
97	LR	A	7-9 leaves	28 Apr. - 2 May	23-27	1188
		B	anthesis	27-30 May	52-55	2020

*SR='short rains'; LR='long rains'
**growth stage for maize in C_g plots
†Days after emergence

weeks of maize growth and the second after anthesis; details of the timing of coring in each season are provided in Table 3.1.

Soil cores were collected using a 4.8 cm i.d. corer that was driven into the ground with a hydraulically-powered hammer and extracted using a ball clamp and jack. Cores were always taken to the depth of the bedrock and, after extraction, they were separated into increments 0.2 m in length.

At each sampling, cores were collected in three replicates of each treatment. Coring in the fourth replication (plots 10, 11 and 12 in Fig. 3.1) was not possible because of permanent installations of instruments used in the study of the soil water balance (R6364). Three sets of cores were extracted from within each of the plots sampled. Each set of cores was taken along a transect between a maize plant or tree and the midpoint between rows (Fig. 3.2). The locations of each transect within the plots were selected randomly, although the area within 2 m of the vetiver grass strip was excluded. Over the four growing seasons, coring was never repeated at any location.

There were three cores per set in the C_g and T_d plots and six cores in the CT_d treatment; thus, at each sampling, a total of 54 cores (6 positions x 3 sets x 3 plots) were collected from the CT_d plots and 27 (3 positions x 3 sets x 3 plots) from the C_g and T_d treatments. Modifications to this sampling regime used only in the 1996 long rains reduced the number of cores collected to two per set in T_d plots.

Within a few hours of collection, roots in the samples were carefully washed out of the soil over a 0.5 mm sieve. Root samples were then placed in a small amount of 9 % (v/v)

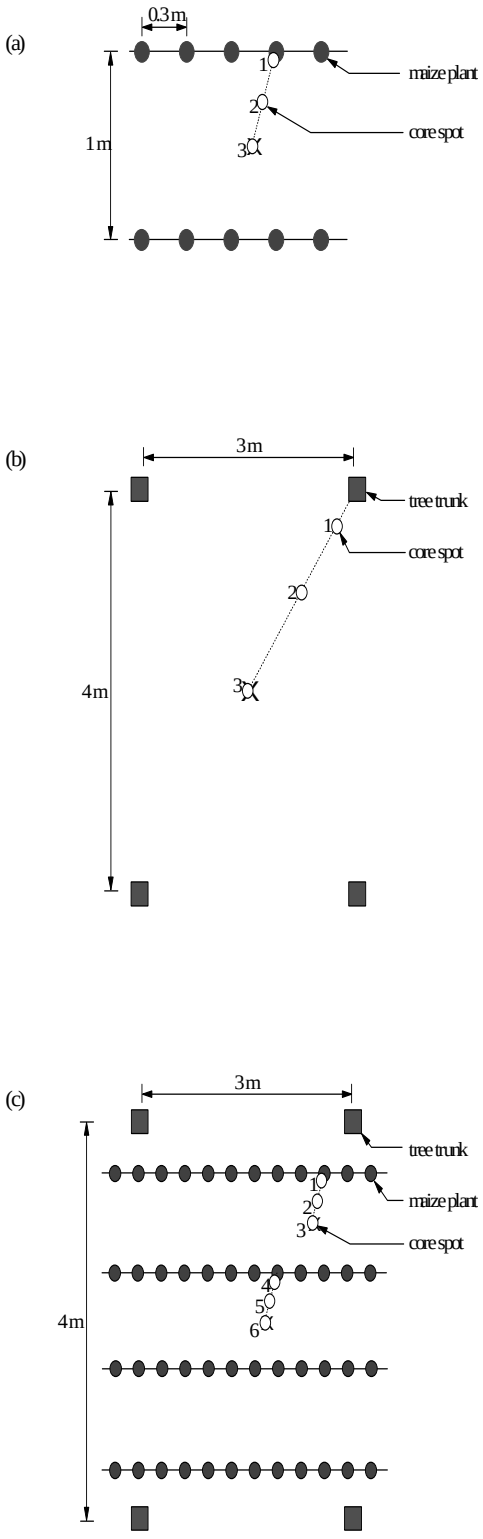

Figure 3.2: Configuration of locations of soil cores extracted from:(a) maize-only plots (C_g treatment); (b) dispersed trees only (T_d); and (c) dispersed trees with maize understorey (CT_d). Position numbers are marked on each core spot. Positions 1,2 and 3 were 2.5, 26 and, nominally, 52 cm from the closest maize plant in the C_g plots, and 50, 125 and 250 cm from the tree trunk in the T_d plots. The coring configuration in the C_g plots was repeated for two plants in the CT_d plots which lay, approximately, along the transect between the tree and the mid-point of the plot.

vinegar solution and stored in a refrigerator until manually sorted by a team of workers into maize and *G. robusta* components, which were readily distinguished by colour and morphology; other organic debris and dead roots were discarded. *G. robusta* is a member of the *Proteaceae* family with proteoid roots, which are characterised by segments of roots with tightly-packed clusters of rootlets. These were removed and kept separately from the main sample. Before sorting was completed, each sample was checked by a single supervisor to ensure that roots were classified as consistently as possible.

3.3.2 *Measurement of root length*

The length of roots in each sample was determined by digital image analysis. Prior to analysis, each sample was stained with 0.01 % (w/w) methyl violet. Samples were spread randomly over a transparent sheet and then scanned using a flat-bed scanner (ScanJet IIcx, Hewlett Packard Co., Palo Alto CA, USA.) and desktop computer. Samples of proteoid roots were prepared in the same way, but were scanned after shaving the rootlets off each root in water and then collecting them by filtration. The length of roots in each digital image obtained was determined using specialised image analysis software (DT-Scan, Delta-T Ltd., Cambridge).

Once measured, root lengths were divided by the volume of the original soil sample to give root length densities. Thus, root length densities were measured for maize and both proteoid rootlets and ordinary, non-proteoid roots of *G. robusta*. Dry weights of all root samples were subsequently measured, after drying the samples in an oven at 70 °C.

3.3.3 *Analysis of root length data*

To compare quantities of roots among treatments, root lengths per tree and per maize plant were calculated from the profiles of root length density. This was accomplished by integrating root length densities over the depth of each core and the area of soil for which each core was assumed to be representative (Fig. 3.3). Root lengths were normalised to 12 m^2 of land-surface area for each tree and to 0.3 m^2 for each maize plant.

Although it may appear a gross extrapolation to estimate root lengths for whole plants from measurements made on small soil cores, total root lengths determined in this way are equivalent to weighted mean root length densities multiplied by the volume of soil occupied by each tree or maize plant, where data are weighted by the volume of soil represented by each root sample. As interpretation of the results was more complex if data were expressed as mean root length densities, analyses were performed on root lengths per tree or per maize plant. The significance of differences among treatments were compared by analysis of variance, with soil depth used as a covariate.

To compare root distributions among treatments, the depth of 50 % cumulative root length (d_{50}) was determined for each soil core. Non-linear regression was used to fit the function (Gale and Grigal, 1987)

$$f_c = 1 - \beta^d \qquad (3.1)$$

to the profile of cumulative root fraction (f_c), from the soil surface downwards, for each soil core, where d is depth (in cm) and β is a regression coefficient. Values of d_{50} for each core were then calculated from

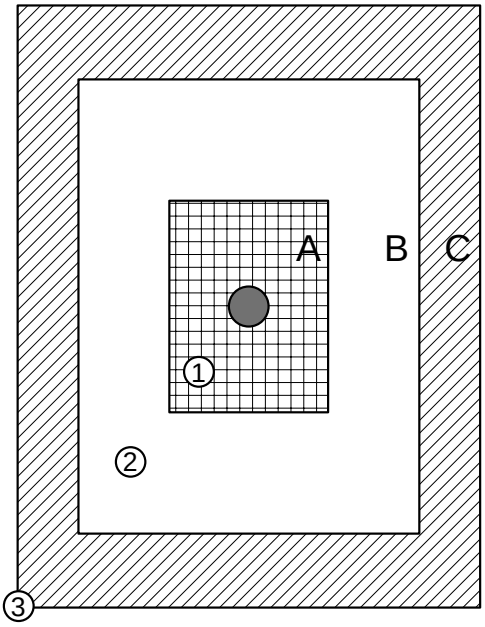

Figure 3.3: To estimate root length per tree or per plant, root lengths measured in the cores marked 1, 2 and 3 were integrated over the areas marked A, B and C, respectively, where the stem of the tree or maize plant was at the centre of area A. Root lengths per tree in CT_d plots were estimated by integration of root lengths from six cores over six areas, rather than three.

$$d_{50} = \frac{\ln(0.5)}{\ln(\beta)} \tag{3.2}$$

and differences among treatments were assessed by analysis of variance, using the depth of each core as a covariate.

3.4 Observation of Root Growth Using Minirhizotrons

Minirhizotrons are devices that allow *in situ* observation of plant roots. They were deployed in this project to enable changes in root lengths to be assessed over shorter time periods than was possible by soil coring. Changes in numbers of roots observed in minirhizotrons over intervals between corings were used to estimate dynamics in root growth.

3.4.1 *Minirhizotron design*

A new minirhizotron was developed for use in this project, based on the design by Gijsman *et al*. (1991). As illustrated in Fig. 3.4, it comprised a square aluminium frame that fits into an access hole in the ground, which was made using a square soil corer fitted to the hydraulic hammer. Once installed in the soil, the frame was lined with a sealed, rubber bladder that was inflated to fill the access hole; the presence of air-filled gaps at the interface between the soil and minirhizotron, in which roots can proliferate, was thus minimised using this approach. To observe root growth on the walls of the access hole,

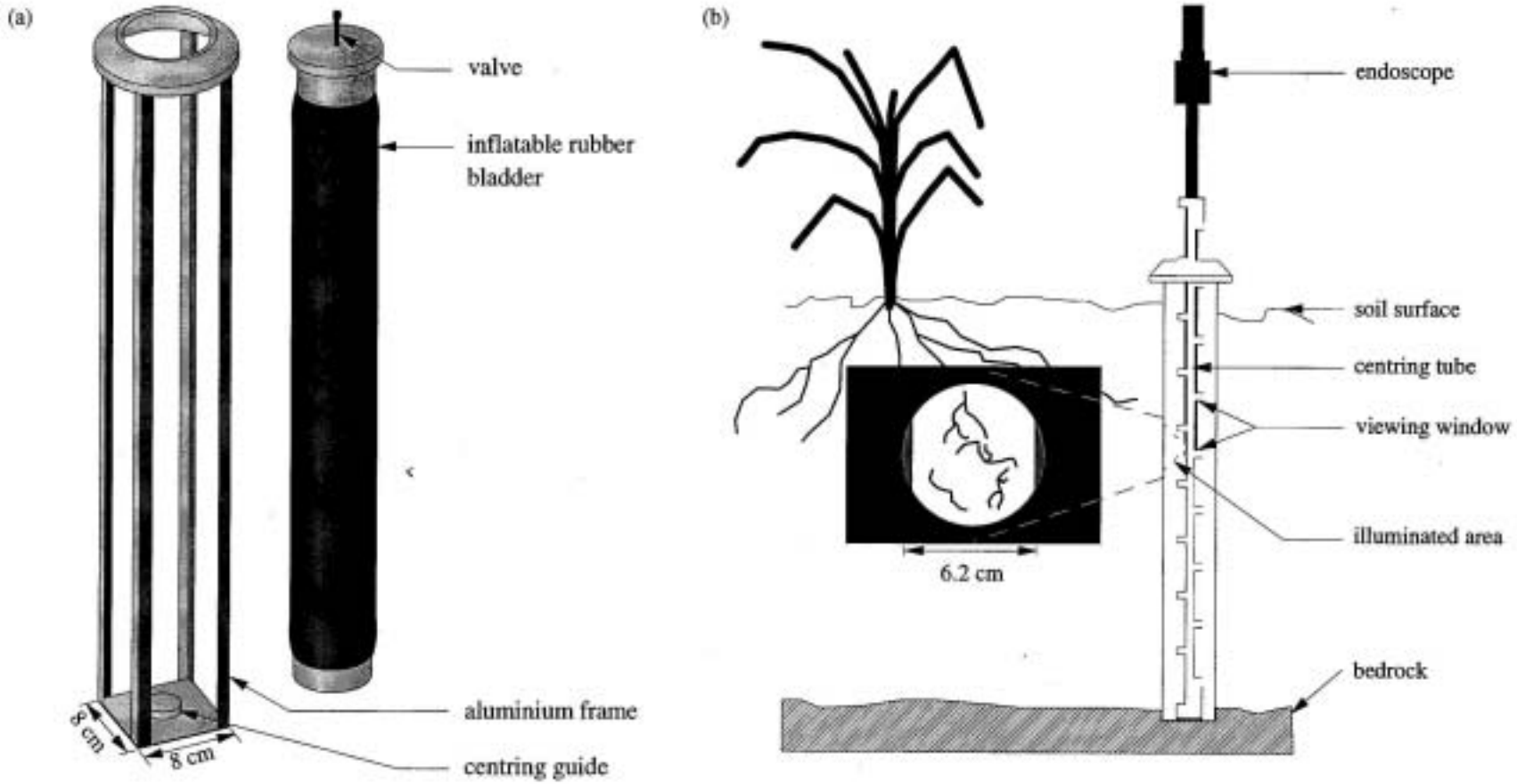

Figure 3.4: (a) Minirhizotron frame and rubber bladder, which was inflated to fill the air space within the frame when installed in the soil. The length of the frame was customised at each installation to extend from the soil surface to underlying bedrock, as depicted in (b), which shows use of an endoscope to view roots on a soil face of the minirhizotron, after removal of the rubber bladder. The endoscope was positioned using the centring tube and, in practice, a tripod on the soil surface. Photographs of roots (inset in (b)) were taken with a camera attached to the endoscope.

the bladder was deflated and removed. An endoscope and light source, positioned by a plastic guide tube, was then lowered into the access hole to allow viewing of the unobscured, bare walls of the minirhizotron (Fig. 3.4). A circle of the soil face with an area of approximately 30 cm^2 could be seen and photographed using an SLR camera attached to the endoscope.

3.4.2 *Placement of minirhizotrons and capture of images*
Fifteen minirhizotrons were installed at the CIRUS site in December, 1995; six were located in one T_d and one CT_d plot and three in a C_g plot, using the configuration shown in Fig. 3.5. Each access hole reached the level of the bedrock. The minirhizotrons were left undisturbed until April, 1996 when, after some testing of lighting and exposure, photographs were taken at depth intervals of 10 cm. Capture of images from the minirhizotrons was then repeated approximately weekly between: (i) April 20 and May 11, 1996; (ii) November 2, 1996 and January 2, 1997; and (iii) April 12 and May 31, 1997.

3.4.3 *Analysis of images*
To determine the timing of root growth and death between soil corings, roots in the images from the minirhizotrons were counted. A 1 x 1 cm grid on a transparent sheet was placed over the images, which were ~9 cm in diameter, and intersections between roots in the image and the grid were marked on the transparent sheet and counted. The sheet was then placed over photographs from subsequent weeks in series and intersections with new roots marked and counted. The death of roots was also recorded. Roots were counted as dead when they appeared shrunken and discoloured.

3.5 Estimation of Tree Root Length Using Fractal Branching Models
3.5.1 *Sampling of roots*
The utility of using the fractal characteristics of root branching to estimate tree root lengths, on the basis of the theoretical formulation devised by van Noordwijk *et al*. (1994), was tested by comparing output from a branching algorithm and results from soil coring. This test was conducted on four groups of four trees in the complementary plots at the CIRUS site; the four trees in each group were at the corners of a 4 x 3 m unit, or cell, of the planting grid.

Soil was removed near the base of each tree and the diameter of each root growing from the base of the trunk was recorded. Nine soil cores were then taken from the grid cell bounded by each set of trees; one each at distances of 0.5 and 1.25 m along transects between the trees and the midpoint of each cell, where the ninth core was taken. Root length densities were determined using the methods described in Section 3.3 for soil samples obtained from the cores.

After coring was completed, up to 3 roots of each tree were selected and recovered from the soil by excavation between the trunk and root tips. Care was taken to trace and recover as much of each root as possible, but a large proportion of the fine roots were inevitably left in the soil. The diameters at the trunk of the roots excavated ranged from 10 to 33 mm. A total of 32 roots were recovered in this way from the 16 trees.

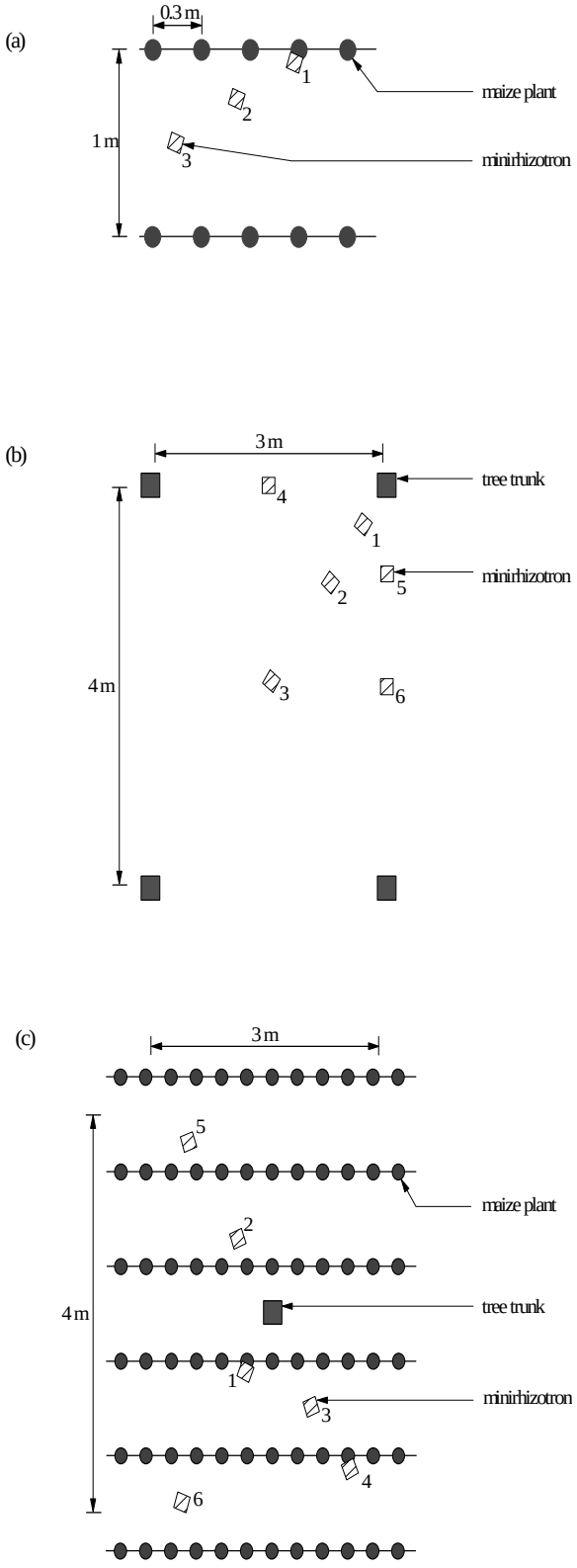

Figure 3.5: Configuration of locations of minirhizotrons in: (a) the maize-only plot (C_g treatment); (b) the plot with dispersed trees only (T_d); and (c) the plot with dispersed trees and maize understorey (CT_d). Locations of coring spots (Fig. 2) match these configurations, with the addition of three locations in the T_d plot, except that only a single minirhizotron is assigned to any maize plant, to avoid the minirhizotrons blocking one another.

3.5.2 *Assessment of branching characteristics*
To assess the branching characteristics for the trees, branching points of the excavated roots were examined. The number of branches at each branching point were counted, the lengths of links between branches were measured and the diameter of all branches before and after each branching point were measured using callipers with a resolution of 0.1 mm. The minimum number of measurements made on each root covered all branches in a series between the point where the root was severed near the trunk and the tip of a terminal root link; branching characteristics were thus assessed for roots of all sizes, from large structural roots to fine roots.

Branching characteristics were defined using four parameters. These were:

(i) The number of branches at each branching point (n_b).
(ii) The ratio α, which was calculated as (van Noordwijk and Purnomosidhi, 1995)

$$\alpha = \frac{D_b^{\,2}}{\sum_{i=1}^{n_b} D_{ai}^{\,2}} \quad , \tag{3.3}$$

where D_b is the root diameter before branching and D_{ai} is the diameter of each branch after the branching point. The value of α is determined by the change in cross-sectional area at each branching point and it thus describes how rapidly root size declines at each branching point.
(iii) The ratio q, which was calculated using (van Noordwijk and Purnomosidhi, 1995)

$$q = \frac{\left(D_a^*\right)^2}{\sum_{i=1}^{n_b} D_{ai}^{\,2}} \quad , \tag{3.4}$$

where D_a^* is the diameter of the largest branch at each branching point. The value of q depends on whether branching tends to result in roots of approximately the same size ('dichotomous' branching) or in a dominant root and one or more much smaller branches ('herring bone' branching).
(iv) The length of links between branching points (L_l)

To estimate tree root lengths from root diameters using fractal branching models, the branching characteristics of roots must not vary with root size; thus, n_b, α, q and L_l must be independent of scale (van Noordwijk *et al*., 1994). This assumption was tested for *G. robusta* by plotting each variable against root diameter.

3.5.3 *Recursive branching algorithm for estimation of root lengths*
The BASIC listing for a recursive branching algorithm for estimating the number of links comprising a tree root is given in Appendix A. The coding shown was derived from an algorithm supplied by Dr. Meine van Noordwijk of ICRAF.

The branching algorithm was used to estimate the number of links in the root systems of the 16 test trees. Input data for these estimations were the diameter of each root at the

base of each tree, the minimum root diameter, representative values of α and q and their approximate ranges of variation.

To enable comparison of output from the branching algorithm to the root lengths determined by soil coring, it was assumed that one quarter of all links were present within the grid cell at the centre of each set of four trees. Root lengths from soil coring for the 12 m^2 of each grid cell were estimated by extrapolating from the measured root length densities (Section 3.3.3). These root lengths were then compared to the product of the number of links in each grid cell and the link length (L_l).

3.6 Measurement of Sap Flow in Tree Roots

For trees and crops to be complementary in their use of water, the trees must utilise water from below the rooting zone of the crop. This suggests that complementarity in water use in agroforestry can be assessed by comparing uptake of water by lateral tree roots growing near the soil surface and deeply-penetrating vertical roots. The dynamics of water uptake by roots of *G. robusta* were investigated, therefore, by comparing rates of sap flow in lateral and vertical roots.

3.6.1 *Use of sap flow gauges on roots*

Constant-power sap flow gauges were used to measure sap flow in roots near the bases of *G. robusta* trees. This technique for measuring sap flow, which was reviewed and contrasted with other methods by Smith and Allen (1996), is based on the heat balance principle. A short, insulated section of stem or root is heated with an electric heater and the power supplied to the heater, output from a radial thermopile and the gradients in temperature across the heater, ΔT_a and ΔT_b (Fig. 3.6), are used to quantify components of the heat balance of the gauge. The residual of the heat balance is the heat absorbed by the moving sap stream (q_f), from which the mass rate of sap flow (F) is calculated using (Sakuratani, 1981; Baker & van Bavel, 1987)

$$F = \frac{q_f}{c_s \Delta T} \quad , \tag{3.5}$$

where $\Delta T = (\Delta T_a + \Delta T_b)/2$, the mean change in temperature across the heater, and c_s is the specific heat capacity of sap.

When sap flow in roots is measured, constant-power sap flow gauges have an important advantage over other techniques that could be used because their design is symmetrical. If sap flow reverses direction in roots, output from the gauge simply changes sign (Fig. 3.6).

3.6.2 *Collection of sap flow data*

Constant-power sap flow gauges (Dynagages, Dynamax Inc., Houston TX, USA) were installed on roots after excavating around trees up to approximately 0.4 m from the base of the trunk. Roots that were of a suitable size and sufficiently straight to accommodate a sap flow gauge were then selected and excavations extended as required. Soil was removed to a depth of 0.2 m around lateral roots and a depth of 0.4 m around vertical roots.

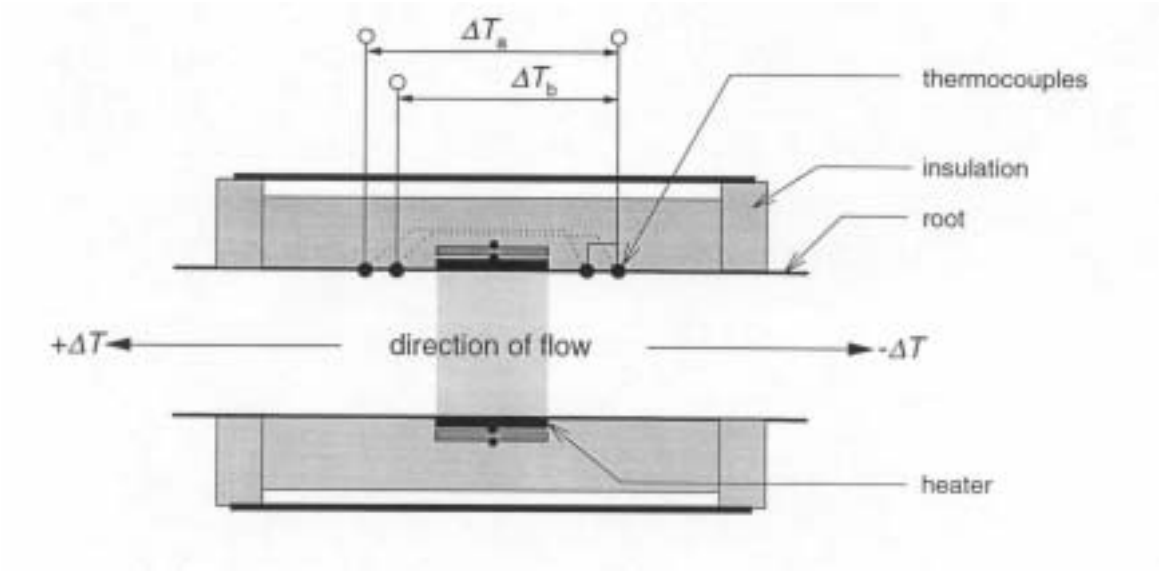

Figure 3.6: Cross-sectional view of a heat-balance sap flow gauge installed on a root, showing the symmetrical arrangement of the thermocouple junctions used to measure the gradients in temperature across the heater, ΔT_a and ΔT_b; when the direction of flow is reversed, the mean temperature gradient (ΔT) changes sign.

Installations were made during three periods; a description of the roots and sizes of gauge used in each case are listed in Table 3.2. Installation 1 was made between November 26 and December 17, 1996. Rainfall ceased for the season on November 29, when the seasonal total had reached only 157 mm. Installation 2 was made on roots of a second tree between March 21 and April 15, 1997, enabling changes in the dynamics of sap flow associated with the onset of rains to be recorded, as the dry season ended with 50 mm of rain on March 30. The final period, Installation 3, was between June 13 and July 1, 1997, when gauges were installed on roots of a third tree. This period occurred after the end of the long rains, but 45 mm of irrigation was applied to a 6 x 8 m area centred on the tree between June 23 and 25.

Shelters constructed from polythene prevented rain flooding the excavations and diverted stemflow away from the exposed roots. To minimise the influence of fluctuations in ambient conditions on the performance of the gauges, black netting was suspended over the shelter, shading the gauges from direct sunlight, and sections of roots left exposed after installation of the gauges were insulated with foam pipe lagging and covered with aluminium foil. With these precautions, problems identified by Lott *et al*. (1996) with the use of sap flow gauges on roots were not encountered.

Output from the gauges were recorded using an AM416 multiplexer and 21X data logger (Campbell Scientific Ltd., Shepshed, UK); measurements were made every 30 s and logged as 10 min averages. The temperature of the heated section of root was measured

Table 3.2: Roots for which sap flow was measured during three periods of observation. The nominal diameter of the gauge used and the diameter of the root at the midpoint of the gauge are given, with the cross-sectional area (A_x) of each root at the base of the trunk and the summed A_x of all vertical or lateral roots of each tree.

Installation	Root description	Gauge diameter* (mm)	Root diameter (mm)	A_x (cm^2)	Total A_x (cm^2)
1	near-surface lateral	25	30	12.9	57.0
	vertical	16	15	5.7	38.8
2	near-surface lateral	19	17	4.4	101.9
	vertical	25	28	13.6	63.0
3	near-surface lateral	16	18	5.5	162.0
	sub-surface lateral, descending at 15° from horizontal, 0.3 m below surface	25	29	7.9	9.4
	vertical	19	22	3.4	70.4

*nominal size of gauge

in all cases, by placing a thermocouple junction beneath the heater, and used to estimate a storage term in the heat balance of the gauge (Smith and Allen, 1996).

To deduce radial heat fluxes from sap flow gauges, and thus enable determination of q_f, a constant representing the thermal conductance of the gauge, often called the sheath conductance (K_{sh}), must be evaluated for each new installation. This is done using data collected during periods when there is no sap flow (Smith and Allen, 1996). To ensure that this condition was met, K_{sh} was determined after sap flow was stopped at the end of each period of measurement by severing the root below the distal end of the gauge.

3.6.3 *Determination of soil and leaf water potentials*

Profiles of soil water content were measured over each period of observation of sap flow in roots using a neutron probe (IH II, Didcot Instrument Co., Abingdon, UK). Measurements were made in 45-mm diameter aluminium access tubes which had been in place since 1993 for the study of the soil water balance (see FRP projects R4853 and R6364; Wallace *et al*., 1995). For Installation 1, these measurements were made in a plot with a similar soil depth and the same configuration of trees, approximately 80 m from the tree instrumented with sap flow gauges. For Installations 2 and 3, measurements were

made using access tubes 1.0 and 1.8 m upslope from the base of the instrumented trees. Readings were taken regularly at depth increments of 0.2 m, between 0.2 m and the underlying bedrock.

For Installations 1 and 2, soil water potentials were calculated from measured soil water contents using water retention curves for the five soil horizons identified at the site. The retention characteristics of each horizon were measured by Wallace *et al*. (1995). For Installation 3, soil water potentials between the depths of 0.1 m and the bedrock were measured every 0.1 m using an array of tensiometers located 1 m upslope from the trunk of the tree.

During Installations 1 and 3, a pressure chamber was used to measure the water potentials of leaves from the crowns of the instrumented trees. Measurements were made at regular intervals between the pre-dawn period and sunset on several days; mean leaf water potentials were determined from a minimum of three leaves at each time interval.

3.7 Measurement of the Hydraulic Conductances of Roots

During uptake by roots, water moves down gradients in water potential between the soil and xylem of the root, crossing the root endodermis during its radial passage across the root. Using an Ohm's Law analogy, uptake of water per unit of root length (U_l) can thus be described by

$$U_l = \frac{\left(\psi_s - \psi_r\right)}{\left(1/\kappa_s + 1/\kappa_r\right)} \tag{3.6}$$

where ψ_s and ψ_r are the water potentials of the soil and roots at the base of the stem, respectively, and κ_s and κ_r are the hydraulic conductivities of soil and roots, expressed per unit of root length. As defined here, κ_r incorporates a radial and an axial component (Huang and Nobel, 1994). κ_s is dependent on the hydraulic characteristics of the soil (Gardner, 1960; Rowse *et al*., 1983), which can be determined using standard methods, but determination of κ_r in the field was previously difficult.

Recent developments in instrumentation, however, have made direct measurement of the hydraulic conductances of roots in the field possible on a routine basis (Tyree *et al*., 1995). A device, called a high pressure flow meter (HPFM), is used to force water back through roots from a cut surface towards the root tips (Fig. 3.7(a)). Although the root must be severed, it is otherwise undisturbed. Rates of flow into the root are measured using a mass flow meter over a range of pressures and hydraulic conductances are then determined from the slope of the linear portion of the plot of flow against pressure (Fig. 3.7(b)). Division of these conductances by root length gives κ_r.

Knowledge of the hydraulic conductivities of tree and crop root systems is a key to understanding the mechanisms controlling the partitioning of water, and therefore the extent of competition, in agroforestry systems. Such information has not been available previously. A programme of measurement with the HPFM was consequently undertaken at the CIRUS trial to determine the hydraulic conductivities of roots of maize and *G. robusta*.

3.7.1 *Determination of the hydraulic conductivity of roots of* G. robusta

Between November 4 and December 17, 1996, an HPFM (Dynamax Inc., Houston TX, USA) was used to measure the hydraulic conductances of 65 roots from 23 *G. robusta* trees in the complementary plot of the CIRUS trial. Measurements were made after excavating around the base of the trunk of each tree on roots selected to cover a broad range of diameters; the diameters of the roots chosen ranged from 1.0 to 34.3 mm.

Each measurement was made after severing the root near the base of the trunk and clearing debris from the cut surface of the root with a razor blade. A suitably-sized compression fitting was then selected and used to seal the water line (Fig. 3.7(a)) from the HPFM to the root. A supply of compressed nitrogen gas to the captive air tank (Fig. 3.7(a)) was then used to increase the pressure of the water supply to the root from 0 to ~500 kPa (relative to atmospheric pressure) over a period of ~90 s. The mass flow rate of water into the root and pressure at the water outlet from the HPFM were logged on a laptop computer. The hydraulic conductance of the root was then determined by using linear regression to find the slope of the linear portion of the plot of flow against pressure (Fig. 3.7(b)).

For 32 of the 65 roots, the root was carefully excavated after the measurement was completed. As much of each root as possible was recovered from the soil, washed and cut into small pieces. The total length of root recovered was then measured by digital image analysis, as described in Section 3.3.

Root lengths determined after excavation inevitably underestimated true root lengths because much of each root remained in the soil. Consequently, the fractal branching model described in Section 3.5 was used to estimate corrected root lengths for the 32 excavated roots and the 33 roots that were not excavated. These estimates were made using the diameters of the roots at the point where they were severed and the values of α and q determined from the investigation described in Section 3.5. The branching model was calibrated against root lengths measured by soil coring (see Section 4.4).

3.7.2 *Determination of the hydraulic conductivity of maize roots*

The HPFM was used to measure the hydraulic conductances of maize roots between May 8 and 30, 1997. Measurements were made for whole root systems, as it was not possible to attach the water line from the HPFM to individual maize roots, because they were too fragile. This meant that measurements could only be made after stem elongation; measurements were made on 32 plants between the growth stages of 11 leaves and anthesis.

Hydraulic conductances of maize root systems were measured after cutting the stem above the soil surface, leaving a sufficient length of stem (~5 cm) to permit fitting of the coupling to the water line from the HPFM. At least two days prior to making each measurement, the blades and sheaths of the bottom four or five leaves of each stem were removed. This was sufficient time for the vascular tissue exposed at each leaf node to be plugged, thus preventing leakage of water when the stems were pressurised by the HPFM.

The lengths of the root systems of the 32 plants on which measurements were made were estimated by soil coring. Cores were taken at three positions adjacent to each plant, as

(a)

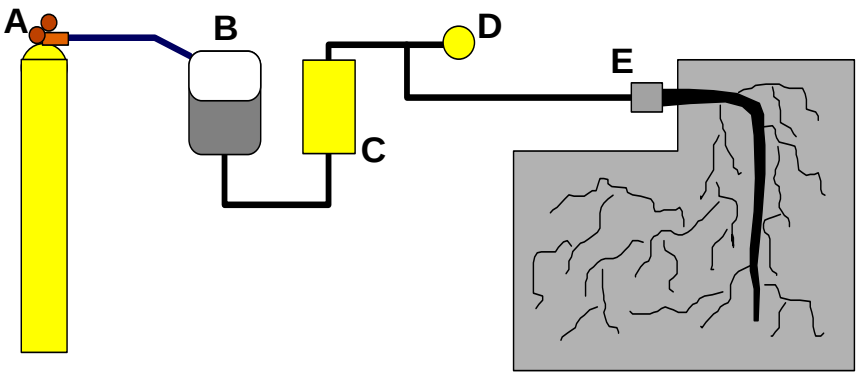

(b)

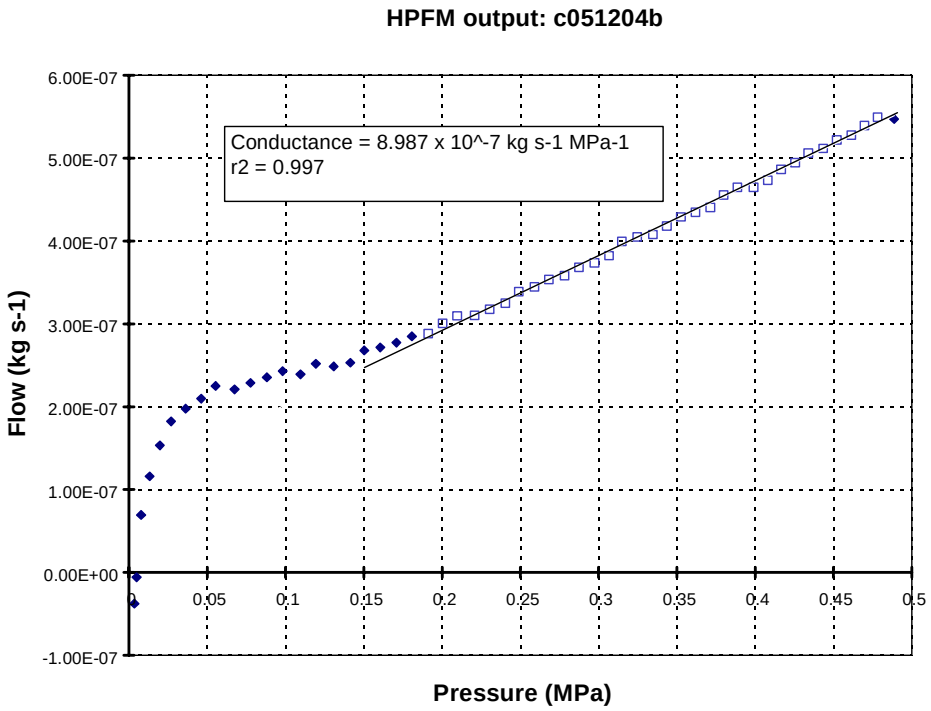

Figure 3.7: (a) The components of a high pressure flow meter (HPFM) used to measure the hydraulic conductances of roots using the method developed by Tyree *et al*. (1995). Compressed gas (A) is used to pressurise water in a captive air tank (B), from 0 to ~500 kPa in ~90 s, forcing water into a severed root (E). The flow rate of water into the root is measured with a mass flow meter (C) and the pressure at the outlet is measured with a pressure transducer (D). When flow is plotted against pressure, the slope of the linear portion of the curve is the hydraulic conductance of the root, as shown in (b)

described in Section 3.3. The length of roots recovered from each core was then measured and extrapolated to the 0.3 m^2 occupied by each plant.

3.8 Model of Water Uptake by Tree and Crop Roots in Agroforestry

A model of water uptake by the root systems of trees and crops in agroforestry mixtures was developed. The model is based on mechanistic principles and is intended for incorporation into models of tree and crop growth and the soil water balance in agroforestry systems. The model is based on implementation for two co-existing species of the Campbell model for water uptake by roots (Campbell, 1985, 1991) in a 2-dimensional soil water model. It is presently written in CSMP, a modelling language derived from FORTRAN that was designed for solving non-linear numerical problems.

3.8.1 *2-dimensional soil water model*

A 2-dimensional soil water model developed by Ragab *et al*. (1984) was chosen as the foundation for the model of water uptake in agroforestry. Their model is based on Darcy's Law and the continuity equation, where for 1-dimension, change in volumetric soil water content (θ) with time (t) is found from

$$\frac{\partial \theta}{\partial t} = \frac{\partial}{\partial z} K \left(\frac{\partial \psi_m}{\partial z} + 1 \right), \tag{3.7}$$

where z is depth, K is soil hydraulic conductivity and ψ_m is the matric potential of soil expressed in m of water. Ragab *et al*. utilised a form of this equation in which fluxes are expressed in terms of matric flux potentials, which combine K and ψ_m into a single variable, ϕ.

A block of soil - the 'flow domain' - is divided into a grid of compartments with the dimensions along the x, y and z axes of Δx, Δy and Δz. Flow occurs only in the x and z directions and there is no flow through any boundary of the flow domain. Evaporation from the soil surface and drainage are thus ignored in the present model; when implemented in a model of the soil water balance, however, these assumptions would be unnecessary. Rates of flow vertically between compartments (q_z) are calculated using

$$q_z = \left[\frac{\Delta \phi}{\Delta z} + \overline{K} \right] \Delta x \Delta y \tag{3.8}$$

and rates of flow horizontally (q_x) using

$$q_x = \left[\frac{\Delta \phi}{\Delta x} \right] \Delta z \Delta y \, . \tag{3.9}$$

The hydraulic conductivity $\overline{K}$ is the mean K for two adjacent compartments weighted by θ. Net flow (Δq) into or out of each compartment of the flow domain is calculated using

$$\Delta q_{i,j} = \left(q_{xL} - q_{xR} + q_{vA} - q_{vB} \right)_{i,j} \quad , \tag{3.10}$$

where subscripts i and j represent the vertical and horizontal co-ordinates of each soil compartment and subscripts L, R, A and B indicate flow into the compartment from the left, right, above and below, respectively. The change in soil water content ($\Delta\theta$) for each time step (Δt) is then

$$\Delta\theta_{i,j} = \frac{\Delta q_{i,j}\Delta t}{\Delta x \Delta y \Delta z} \quad . \tag{3.11}$$

Redistribution of water in the soil is determined by repeating these calculations systematically for each compartment of the flow domain.

3.8.2 *Uptake of water by trees*

The flow domain for the model of water uptake by roots is defined as a block of soil with a breadth of 2 m in the x direction and a z dimension determined by the depth of bedrock, but assumed here to be 1.6 m. The soil block is divided into eight compartments along the x axis and 16 compartments along the z axis. Each compartment has dimensions of Δx=0.25 m, Δz=0.10 m and Δy=3 m. The soil block thus forms one half of a 3 x 4 m grid cell from the CIRUS trial; it is therefore assumed to contain half of a tree root system, connected to half the trunk and crown of a tree located at one edge of the soil block. Uptake and redistribution of water is assumed to be uniform in the y direction.

Uptake of water from the soil is described by the electrical analogue in Fig. 3.8, which shows water potentials along the pathway of flow between the soil and crown of the tree connected by resistances for different segments of the pathway. These resistances are the reciprocals of conductances. Steady flow is assumed in the soil and plant and thus the flow path contains no capacitance. The transpiration rate (E) is determined primarily by atmospheric driving forces and the surface and aerodynamic conductances in the vapour phase; the water potentials in Fig. 3.8 therefore result mainly from an imposed value of E, although feedbacks between stomatal conductance and low leaf water potentials also influence E (Campbell, 1991).

To calculate water uptake from each compartment of the flow domain, the resistances in the flow pathway in Fig. 3.8 must be known, as must the soil water potential for each compartment and E_v, the transpiration rate dependent on processes in the vapour phase. E_v is the transpiration rate that would occur without limitations resulting from stomatal responses to leaf water potential; it is the rate of uptake from the flow domain which occurs when leaf water potentials have no effect on the surface conductance. For the purposes of development of the uptake model, E_v is currently assumed to follow a sine function between 0600 and 1800 daily, peaking at midday. The Penman-Monteith equation could be used to calculate E_v if the influence of leaf water potential on the surface conductance term was ignored.

The major resistances in the flow pathway are the soil resistance (R_s), the root resistance (R_r) and the resistances to liquid phase transport in the stem and leaf (R_l). R_s is defined as the resistance per unit length of root to the flow of water from the bulk soil to the surface of the root and R_r is the combined resistance per unit length to radial flow into roots and axial flow along roots.

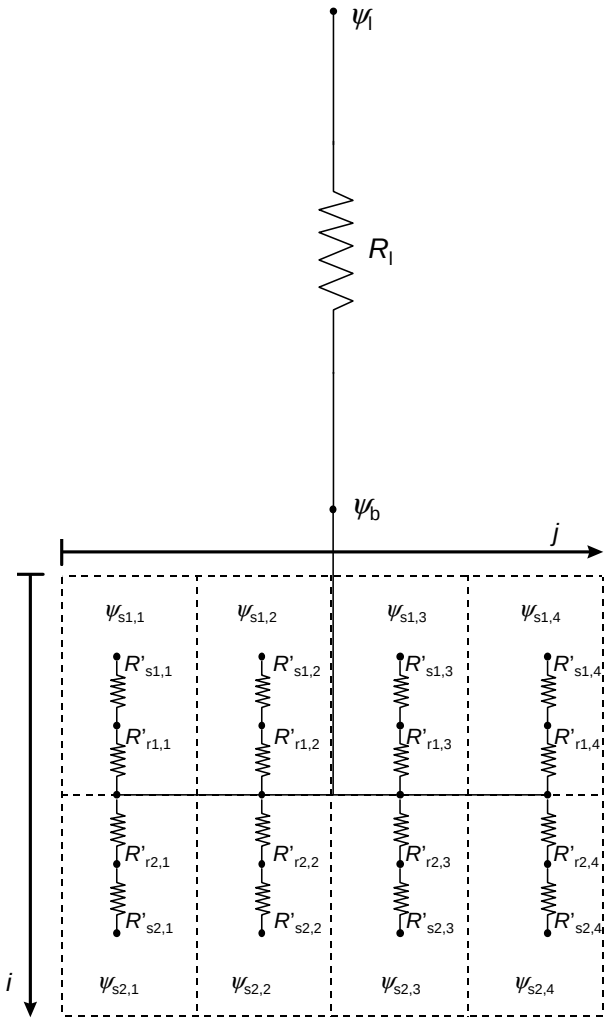

Figure 3.8: The electrical analogue used to model uptake of water by roots. Here, a flow domain containing a single plant is composed of eight compartments, each identified by the subscripts *i* and *j*, their vertical and horizontal co-ordinates. The rate of abstraction of water by roots in each compartment is calculated using Equations 3.12 to 3.18, from: the gradients between leaf water potential (ψ_l), the potential at the base of the stem (ψ_b) and the soil water potential in each compartment ($\psi_{si,j}$); and the resistances to flow in the soil ($R'_{si,j}$), the roots ($R'_{ri,j}$) and the leaves and stem (R_l). For the model of uptake in agroforestry, two resistance networks are present in the flow domain, one for the trees and one for the crop.

R_s for compartment *i,j* is calculated from the soil hydraulic conductivity, *K*, for the compartment using

$$R_{si,j} = \frac{-\ln\left(L_{vi,j}\pi r^2\right)}{4\pi K_{i,j}} \ , \tag{3.12}$$

which was derived by Rowse *et al*. (1983) from equations given by Gardner (1960). Here, L_v is root length density and *r* is the radius of the root. The bulk soil resistance for compartment *i,j* ($R'_{si,j}$) is

$$R'_{si,j} = \frac{R_{si,j}}{L_{vi,j}V} \tag{3.13}$$

where *V* is the volume of the compartment.

R_r is $1/\kappa_r$, where κ_r is the hydraulic conductivity of roots measured using the HPFM, as described in Section 3.7. The bulk root resistance for compartment *i,j* ($R'_{ri,j}$) is then

$$R'_{ri,j} = \frac{1}{\kappa_r L_{vi,j}V} \ . \tag{3.14}$$

To enable calculation of actual *E* (E_a) and leaf water potential (ψ_l), a weighted mean soil water potential ($\overline{\psi}_s$) for the entire flow domain is determined from

$$\overline{\psi}_s = \frac{\Sigma\left[\left(\psi_{mi,j} - z_{i,j}\right)\Big/\left(R'_{si,j} + R'_{ri,j}\right)\right]}{\Sigma\left[1\Big/\left(R'_{si,j} + R'_{ri,j}\right)\right]} \ . \tag{3.15}$$

Newton-Raphson iteration is then used to find values of E_a and ψ_l which satisfy both

$$\psi_l = \overline{\psi}_s - E_a\left(R_l + R'_{sr}\right) \ , \tag{3.16}$$

where $R'_{sr} = 1\Big/\Sigma\left[1\Big/\left(R'_{si,j} + R'_{ri,j}\right)\right]$, and

$$\frac{E_a}{E_v} = 1 + \left(\frac{\psi_l}{c_\psi}\right)^a \ , \tag{3.17}$$

which is an approximation of the change in E_a resulting from stomatal response to changes in ψ_l (Campbell, 1991); *a* and c_ψ are species-dependent fitting parameters.

Uptake from each compartment of the flow domain ($q_{ri,j}$) is then calculated using

$$q_{\mathrm{ri},j} = \frac{\left(\psi_{\mathrm{mi},j} - z_{i,j} - \psi_{\mathrm{b}}\right)}{R'_{\mathrm{si},j} + R'_{\mathrm{ri},j}} \tag{3.18}$$

where ψ_{b}, the water potential at the base of the stem, is

$$\psi_{\mathrm{b}} = \overline{\psi}_{\mathrm{s}} - \left(E_{\mathrm{a}} R'_{\mathrm{sr}}\right) \tag{3.19}$$

To account for the effect of uptake on the soil water balance, Equation 3.10 becomes

$$\Delta q_{i,j} = \left(q_{\mathrm{xL}} - q_{\mathrm{xR}} + q_{\mathrm{vA}} - q_{\mathrm{vB}}\right)_{i,j} - q_{\mathrm{ri},j} \tag{3.20}$$

and $\Delta\theta$ is calculated using Equation 3.11.

3.8.3 *Uptake of water by a mixture of trees and crops*

To compute the partitioning of water between trees and crops occupying the same soil volume, values of $q_{\mathrm{r}}^{\mathrm{t}}$ and $q_{\mathrm{r}}^{\mathrm{c}}$, the uptake from each soil compartment by tree and crop roots respectively, are calculated by executing Equations 3.12 through 3.18 twice; the calculations are made first for tree roots and then crop roots. Root resistances in each compartment for the two species depend on their respective distributions of roots, while soil resistance depends on the aggregated root length density for each compartment, as the volume of soil from which water is available to the roots of one species is reduced by the presence of roots of the other species. As a single crop plant occupies 0.3 m^2, there are 20 plants in the flow domain of the model and the value of R_{l} for the crop is calculated by treating the 20 stems as parallel resistors. Net flow of water into each soil compartment, from Equation 3.10, thus becomes

$$\Delta q_{i,j} = \left(q_{\mathrm{xL}} - q_{\mathrm{xR}} + q_{\mathrm{vA}} - q_{\mathrm{vB}}\right)_{i,j} - q_{\mathrm{ri},j}^{\mathrm{t}} - q_{\mathrm{ri},j}^{\mathrm{c}} \quad . \tag{3.21}$$

An explanation of the required input data for the model are given in Appendix B and a listing of the model code is given in Appendix C. The present version runs with a variable time step, with a maximum value of 1 h, that is varied to ensure that changes in θ between time steps remain below a prescribed limit. Subsequent versions of the model will be developed using a fixed time step.

4. OUTPUTS: RESEARCH RESULTS

4.1 Rainfall During the Project

Rainfall at the Machakos Research Station between the beginning and end of the field studies for the project is plotted in Fig. 4.1. Rainfall was close to the seasonal average in the 1995 short rains and the 1997 long rains, but well-below average in the two rainy seasons of 1996. However, in all seasons except the 1997 long rains, substantial dry spells began within 12 days or less of the emergence of the maize crop. Thus, the distribution of rainfall in the first three seasons of the project was poor, causing the young maize plants to be exposed to dry conditions. In contrast, during the 1997 long rains, conditions for crop growth were good, as there was frequent and abundant rainfall for approximately 30 days after the emergence of the maize.

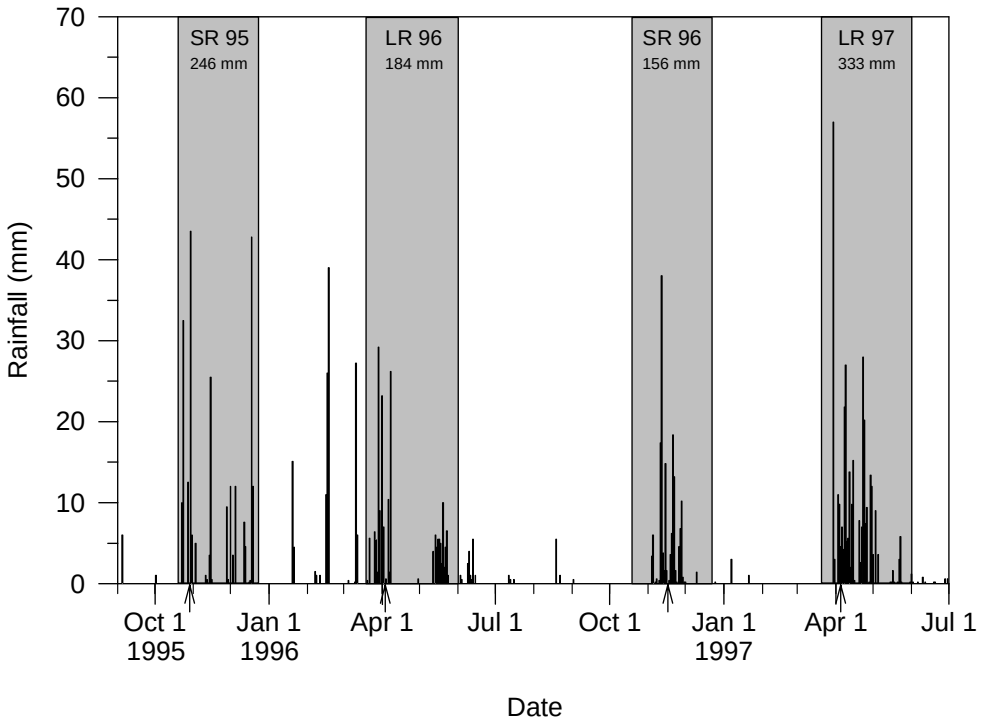

Figure 4.1: Rainfall at Machakos Research Station, Kenya, between September 1995 and July 1997. The shaded areas mark the average timing of the short rains (SR) and long rains (LR) (Wallace *et al*., 1995) and the arrows along the x-axis mark the date of maize emergence in each season. Total rainfall in each season is given at the top of each shaded bar.

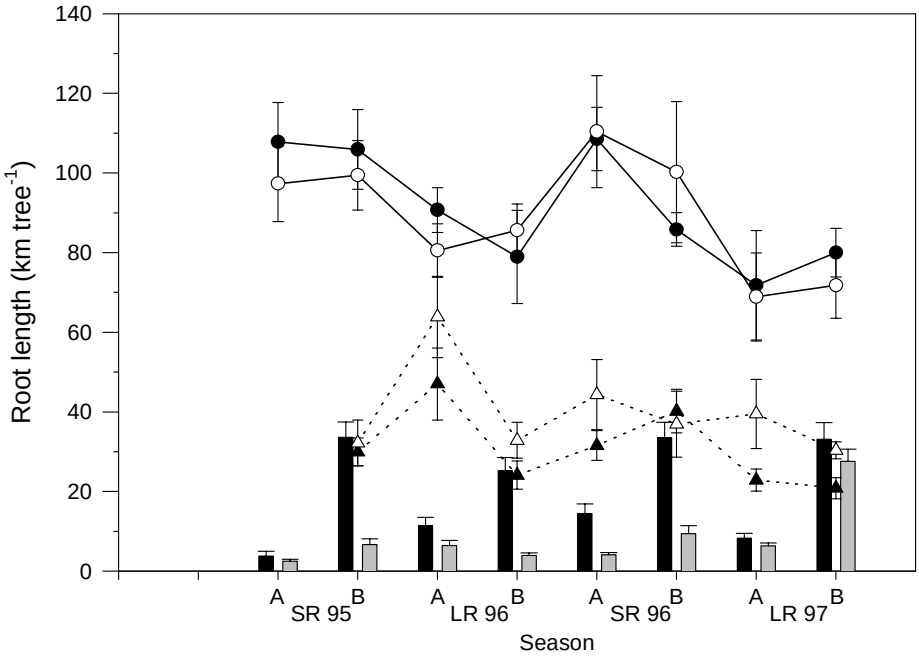

Figure 4.2: Root lengths per tree (ie. normalised to 12 m^2 of ground area) determined for the CIRUS plots, 1995 - 1997. The lines show ordinary (circles) and proteoid (triangles) root lengths for *G. robusta* in T_d (open symbols) and CT_d (closed symbols) plots; the bars show maize root lengths for C_g (black bars) and CT_d (light grey bars) plots. Seasons are denoted by 'SR' for short rains and 'LR' for long rains; timings of the A and B corings are given in Table 3.1. Error bars show ±1 se.

4.2 Tree and Crop Root Lengths

4.2.1 *Root lengths per tree*

A summary of the determinations of root length made for the CIRUS trial between 1995 and 1997, from a total of 9850 root samples, is shown in Fig. 4.2. Mean root lengths per tree, estimated by extrapolating from root lengths measured in soil cores, are shown for each of the eight times cores were collected. The population of roots was dominated consistently by ordinary, non-proteoid tree roots, which had a mean root length per tree of 90 ±2.6 km for the T_d and CT_d plots over all seasons. Proteoid rootlets increased the root length per tree by an average of 35 ±1.8 km. When mixed with trees, the mean length of maize roots per tree for all seasons was much less, at just 8 ±0.8 km; this was also less than the mean maize root length for a comparable area of the maize-only crop, which was 20 ±1.7 km for an area of 12 m^2, the area occupied by a single tree in the tree-crop mixture.

Analysis of variance showed that proximity of a maize plant to a tree in the CT_d plots had no significant ($P<0.05$) effect on root lengths per maize plant (Table 4.1). When root lengths for maize in the monocrop and the tree-crop mixture were compared (Table 4.2),

differences were significant ($P<0.01$) unless samples were from (i) the early vegetative

Table 4.1: Differences in root lengths (L_r) for maize plants in CT_d plots either closest to (Plant 1) or furthest from (Plant 2) the base of the tree. Values of L_r are means adjusted to a common soil depth.

				L_r (m plant^{-1})		
Year	Season[a]	Coring	Growth stage[b]	Plant 1[c]	Plant 2[c]	sign.[†]
95	SR	A	5-7 leaves	62.7	63.3	nsd
		B	tasselling/anthesis	175.2	160.4	nsd
96	LR	A	7-8 leaves	138.6	183.8	nsd
		B	anthesis	85.2	110.4	nsd
	SR	A	7-9 leaves	131.2	74.7	nsd
		B	anthesis	178.7	290.0	nsd
97	LR	A	7-9 leaves	183.0	135.2	nsd
		B	anthesis	697.4	678.9	nsd

[a]SR='short rains'; LR='long rains'
[b]growth stage for maize in C_g plots
[c]closest plant to tree = 1; furthest plant from tree =2
[†]nsd = no significant differences; * = significant (P<0.05); ** = significant (P<0.01)

Table 4.2: Differences in root lengths (L_r) of maize in the monocrop (C_g) or mixed with trees (CT_d). Data are normalised to 12 m^2, the area occupied by a single tree. Values of L_r are means adjusted to a common soil depth.

				L_r (km tree^{-1})[c]		
Year	Season[a]	Coring	Growth stage[b]	C_g	CT_d	sign.[†]
95	SR	A	5-7 leaves	3.8	2.5	nsd
		B	tasselling/anthesis	34.5	5.8	**
96	LR	A	7-8 leaves	6.3	9.3	nsd
		B	anthesis	22.7	6.4	**
	SR	A	7-9 leaves	15.5	3.0	**
		B	anthesis	34.1	8.8	**
97	LR	A	7-9 leaves	8.3	6.4	nsd
		B	anthesis	33.3	27.4	nsd

[a]SR='short rains'; LR='long rains'
[b]growth stage for maize in C_g plots
[c]ie. root lengths normalised to 12 m^2 of land surface area
[†]nsd = no significant differences; * = significant (P<0.05); ** = significant (P<0.01)

Table 4.3: Differences in root lengths (L_r) for *G. robusta* trees in tree-only stands (T_d) or mixed with maize (CT_d). Data are normalised to 12 m^2, the area occupied by a single tree. Values of L_r are means adjusted to a common soil depth.

				L_r (km $tree^{-1}$)[c]		
Year	Season[a]	Coring	Growth stage[b]	T_d	CT_d	sign.[†]
95	SR	A	5-7 leaves	100.9	104.2	nsd
		B	tasselling/anthesis	105.5	99.7	nsd
96	LR	A	7-8 leaves	80.7	90.5	nsd
		B	anthesis	85.5	72.5	nsd
	SR	A	7-9 leaves	118.9	100.0	nsd
		B	anthesis	100.4	85.6	nsd
97	LR	A	7-9 leaves	68.4	72.2	nsd
		B	anthesis	72.5	79.3	nsd

[a]SR='short rains'; LR='long rains'
[b]growth stage for maize in C_g plots
[c]ie. root lengths normalised to 12 m^2 of land surface area
[†]nsd = no significant differences; * = significant (P<0.05); ** = significant (P<0.01)

Table 4.4: Differences in lengths of proteoid rootlets (L_r) for *G. robusta* trees in tree-only stands (T_d) or mixed with maize (CT_d). Data are normalised to 12 m^2, the area occupied by a single tree. Values of L_r are means adjusted to a common soil depth.

				L_r (km $tree^{-1}$)[c]		
Year	Season[a]	Coring	Growth stage[b]	T_d	CT_d	sign.[†]
95	SR	A	5-7 leaves	--	--	--
		B	tasselling/anthesis	34.9	27.2	nsd
96	LR	A	7-8 leaves	63.8	62.4	nsd
		B	anthesis	32.9	24.0	nsd
	SR	A	7-9 leaves	49.1	26.7	*
		B	anthesis	40.4	36.6	nsd
97	LR	A	7-9 leaves	39.3	23.0	nsd
		B	anthesis	30.0	21.2	nsd

[a]SR='short rains'; LR='long rains'
[b]growth stage for maize in C_g plots
[c]ie. root lengths normalised to 12 m^2 of land surface area
[†]nsd = no significant differences; * = significant (P<0.05); ** = significant (P<0.01)

Table 4.5: Differences in root lengths (L_r) for maize and *G. robusta* trees in mixed stands. Data are normalised to 12 m^2, the area occupied by a single tree.

				L_r (km $tree^{-1}$)[c]		
Year	Season[a]	Coring	Growth stage[b]	maize	*G. robusta*	sign.[†]
95	SR	A	5-7 leaves	2.5	107.8	*
		B	tasselling/anthesis	6.7	105.9	*
96	LR	A	7-8 leaves	6.4	90.7	*
		B	anthesis	3.9	72.5	*
	SR	A	7-9 leaves	4.1	108.5	*
		B	anthesis	9.4	85.8	**
97	LR	A	7-9 leaves	6.4	71.8	nsd
		B	anthesis	27.5	80.0	*

[a]SR='short rains'; LR='long rains'
[b]growth stage for maize in C_g plots
[c]ie. root lengths normalised to 12 m^2 of land surface area
[†]nsd = no significant differences; * = significant ($P<0.05$); ** = significant ($P<0.01$)

growth stage or (ii) the 1997 long rains, when rainfall was good. Results from all seasons fit this pattern, except the 1996 short rains, as differences in maize root lengths were significant ($P<0.01$) at the early vegetative growth stage; however, in this case the root samples had been collected a few days later and at a more advanced growth stage than previously. Thus, when rains were poor and dry spells occurred prior to anthesis, the trees suppressed maize root growth after development of the crop had progressed past the seventh or eighth leaf, about 21 d after emergence. With abundant and well-distributed rains, however, the trees did not affect the growth of maize roots.

Comparison of results in tree-only and mixed plots showed that maize did not significantly ($P<0.05$) affect ordinary, non-proteoid root lengths for *G. robusta* (Table 4.3). The effects of maize on proteoid root lengths for *G. robusta* were also not significant ($P<0.05$) in most seasons, although they were consistently higher in the tree-only treatment and significantly ($P<0.05$) higher on one occasion (Table 4.4). There is a suggestion, therefore, that proliferation of proteoid rootlets may be suppressed by the maize crop.

Comparison of root lengths for maize and non-proteoid roots of *G. robusta* in CT_d plots demonstrated that tree roots always dominated the root population in the tree-crop mixture, even when rainfall was good (Table 4.5). Root lengths were significantly ($P<0.05$) less for maize than the trees on all occasions but one, when variability in tree root lengths was unusually high.

4.2.2 *Root length distributions*

Examples of profiles of root length density for *G. robusta* and maize are shown in Figs. 4.3 to 4.6. Such profiles were determined for all seasons of the study, but only those from the 1996 short rains, when rainfall was below average and poorly distributed, and the 1997 long rains, when rainfall was well distributed, are shown. An example of the profile for the density of proteoid rootlets is given in Fig. 4.7.

In all seasons, root length densities for non-proteoid and proteoid roots of *G. robusta* declined approximately exponentially from the surface downwards (Figs. 4.3 to 4.7), with mean values at the top of the profile for each time of sampling ranging from 1.1 to 1.7 cm cm^{-3} for non-proteoid roots. However, root length densities for tree roots did not appear to vary with distance from the tree (Figs. 4.3 to 4.6); thus, the trees occupied the available soil volume uniformly in both the T_d and CT_d plots.

Root length densities for maize also appeared to decline approximately exponentially with depth, but were usually highest near the base of the plant (Figs. 4.3 to 4.6). At the early vegetative growth stage, maximum root length densities were similar for the maize-only and mixed crops, with mean values at the top of the profile ranging between 0.25 and 0.5 cm cm^{-3} (Figs. 4.3 and 4.5). In seasons when rainfall was poor, root length densities for maize in the tree-crop mixture were similar at anthesis, indicating that there was little further growth of maize roots (Fig. 4.4). In the maize-only plots, however, mean root length densities for maize at the top of the profile increased to between 0.8 to 1.0 cm cm^{-3} by anthesis even in seasons with low rainfall (Fig. 4.4). When rainfall was good, in the 1997 long rains, such a contrast between the maize-only and mixed crops in root growth prior to anthesis did not occur (Fig. 4.6).

To compare root distributions among treatments, the depth of 50 % root length (d_{50}) was determined for each soil core collected. This was accomplished by fitting an exponential model to cumulative root length with depth (see Section 3.3.3) and calculating the depth at which cumulative root length reached 50 % (Fig. 4.8(a)). Curves fitted to data from all seasons for ordinary and proteoid tree roots and for maize roots from the monocrop and mixed plots are shown in Fig. 4.8.

The distribution of ordinary, non-proteoid roots of *G. robusta* tended to be slightly shallower in mixed plots than in tree-only stands, but this effect of maize on tree root distribution was small and not significant ($P<0.05$) in most seasons (Table 4.6). Effects of maize on distributions of proteoid root lengths were consistently non-significant ($P<0.05$) (Table 4.7).

The distribution of roots was usually significantly ($P<0.01$) deeper for tree roots than maize roots in mixed plots (Table 4.8), and maize roots were significantly ($P<0.05$) more deeply distributed in the monocrop than the tree-crop mixture, whether rains were poor or not (Table 4.9). Thus, the penetration of maize roots into the soil was suppressed by the trees.

4.2.3 *Root lengths and competition*

In the below-ground environment of the CIRUS site, where there was no water table and downward root growth was constrained by bedrock at shallow depths, maximum root length densities for *G. robusta* were always found at the top of the soil profile. *G. robusta*

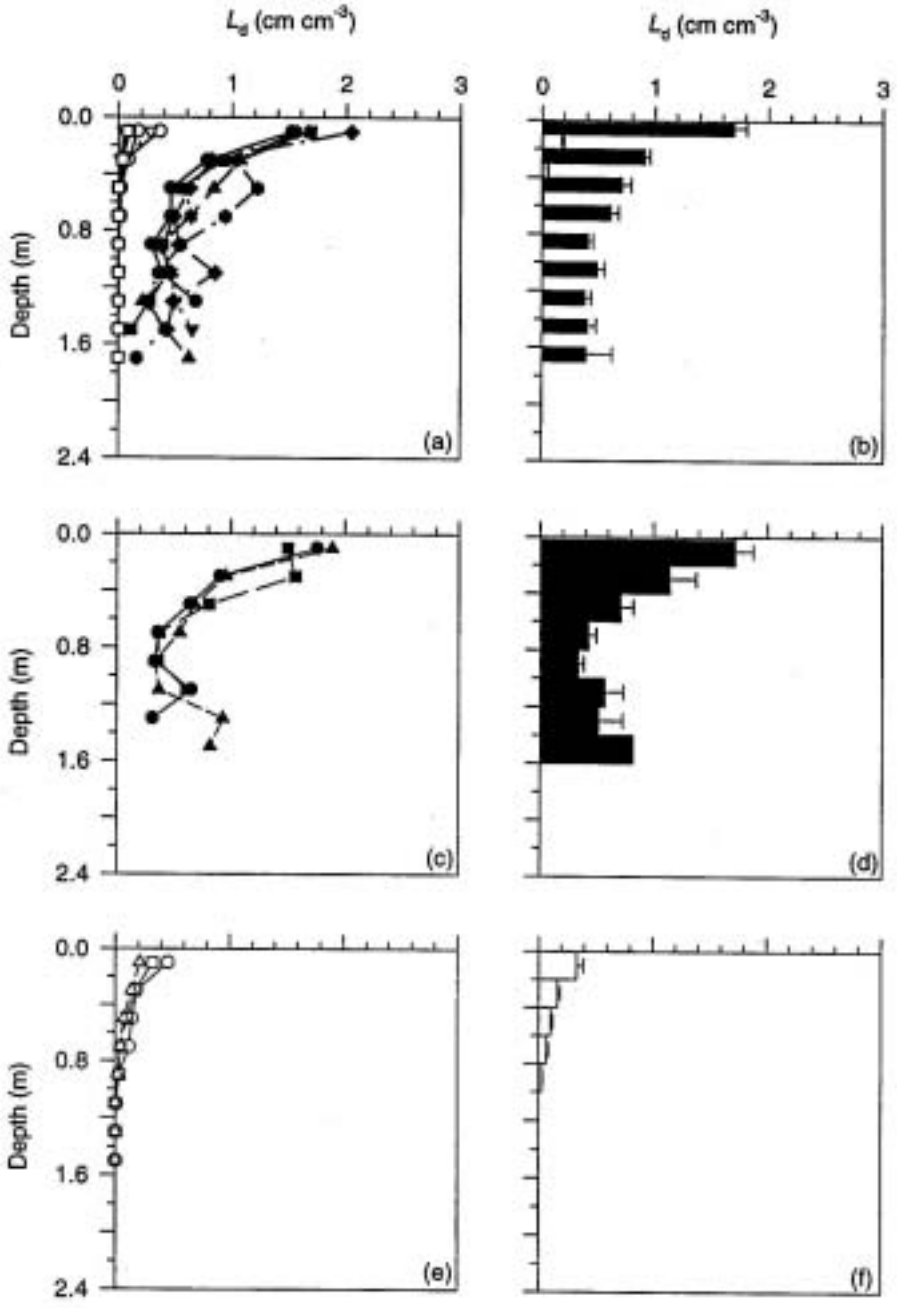

Figure 4.3: Root length densities (L_d) at 22-26 days after maize emergence in the short rains 1996, for (a) maize (open symbols) and *G. robusta* trees (closed symbols) in CT_d plots; (c) *G. robusta* in T_d plots; and (e) maize in C_g plots. The symbols denote (see Fig. 4.2) core positions: 1 (●); 2 (■); 3 (▲); 4 (▼); 5 (◆); and 6 (•). L_d (+1 s.e.) averaged over all core positions are shown for (b) CT_d plots, with maize root lengths shown by open bars; (d) T_d plots; and (f) C_g plots.

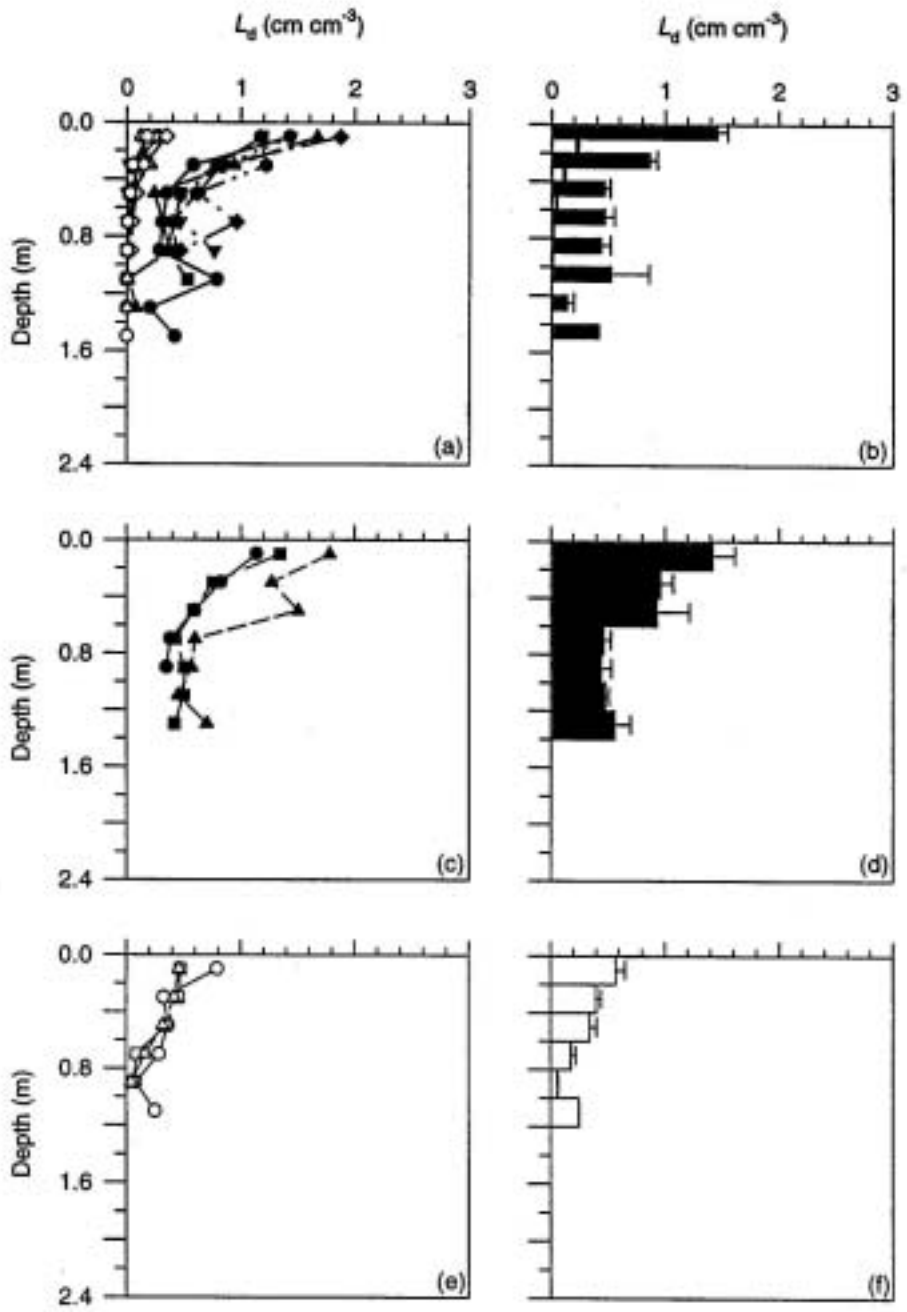

Figure 4.4: Root length densities (L_d) at maize anthesis in the short rains 1996, for (a) maize (open symbols) and *G. robusta* trees (closed symbols) in CT_d plots; (c) *G. robusta* in T_d plots; and (e) maize in C_g plots. The symbols denote (see Fig. 4.2) core positions: 1 (●); 2 (■); 3 (▲); 4 (▼); 5 (◆); and 6 (•). L_d (+1 s.e.) averaged over all core positions are shown for (b) CT_d plots, with maize root lengths shown by open bars; (d) T_d plots; and (f) C_g plots.

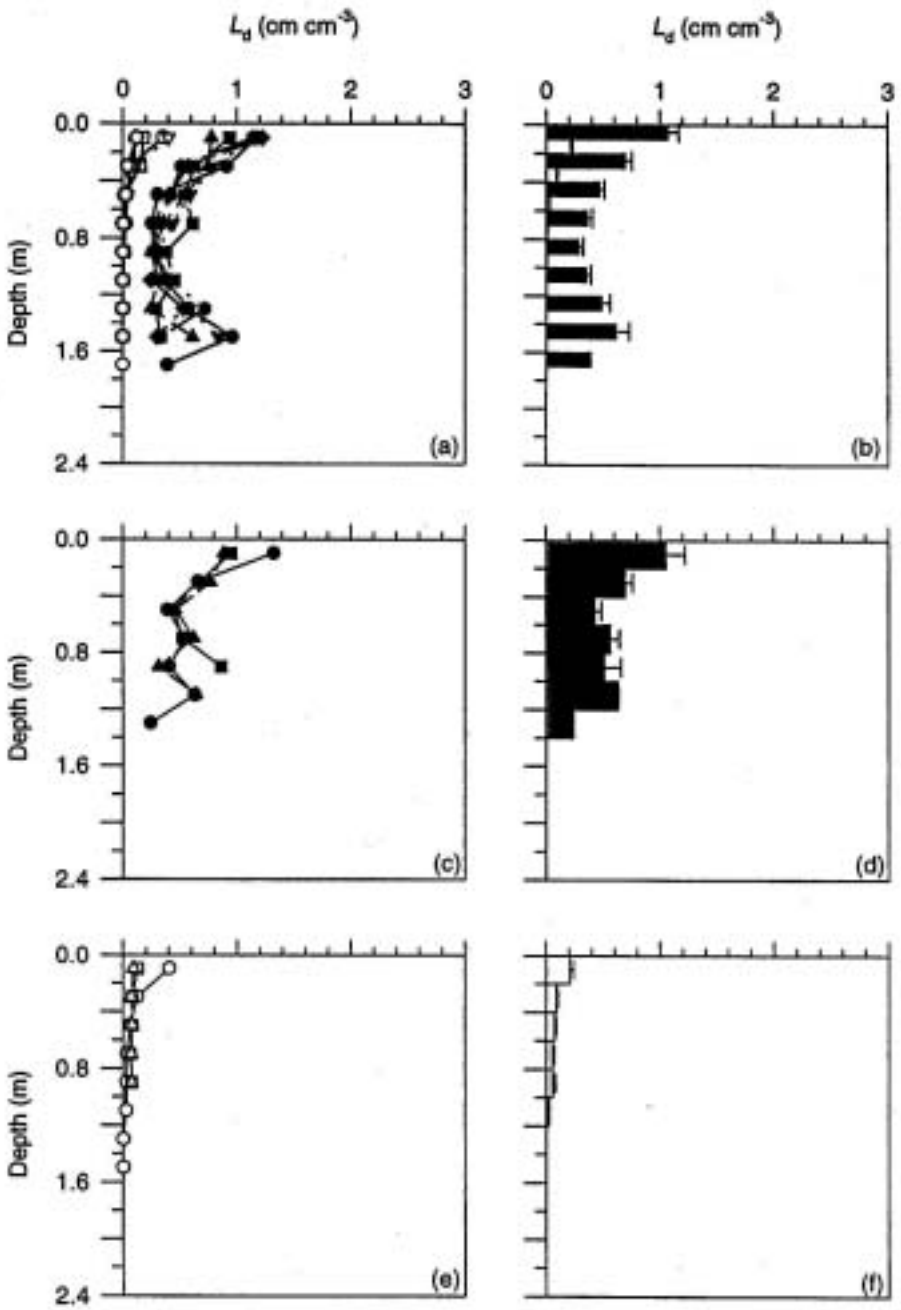

Figure 4.5: Root length densities (L_d) at 23-27 days after maize emergence in the long rains 1997, for (a) maize (open symbols) and *G. robusta* trees (closed symbols) in CT_d plots; (c) *G. robusta* in T_d plots; and (e) maize in C_g plots. The symbols denote (see Fig. 4.2) core positions: 1 (●); 2 (■); 3 (▲); 4 (▼); 5 (◆); and 6 (•). L_d (+1 s.e.) averaged over all core positions are shown for (b) CT_d plots, with maize root lengths shown by open bars; (d) T_d plots; and (f) C_g plots.

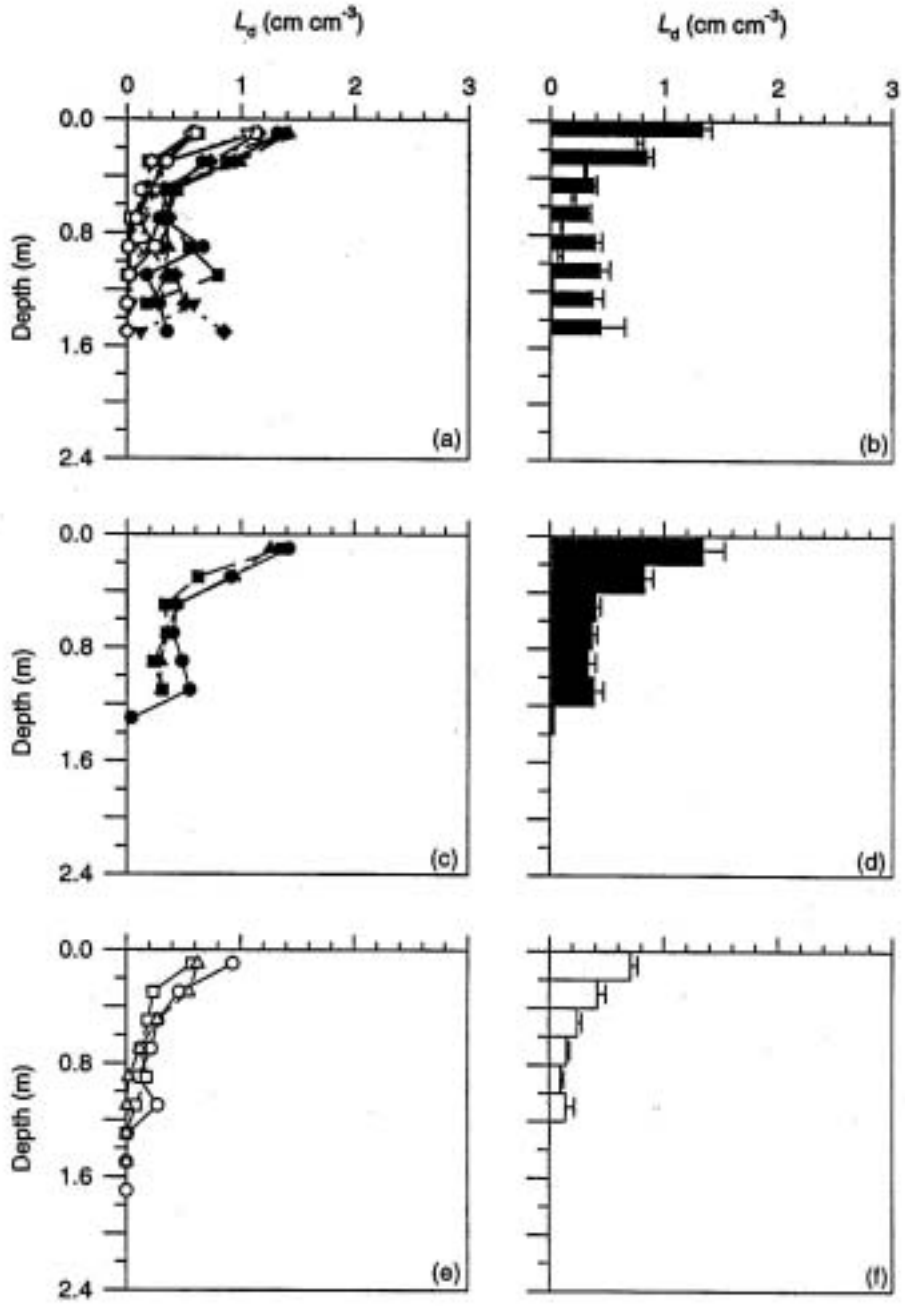

Figure 4.6: Root length densities (L_d) at maize anthesis in the long rains 1997, for (a) maize (open symbols) and *G. robusta* trees (closed symbols) in CT_d plots; (c) *G. robusta* in T_d plots; and (e) maize in C_g plots. The symbols denote (see Fig. 4.2) core positions: 1 (●); 2 (■); 3 (▲); 4 (▼); 5 (◆); and 6 (•). L_d (+1 s.e.) averaged over all core positions are shown for (b) CT_d plots, with maize root lengths shown by open bars; (d) T_d plots; and (f) C_g plots.

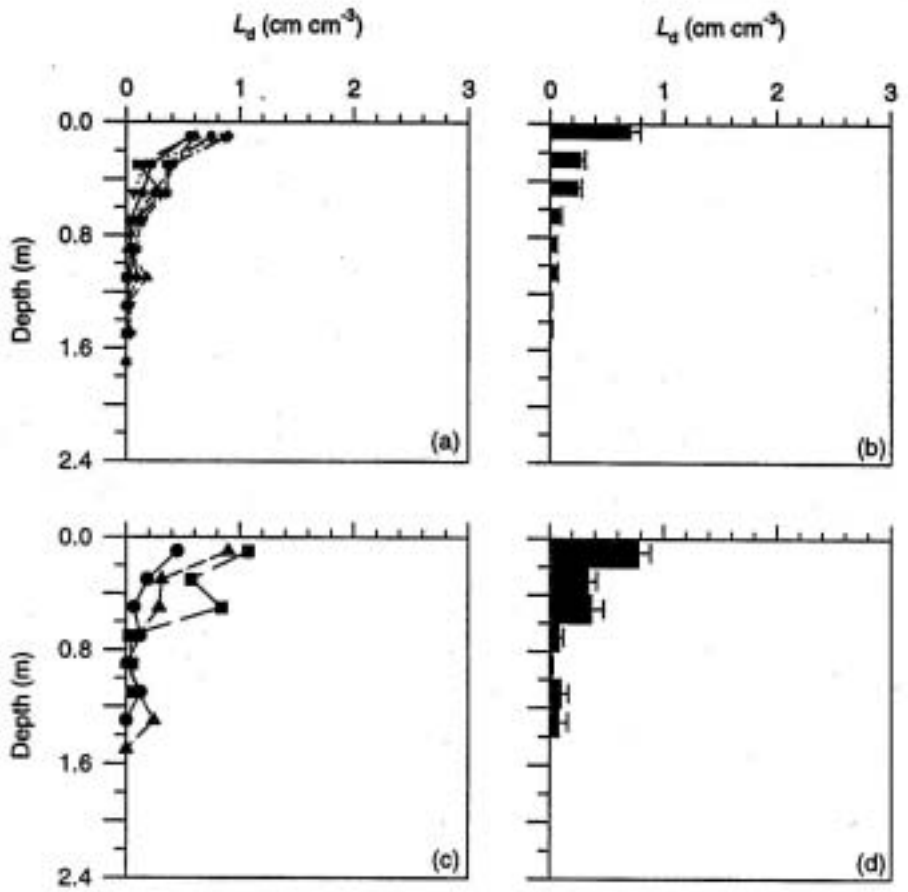

Figure 4.7: Length densities (L_d) of proteoid rootlets at 22-26 days after maize emergence in the short rains 1996 for (a) CT_d plots and (c) T_d plots. The symbols denote (see Fig. 4.2) core positions: 1 (●); 2 (■); 3 (▲); 4 (▼); 5 (◆); and 6 (•). L_d (+1 s.e.) averaged over all core positions are shown for (b) the CT_d and (d) the T_d plots.

Table 4.6: Differences in depth of 50 % cumulative root length (d_{50}) for *G. robusta* trees in tree-only stands (T_d) or mixed with maize (CT_d). Values of d_{50} are means adjusted to a common soil depth.

				d_{50} (m)[c]		
Year	Season[a]	Coring	Growth stage[b]	T_d	CT_d	sign.[†]
95	SR	A	5-7 leaves	0.34	0.31	nsd
		B	tasselling/anthesis	0.35	0.32	nsd
96	LR	A	7-8 leaves	0.28	0.31	nsd
		B	anthesis	0.32	0.31	nsd
	SR	A	7-9 leaves	0.29	0.29	nsd
		B	anthesis	0.28	0.25	*
97	LR	A	7-9 leaves	0.32	0.27	**
		B	anthesis	0.28	0.26	nsd

[a]SR='short rains'; LR='long rains'
[b]growth stage for maize in C_g plots
[†]nsd = no significant differences; * = significant (P<0.05); ** = significant (P<0.01)

Table 4.7: Differences in depth of 50 % cumulative root length (d_{50}) for proteoid rootlets of *G. robusta* trees in tree-only stands (T_d) or mixed with maize (CT_d). Values of d_{50} are means adjusted to a common soil depth.

				d_{50} (m)[c]		
Year	Season[a]	Coring	Growth stage[b]	T_d	CT_d	sign.[†]
95	SR	A	5-7 leaves	--	--	--
		B	tasselling/anthesis	0.18	0.20	nsd
96	LR	A	7-8 leaves	0.26	0.18	nsd
		B	anthesis	0.22	0.17	nsd
	SR	A	7-9 leaves	0.20	0.19	nsd
		B	anthesis	0.17	0.19	nsd
97	LR	A	7-9 leaves	0.23	0.19	nsd
		B	anthesis	0.12	0.16	nsd

[a]SR='short rains'; LR='long rains'
[b]growth stage for maize in C_g plots
[†]nsd = no significant differences; * = significant (P<0.05); ** = significant (P<0.01)

Table 4.8: Differences in mean values of depth of 50 % cumulative root length (d_{50}) for maize *G. robusta* trees in mixed stands.

				d_{50} (m)[c]		
Year	Season[a]	Coring	Growth stage[b]	maize	*G. robusta*	sign.[†]
95	SR	A	5-7 leaves	0.08	0.32	*
		B	tasselling/anthesis	0.09	0.35	nsd
96	LR	A	7-8 leaves	0.20	0.31	nsd
		B	anthesis	0.15	0.32	*
	SR	A	7-9 leaves	0.10	0.30	*
		B	anthesis	0.12	0.25	*
97	LR	A	7-9 leaves	0.13	0.28	nsd
		B	anthesis	0.16	0.27	*

[a]SR='short rains'; LR='long rains'
[b]growth stage for maize in C_g plots
[†]nsd = no significant differences; * = significant (P<0.05); ** = significant (P<0.01)

Table 4.9: Differences in depth of 50 % cumulative root length (d_{50}) for maize in the monocrop (C_g) or mixed with trees (CT_d). Values of d_{50} are means adjusted to a common soil depth.

				d_{50} (m)[c]		
Year	Season[a]	Coring	Growth stage[b]	C_g	CT_d	sign.[†]
95	SR	A	5-7 leaves	0.14	0.08	*
		B	tasselling/anthesis	0.26	0.09	**
96	LR	A	7-8 leaves	0.29	0.21	nsd
		B	anthesis	0.23	0.16	*
	SR	A	7-9 leaves	0.20	0.10	**
		B	anthesis	0.24	0.12	**
97	LR	A	7-9 leaves	0.25	0.13	**
		B	anthesis	0.21	0.16	**

[a]SR='short rains'; LR='long rains'
[b]growth stage for maize in C_g plots
[†]nsd = no significant differences; * = significant (P<0.05); ** = significant (P<0.01)

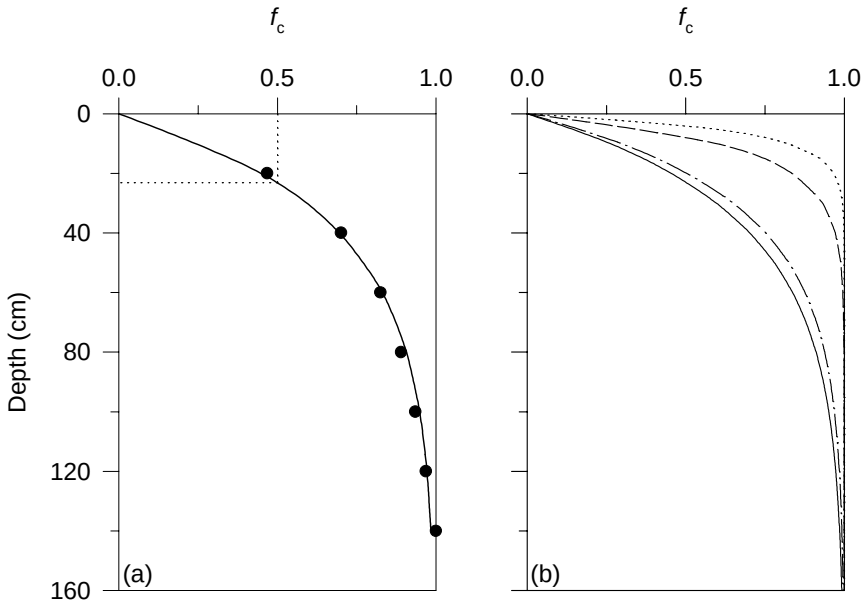

Figure 4.8: (a) Fitting of Equation 3.1 to a profile of cumulative fractional root length (f_c); the dotted lines mark the depth of 50 % root length (d_{50}). (b) Mean profiles of f_c, over all seasons, for ordinary (non-proteoid) roots of *G. robusta* (———), proteoid rootlets of *G. robusta* (– – –), maize at anthesis in the monocrop (—·—·) and in the tree-crop mixture (·····).

is consequently unlikely to exhibit complementarity with maize in use of water resources, at least where below-ground conditions are similar (Schroth, 1995). The consistent dominance of tree roots in the population of roots - at all depths - demonstrates, moreover, that in the tree-crop configuration studied in the CIRUS experiment, *G. robusta* maintained a strong competitive advantage over maize at all times.

G. robusta suppressed downward penetration of maize roots in all seasons, regardless of how rainfall was distributed and whether rainfall was average or below average (Table 4.9). Maize mixed with trees was consequently more vulnerable to drying of the surface layer of the soil during dry spells than the monocrop, with the result that when lengthy dry periods occurred soon after crop emergence, growth of maize roots in the mixture was severely reduced after the early vegetative growth stages (Table 4.2). When rains were poor, maize in the mixture was thus unable to capture a sufficient quantity of below-ground resources to support growth at levels similar to the monocrop. Below-ground competition was therefore one of the principal causes for the severe reductions in crop biomass and grain yields observed by Lott *et al*. (1997) in the CT_d tree-crop mixture.

The dominant position of tree roots in the root population enables them to capture more soil water than the crop and consequently reduce the water available to the crop to levels

that limit growth. Hence, to diminish the impact of below-ground competition on the crop, an appropriate strategy is to take steps to reduce demand for water by the trees and, therefore, the quantity of water they extract from the soil. This can be accomplished by reducing the leaf area of the tree canopy by pruning.

An additional benefit of pruning foliage may be to cause some die back of roots, as a result of a reduction in the supply of photosynthate from the crown (Fownes and Anderson, 1991; van Noordwijk *et al*., 1996). The *G. robusta* trees in the CIRUS trial were severely pruned prior to the 1996 short rains and there appeared to be some reductions in root lengths of the trees in subsequent months (Fig. 4.2). However, without a longer series of measurements, it is not possible to say whether this resulted from pruning or the effects of, for example, cyclical root turnover which may occur annually.

Whatever the cause of the apparent decline in tree root lengths between the 1996 short rains and 1997 long rains, the dominant position of the trees in the root population was not affected. The growth and distribution of maize roots was severely suppressed in the 1996 short rains, despite the large reduction in water use by the trees which must have resulted from pruning the crowns. Uptake of water by the trees, however, remained sufficient to limit the supply of water available to the maize, because rainfall was very low in this season and the established root network of the trees probably enabled them to capture most of the available resource. In the following season, the 1997 long rains, rains were good and maize root lengths were not suppressed by the trees (Table 4.2), but the effect of the trees on penetration of maize roots remained.

While pruning of trees reduces their demand for water, competition for water may still have a substantial impact on crop growth in agroforestry if tree roots continue to dominate the root population after pruning. In such circumstances, the trees remain far more effective at capturing water resources than the crop and thus pruning of the tree canopy is only likely to substantially reduce the impact on the crop of competition for water if the supply available from rainfall exceeds the demands of the trees. The probability of the latter condition is higher after pruning. Thus, while pruning of trees where tree roots are dominant cannot change the relative abilities of the tree and crop root systems to capture water resources, it will enhance the likelihood that rain in a season will be sufficient to support the growth of both trees and a crop.

4.3 Observation of Root Growth Using Minirhizotrons

A series of photographs of roots of *G. robusta* are shown in Fig. 4.9. These photographs were taken at weekly intervals at a depth of 0.7 m in the T_d plot during a dry spell in the cropping season. The young, white roots pictured at the start of the sequence gradually darkened, shrank and began to disappear by the final week in the series. As these roots aged, however, no new roots appeared to replace them, possibly because the soil was very dry.

Another series of photographs, in Fig. 4.10, shows maize roots in the C_g plot during the same period. In this case, few roots appear to have died and new roots have appeared by the time the final picture was taken. Root growth may have continued in the maize-only plot because the soil remained more moist than under the trees over the dry spell.

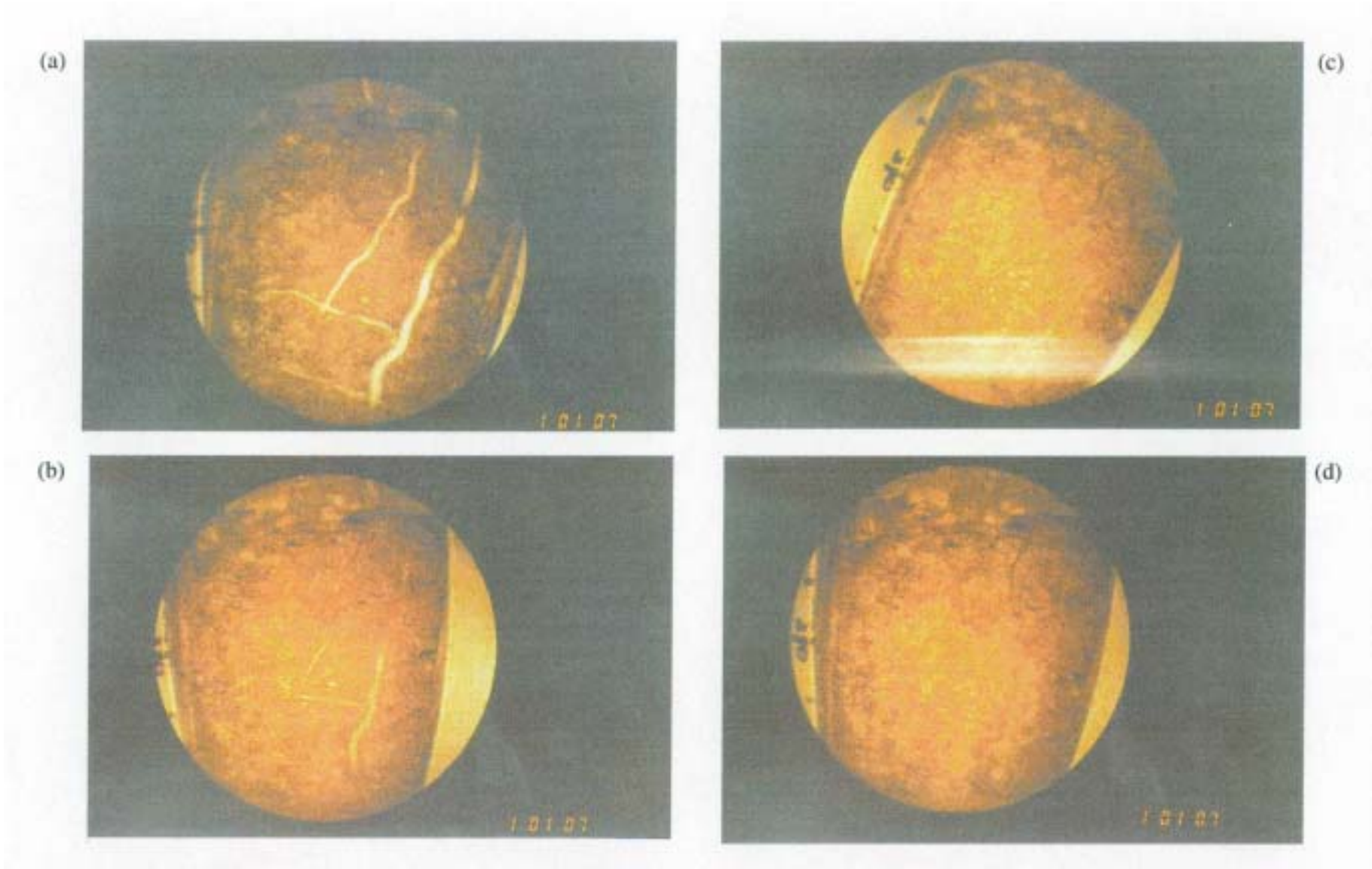

Figure 4.9: Roots of *G. robusta* photographed in a minirhizotron on (a) April 20, (b) April 27, (c) May 4 and (d) May 11, 1996.

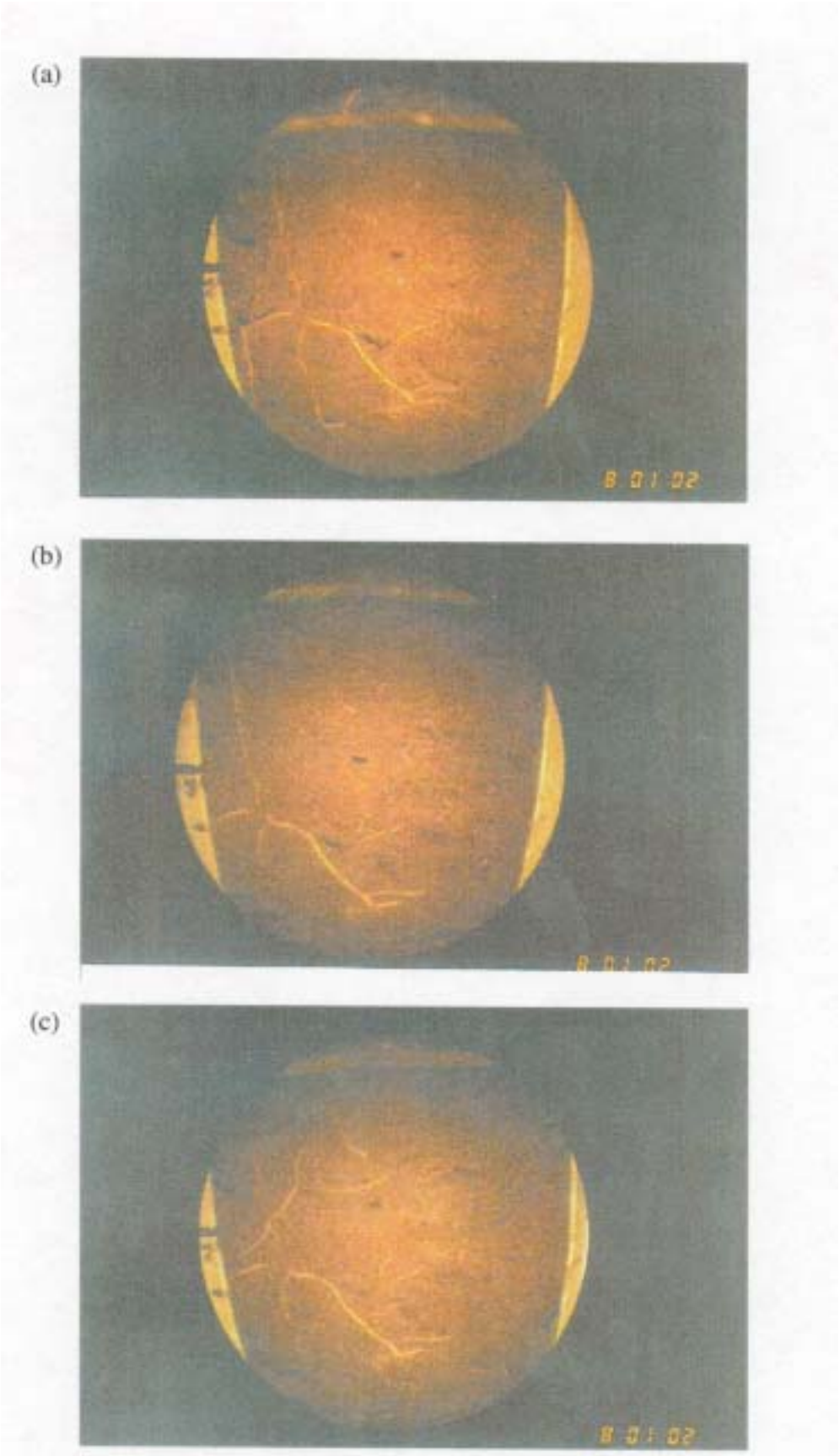

Figure 4.10: Roots of maize photographed in a minirhizotron on (a) April 27, (b) May 4 and (c) May 11, 1996.

These two examples demonstrate how images from the minirhizotron can be used, qualitatively, to assess root dynamics over periods between corings. Unfortunately, however, efforts to derive quantitative information about root growth dynamics by determining changes in root counts in sequences of photographs over time gave ambiguous results. It appears, therefore, that use of minirhizotrons to monitor root growth requires a greater investment of time than was possible in this project. With more time available, observations could have been replicated and ambiguities in the results may have been clarified. However, to undertake such a task, it would have been necessary to devote a very large amount of time to collecting and processing images, to the detriment of other, more fruitful activities undertaken during the project.

4.4 Branching Characteristics of Tree Roots and Estimates of Root Length

4.4.1 *Branching characteristics of roots of* Grevillea robusta

Of 696 root branching points examined, 615 or 88.4 % bore two branches, 9.6 % produced three branches and 2.0 % bore four or more. The mean value of n_b, the number of branches at each branching point, was thus 2.1. As pairs of branching points connected by very short link lengths were easily mistaken for single branching points bearing three or more branches, it is likely that the true proportion of branching points with more than two branches was even smaller than recorded. Consequently, a constant value of n_b=2 can be assumed for *G. robusta*.

Figure 4.11(a) shows that values of the α ratio for *G. robusta* did not vary with root diameter. The assumption that α is independent of scale, required for use of the recursive branching algorithm to estimate root length, was thus fulfilled. However, variation in α was very high, particularly for root diameters (D) of <5 mm. The mean value of α was 1.09 and the median value was 1.02; the latter is likely a better indicator of the central tendency of α because, unlike the mean, its value was not affected by large outliers in the dataset.

Values of the q ratio for roots of *G. robusta* are plotted in Fig. 4.11(b). The range of values was unaffected by D. The fraction of q values >0.9 was 0.75, indicating that the 'herring bone' pattern of branching was most common, but that dichotomous branching occurred at a minority of branching points.

Link lengths (L_l) measured for *G. robusta* are shown in Fig. 4.12(a). Variation in L_l was extremely high, with 1 mm the lowest value recorded and more than 800 mm the highest. However, it is probable that many of the large outliers were measured in error when fragments of branches lost inadvertently during excavation were not detected. When link lengths >100 mm are excluded, it is apparent that L_l does not vary with D (Fig. 4.12(b)). The mean value of L_l recorded was 49 mm and the median value was 22 mm.

The minimum root diameter recorded (D_{min}), which is the diameter of the terminal root links, was 0.1 mm.

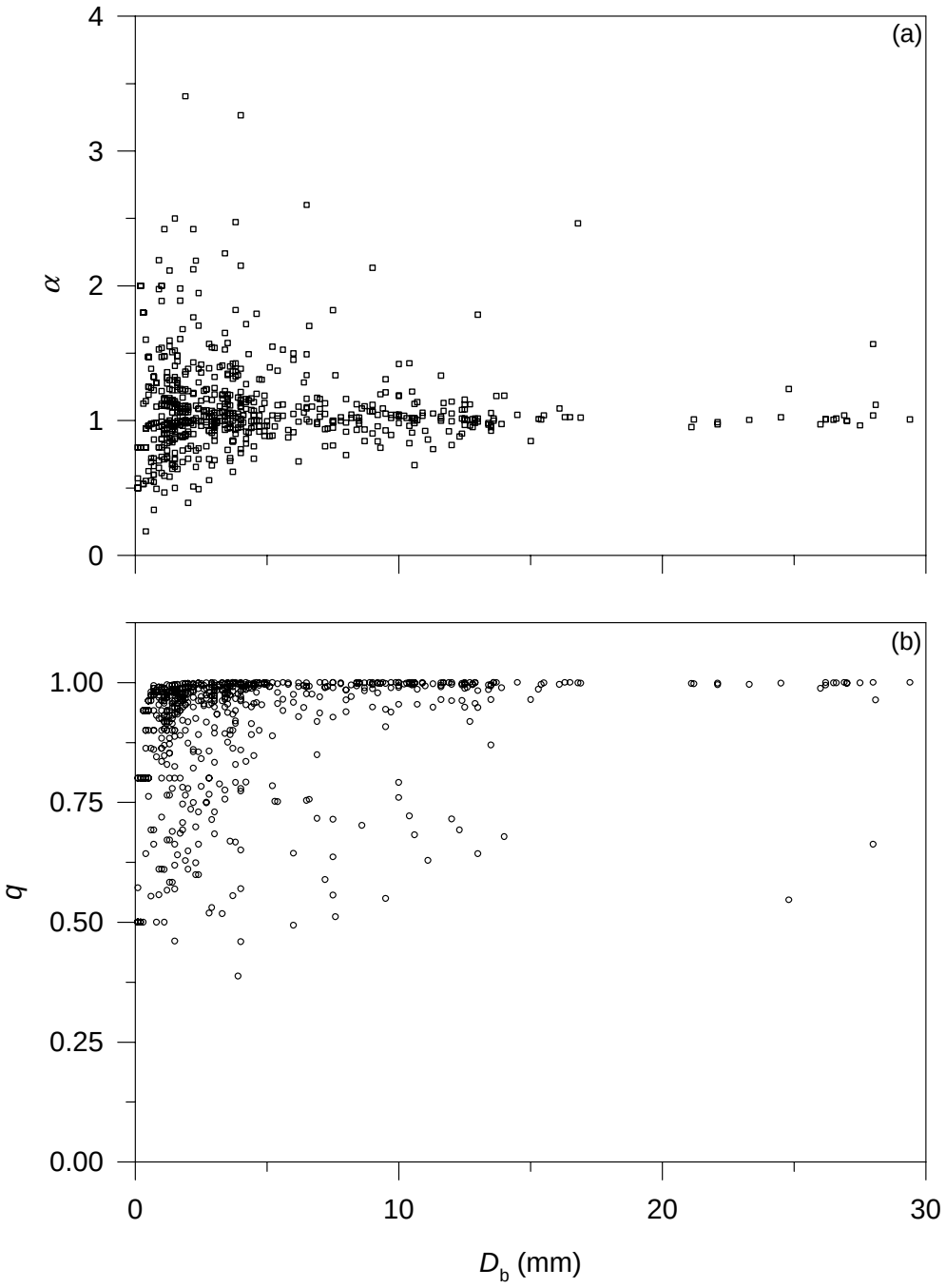

Figure 4.11: Values of (a) α and (b) q for branches of *G. robusta* roots with diameters immediately before the branch of D_b.

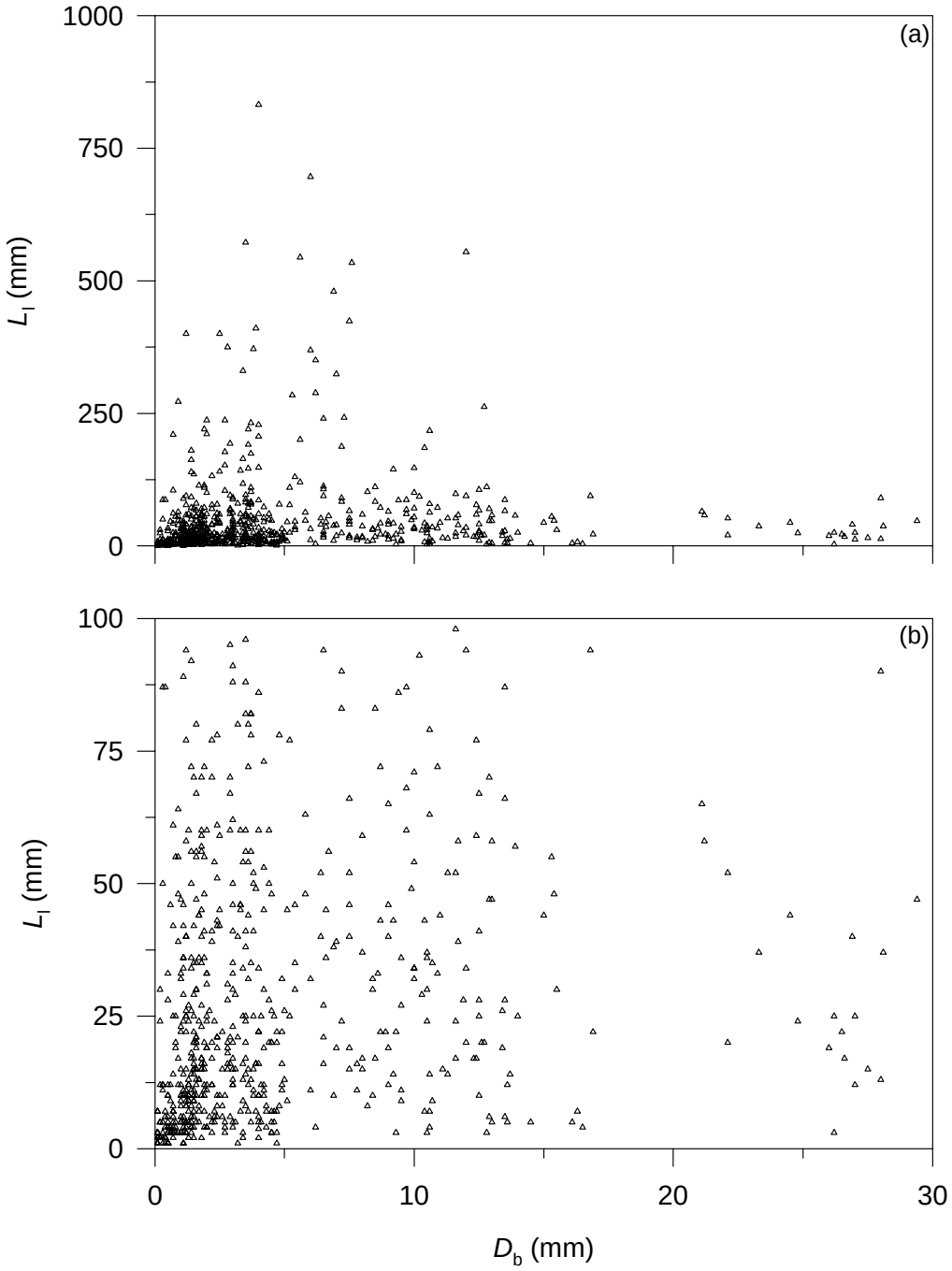

Figure 4.12: (a) Link lengths (L_l) between branching points for *G. robusta* roots with diameters (at the distal end of the link) of D_b. (b) Re-plotting of data for L_l<100 mm.

Table 4.10: Values used to parameterise the recursive branching algorithm (Appendix A) for *G. robusta*.

Parameter	Value	Notes
α	1.0233	median of measured values of α
r_α	0.1408 (for $D_b \leq 5$ mm) 0.0384 (for $D_b > 5$ mm)	α varies randomly within $\pm 2r_\alpha$ in algorithm; variation is higher for root diameters (D_b) ≤5 mm.
f_q	0.748	fraction of measured q values >0.9
D_{min}	0.1 mm	minimum root diameter measured

4.4.2 *Parameterisation of the recursive branching algorithm*

Output from the recursive branching algorithm was extremely sensitive to the values of the branching parameters used. As a consequence, care was taken in selecting the values of these parameters, which are given in Table 4.10. The median value of α ($\breve{\alpha}$) was preferred to the mean, to reduce the influence of large outliers in the dataset that probably resulted from errors in measurement or root growth in unusually constricted locations of the soil. The algorithm includes provision for random variation in α within specified bounds and the bounds chosen were:

$$\breve{\alpha} \pm 2\breve{r}_\alpha \ ,$$

where $\breve{r}_\alpha$ is the median of r_α, the residuals of α, given by

$$r_\alpha = \sqrt{(\alpha - \breve{\alpha})^2} \quad . \tag{4.1}$$

When the bounds of variation in α are defined in this way, 50 % of the values of α generated by the recursive branching algorithm fall within $\pm 1\breve{r}_\alpha$, as was the case in the original dataset. Because variation in α appeared to be higher for roots with smaller diameters, different values of $\breve{r}_\alpha$ were used for $D \leq 5$ mm and $D > 5$ mm (Table 4.10).

4.4.3 *Results from the recursive branching algorithm*

The recursive branching algorithm estimates the number of links (n_l) comprising a root from an initial diameter (D_i). Because of the provision for random variation in α and q, values of n_l determined were means from 100 runs of the algorithm. Values of n_l for the 32 roots on which measurements of branching characteristics were made are plotted in Fig. 4.13; as expected, n_l was approximately proportional to D_i^2, and therefore the cross-sectional area of the root.

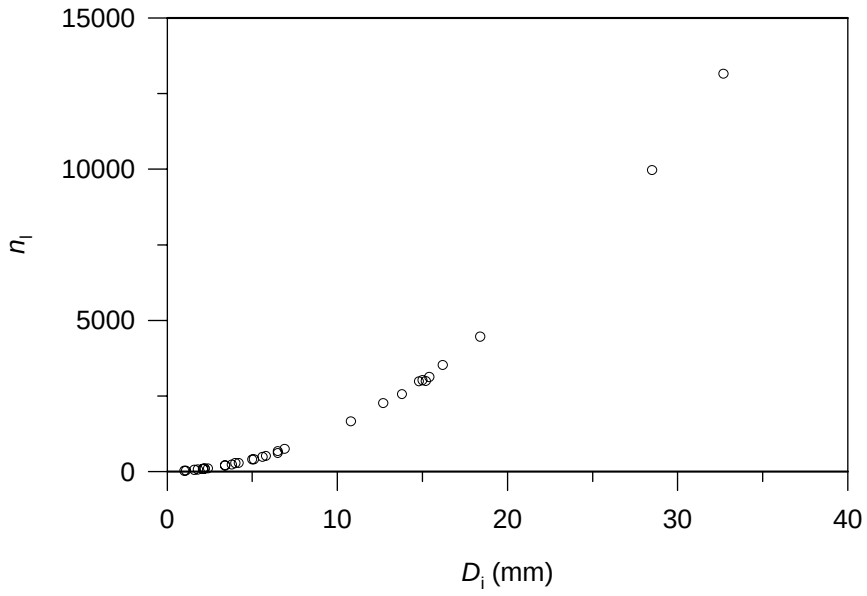

Figure 4.13: The number of links (n_l) estimated using the recursive branching algorithm (Appendix A) for roots of *G. robusta* with initial diameters of D_i.

4.4.4 *Comparison of estimated and measured root length*

The root length determined by soil coring (L_r) for each grid cell at the centre of the four sets of four trees described in Section 3.5 is given in Table 4.11. Root lengths for each grid cell estimated from the output of the recursive branching algorithm ($\hat{L}_r$), as $\hat{L}_r = n_l L_l$, are also given. Whether the mean or median value of L_l was used, $\hat{L}_r$ was a gross underestimate of the measured root length (Table 4.11).

Such large discrepancies between estimated and measured root lengths probably resulted from inaccuracy in the parameterisation of the recursive branching algorithm, as output from the algorithm was very sensitive to small changes in the values of the parameters describing branching characteristics. For example, the approximately 10-fold discrepancy between $\hat{L}_r$ and L_r would be eliminated if, rather than 0.1 mm, actual D_{min} was 0.03 mm (Fig. 4.14). As determination of D_{min} was made using callipers with a resolution limited to 0.1 mm, and because recovery of the finest roots from the soil by excavation is very difficult, such an error in D_{min} is plausible.

Difficulties in accurately determining the parameters describing root branching suggest, therefore, that accurate estimation of tree root lengths on the basis of the fractal characteristics of root branching, as proposed by van Noordwijk *et al*. (1994), is not possible in the field. However, by comparing n_l, estimated using the recursive branching algorithm, and L_r, measured using soil coring, calibration of the fractal method is possible. An 'effective link length' (L_l^{eff}), calculated using

Table 4.11: Root lengths for *G. robusta* estimated by soil cores (L_r) for 3 x 4 m grid cells bounded by a tree at each corner; n_l, the number of root links determined using the recursive branching algorithm; $\hat{L}_r$ (A) and $\hat{L}_r$ (B), estimates of root length from $\hat{L}_r = n_l L_l$, where L_l is mean and median link length, respectively; and L_l^{eff}, the effective link length, from L_r/n_l.

Grid cell	L_r (km)[a]	n_l	$\hat{L}_r$ (A) (km)[†]	$\hat{L}_r$ (B) (km)[†]	L_l^{eff} (mm)
1	60.8	127927	6.2	2.8	476
2	73.9	222541	10.8	4.9	332
3	42.4	176684	8.6	3.9	240
4	43.0	166208	8.1	3.6	259
mean ±se					326 ±54

[a]estimated from soil coring
[†]value (A) calcaulated using the mean link length; value (B) calculated using the median link length

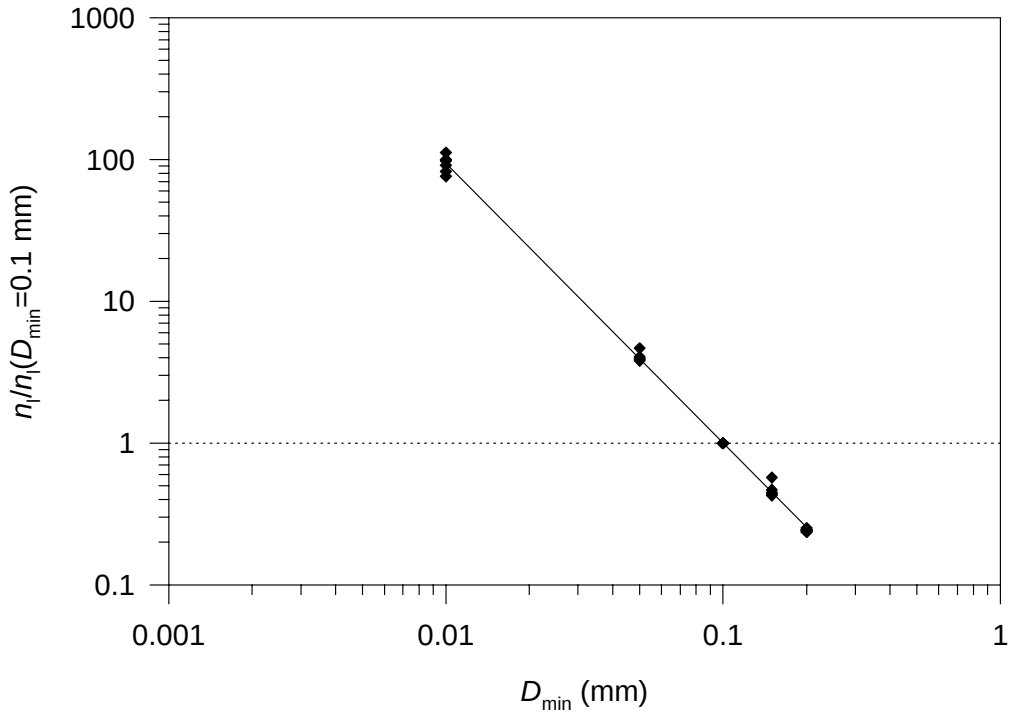

Figure 4.14: The effect of minimum root diameter (D_{min}) on the number of links (n_l) estimated using the recursive branching algorithm; values of n_l are expressed relative to n_l at D_{min}=0.1 mm.

$$L_{\mathrm{l}}^{\mathrm{eff}} = \frac{L_{\mathrm{r}}}{n_{\mathrm{l}}} \tag{4.2}$$

can be used to convert numbers of root links, from the branching algorithm, to estimates of root length; thus,

$$\hat{L}_{\mathrm{r}} = n_{\mathrm{l}} L_{\mathrm{l}}^{\mathrm{eff}} \,. \tag{4.3}$$

The value of $L_{\mathrm{l}}^{\mathrm{eff}}$ for *G. robusta* in the CIRUS trial was much higher than the mean or median of measured link lengths (Table 4.11), but its use provides a means of correcting for errors in the parameterisation of the recursive branching algorithm and results in values of $\hat{L}_{\mathrm{r}}$ that are effectively referenced to soil coring.

The fractal method of estimating tree root lengths can be used in the field, therefore, provided than it is calibrated from a comparison with soil coring. When calibrated in this way, the method enables, for example, lengths of excavated roots to be corrected for losses resulting from breakage during recovery of roots from the soil (Fig. 4.15).

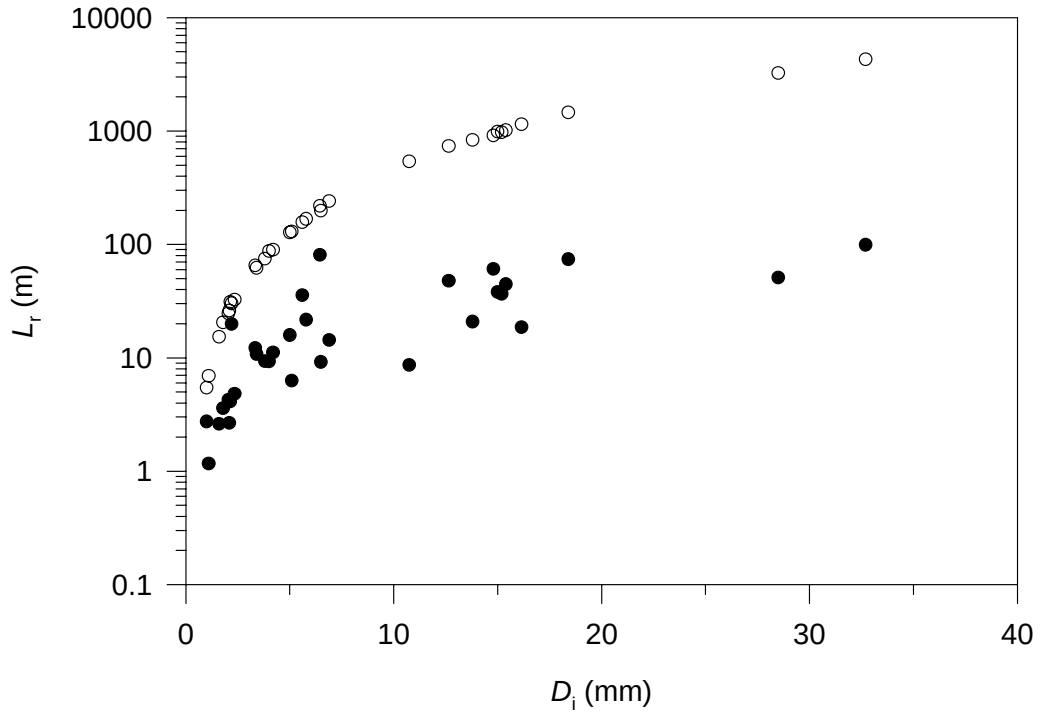

Figure 4.15: Lengths of roots (L_{r}) of *G. robusta* with initial diameters of D_{i} recovered by excavation (closed symbols) or estimated using the recursive branching algorithm and the effective link length (open symbols).

4.5 Sap Flow in Roots of *Grevillea robusta*

Use of sap flow gauges on roots proved to be a valuable method of investigating the dynamics of water uptake by the root systems of trees. We were able to contrast activity of lateral roots near the soil surface with deeply-penetrating vertical roots and our data revealed, for the first time, the process of 'downward siphoning' by tree roots. This is a process that may have very important implications for interactions between trees and crops and for the design and management of agroforestry systems, as it results in the transport of water, via the root systems of trees, between wet soil near the surface and drier subsoil beneath. Observation of downward siphoning was possible because the reversal of flow in roots can be detected using constant-power sap flow gauges.

4.5.1 *Measurement of flow reversal*

The performance of a constant-power sap flow gauge during the reversal of flow in a vertical root is shown in Fig. 4.16. The key to identifying periods of reverse flow was the sign of the temperature gradient across the heated portion of the gauge, ΔT (Fig. 4.16(a)), which was positive when sap warmed by the heater moved towards the trunk, but negative when sap flowed in the opposite direction, towards the root tips. As uptake of heat by the moving sap stream was substantial when ΔT was both positive and negative (Fig. 4.16(b)), flow was measured in both directions.

Data were unreliable, however, near transitions between positive and negative flow because ΔT was then 0 K or close to 0 K, which caused rates of flow (F) calculated using Equation 3.5 to be undefined or erroneously high. Consequently, it was necessary to set F to zero during these periods of transition. This was accomplished using two criteria that were met *concurrently* only during a change in the direction of flow: F was set to zero if $|\Delta T| \leq 2.0$ K *and* $(\Delta T_b - \Delta T_a) \geq 1.0$ K. The latter criterion was effective because it was not met when flow rates were truly high, as $(\Delta T_b - \Delta T_a)$ is proportional to the conductive heat flux from the gauge (Smith and Allen, 1996), which is always low when sap flow is rapid. Filtering of data near periods of transition using these criteria was effective, but resulted in the loss of some resolution in rates of sap flow at these times (Fig. 4.16(c)).

4.5.2 *Sap flow in roots after a poor rainy season*

The record of sap flow in roots from Installation 1 is shown in Fig. 4.17. For the entire period of observation, sap flow in the lateral root was positive, indicating uptake of water from the soil. Uptake continued at substantial rates throughout each night, although nocturnal flow rates declined as the period progressed. In the vertical root, sap flow was negative, or towards the root tips for much of the period. Rates of reverse flow were highest at night and declined as positive flow rates in the lateral root peaked during the day. Later, overnight rates of downward flow in the vertical root gradually declined and, after December 11, sap flow became positive during the middle of the day.

All lateral roots of the tree were severed on December 15. The high rates of sap flow recorded in the lateral root on this day were probably the result of increased uptake compensating for the severing of other roots (Lott *et al.*, 1996), as the gauged lateral was the last to be cut. The following day, sap flow was far higher in the vertical root than on previous days, with much lower rates of downward flow overnight; severing of the laterals thus forced uptake through the vertical roots of the tree. This response to the cutting of roots confirmed that the sap flow gauges were operating correctly.

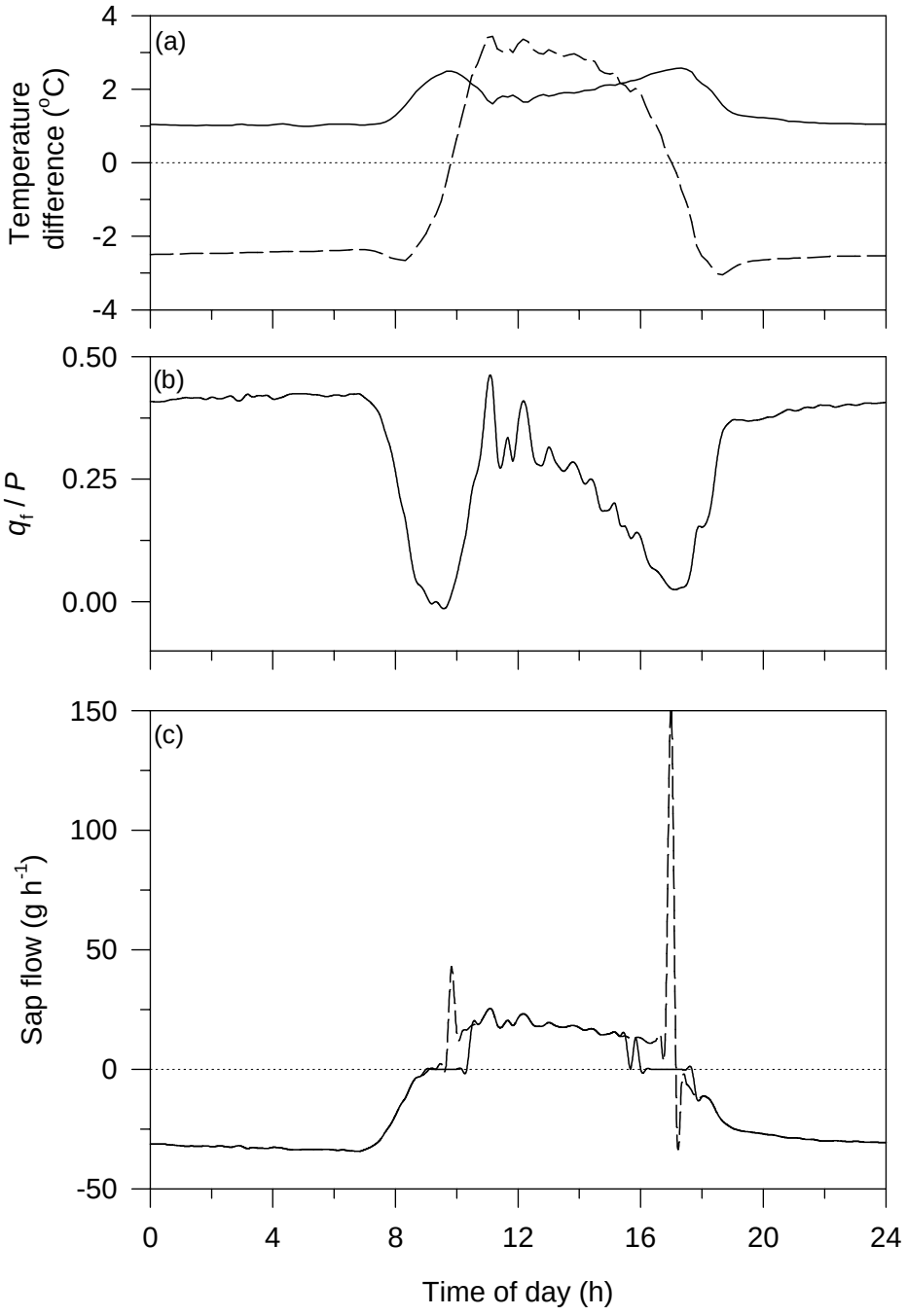

Figure 4.16: Data from a sap flow gauge, installed on a vertical root of *G. robusta*, recorded on December 13, 1996: (a) (ΔT_b-ΔT_a) (———) and ΔT (– – –), where ΔT=(ΔT_a+ΔT_b)/2; (b) the ratio of heat absorbed by the moving sap stream (q_f) to the power supplied to the gauge heater (P); (c) rates of sap flow, before (– – –) and after (———) filtering of data from the period of transition between positive and negative flow, where positive flow was towards the trunk.

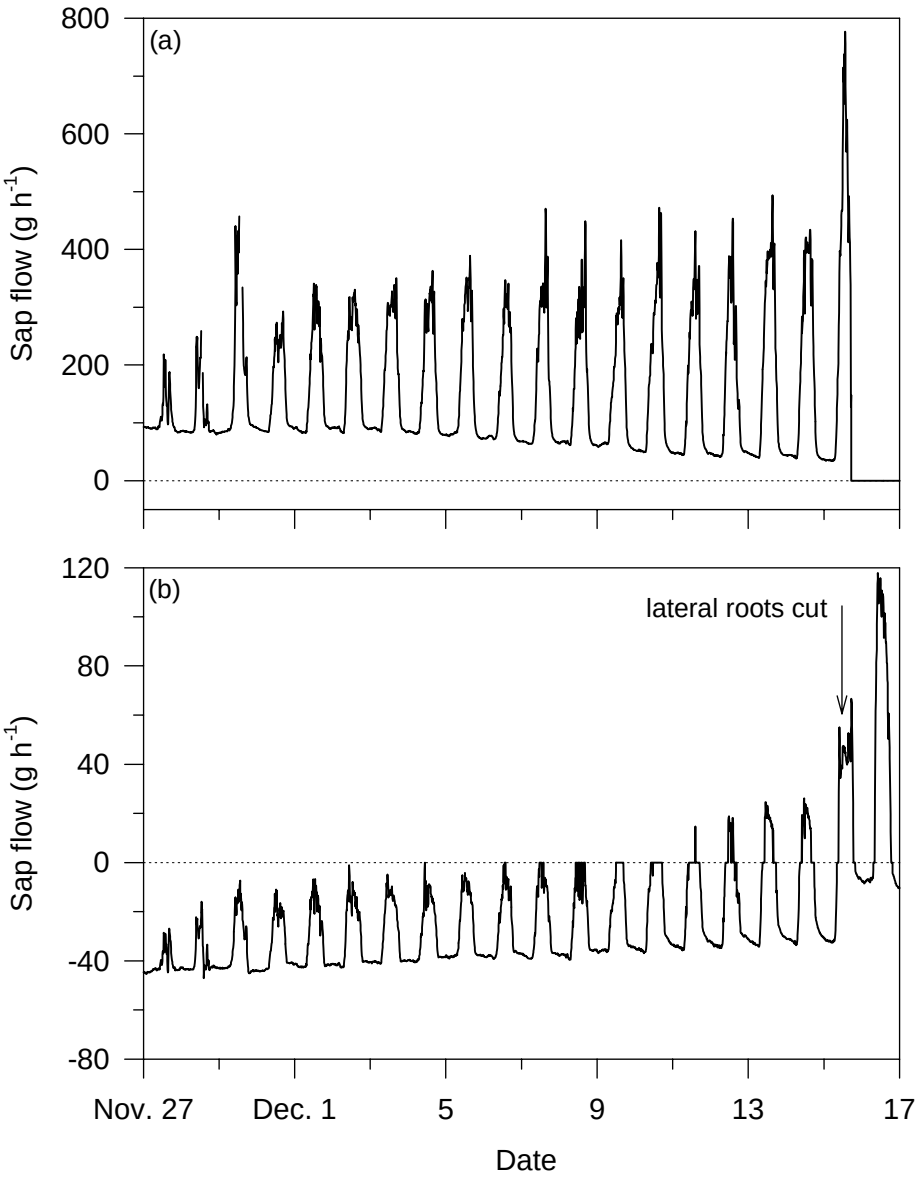

Figure 4.17: Sap flow in (a) a 30-mm diameter lateral root of *G. robusta* and (b) a 15-mm diameter vertical root during Installation 1; positive flow was towards the trunk. All lateral roots of the tree were cut on December 15.

Figure 4.18 shows profiles in soil water potential (ψ_s) during Installation 1. At the start of the period, because the rains had been insufficient to wet the whole profile, there was a strong gradient in ψ_s between the wet surface and drier soil below 0.4 m. Thus, the downward flow of water observed in the vertical root appears to have resulted from the transfer of water, after uptake by lateral roots, along a gradient in ψ_s between the surface layer and drier soil at the bottom of the profile. This is the process of downward siphoning of water by roots; it is the opposite to 'hydraulic lift', which has been observed previously (Richards and Caldwell, 1987; Caldwell and Richards, 1989; Dawson, 1993) and results

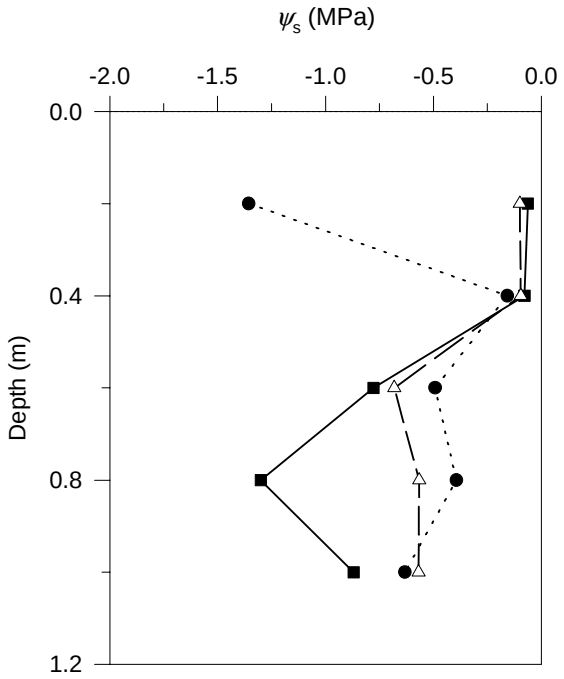

Figure 4.18: Profiles of total soil water potential (ψ_s) on November 28 (■) and December 5 (◬) and 12 (●), 1996, during Installation 1 of sap flow gauges on roots.

in the transfer of water through root systems into dry soil near the surface from more moist soil below.

Downward siphoning of water at night was apparently supplied by nocturnal uptake of water by lateral roots, although some of this uptake may have re-filled storage capacity in the trunk. Prior to December 6, downward siphoning continued throughout the day, indicating that a proportion of the transpiration stream was diverted down into vertical roots. The decline in reverse flow in the vertical root over subsequent days and nights occurred as the surface dried after rainfall ceased on November 29 and the sub-surface layers became wetter, causing the gradient in ψ_s to gradually weaken (Fig. 4.18).

4.5.3 *Sap flow in roots at the onset of the rainy season*

Sap flow in a *G. robusta* root system at the end of the dry season and the effects of the first rains of the wet season on the dynamics of water uptake are shown in Fig. 4.19. Prior to the storm on March 30, rates of sap flow were low in both the vertical and lateral root, with higher uptake by the vertical root, probably because most soil water was available from between the depths of 0.6 and 1.2 m (Fig. 4.20). Within approximately 12 h of the initial wetting of the soil surface by rain, which began near midday on March 30, these patterns of sap movement changed markedly. Uptake of water by the lateral root increased rapidly, quickly exhibiting the same pattern of sap flow seen in the lateral root during Installation 1; rates of sap flow peaked during the day but uptake continued

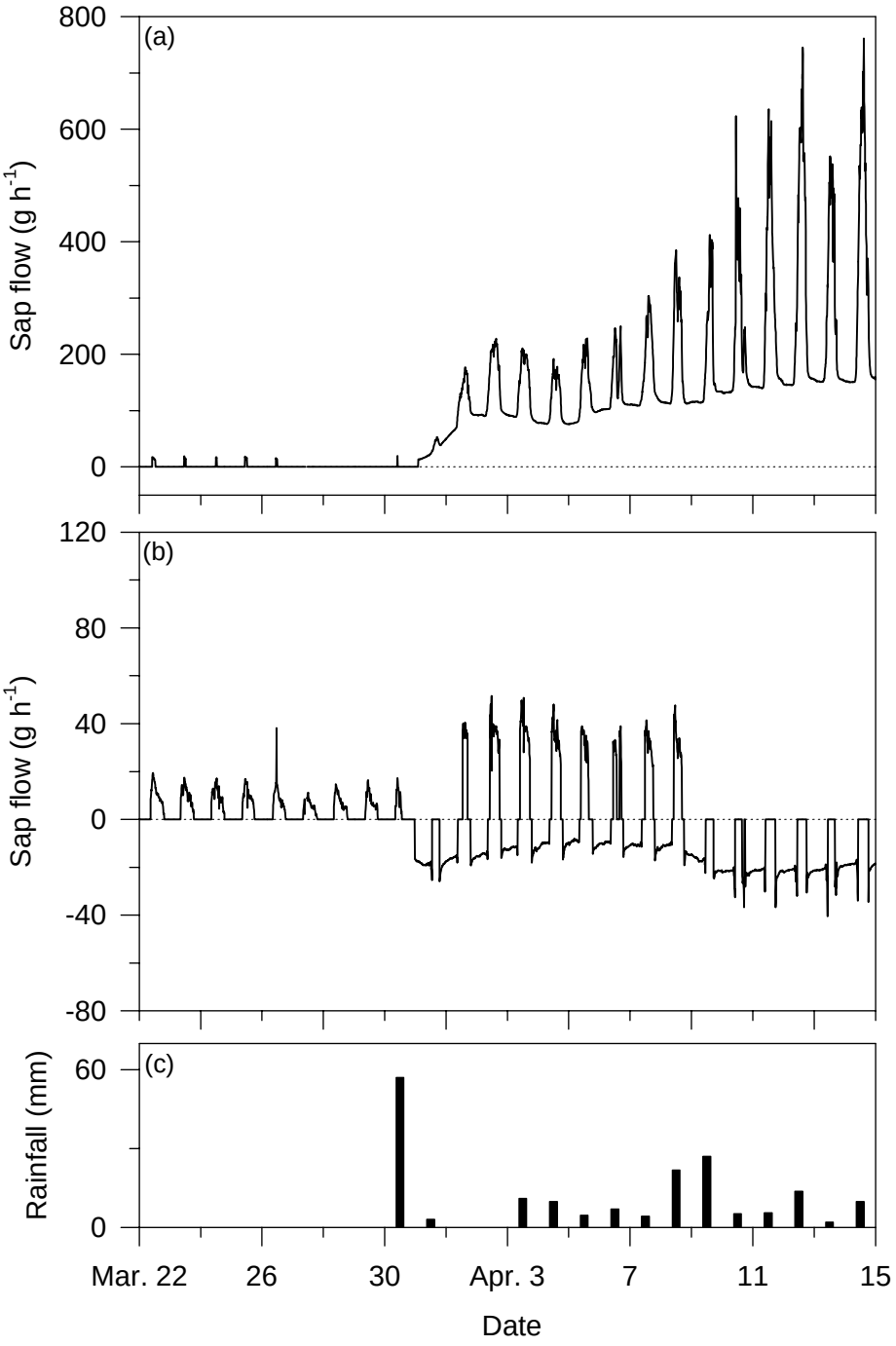

Figure 4.19: Sap flow in (a) a 17-mm diameter lateral and (b) a 28-mm diameter vertical root of *G. robusta* during Installation 2; positive flow was towards the trunk. Rainfall over the period is shown in (c).

throughout the night. In the vertical root, sap flow reversed direction during the night, although negative flow always ceased during the day.

Thus, when the first rains after a long dry period wetted the soil surface and created a vertical gradient in ψ_s (Fig. 4.20), the root system of the tree quickly began siphoning water downwards from the surface. The gradient in ψ_s was about one order of magnitude smaller than during Installation 1, however, and so rates of downward flow in the vertical root were lower in this instance and reverse flow did not continue during the day.

4.5.4 *Uptake of water from soil with a uniform water potential*

Prior to June 24 during Installation 3, total water potential of the soil near the tree instrumented with sap flow gauges was approximately uniform at all depths (Fig. 4.21). Under these conditions, there was substantial uptake of water during the day by all of the gauged roots of the tree, regardless of whether they were lateral or vertical roots (Fig. 4.22). Measurable sap flow did not occur in any of the roots overnight. This indicates that *G. robusta* has a capacity to utilise water from any depth in the soil profile when it is available.

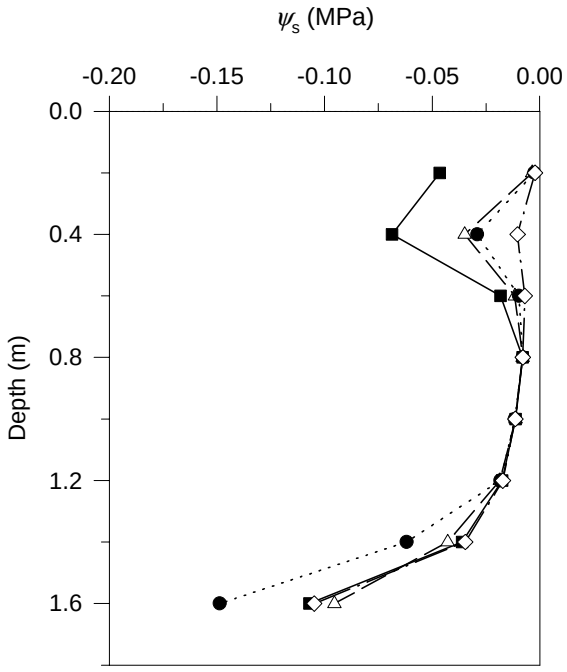

Figure 4.20: Profiles of total soil water potential (ψ_s) on March 27 (■), March 31 (⌓), April 6 (●) and April 9 (◇), 1997, during Installation 2 of sap flow gauges on roots.

4.5.5 *Sap flow in roots after irrigation of the soil surface*
Wetting of the soil by irrigation during Installation 3 was mostly confined to the top 0.3 m of the profile (Fig. 4.21) and the gradient in ψ_s created was small, because soil below this level had retained considerable amounts of water after the recently concluded long rains. The gradient in ψ_s was, however, sufficient to induce changes in the pattern of sap movement (Fig. 4.22): during the nocturnal periods following irrigation between June 24 and 26, uptake of water by the near-surface lateral continued and sap flow was negative in both the sub-surface lateral and the vertical roots. Wetting of the top of the soil profile thus caused downward siphoning of water by the tree, although the rates of downward flow were low because the gradient in soil water potential was small.

4.5.6 *Effects of downward siphoning on the soil water balance*
Approximation of rates of sap flow in whole root systems can be attempted by extrapolating from sap flow in single roots on the basis of the cross-sectional area of roots at the base of the trunk. When sap flow measured in Installation 1 was extrapolated to the whole root system on this basis, using root cross-sectional areas in Table 3.2, the mean proportion of water taken up by lateral roots each day that was diverted downwards into vertical roots was 0.26. During Installations 2 and 3, rates of flow in vertical roots were lower and so this fraction was smaller.

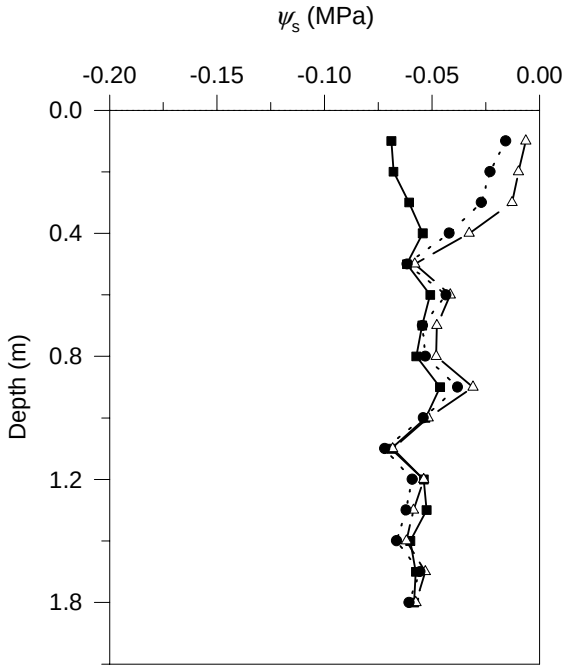

Figure 4.21: Profiles of total soil water potential (ψ_s) on June 18 (■), 26 (△) and 29 (●), 1997, during Installation 3 of sap flow gauges on roots.

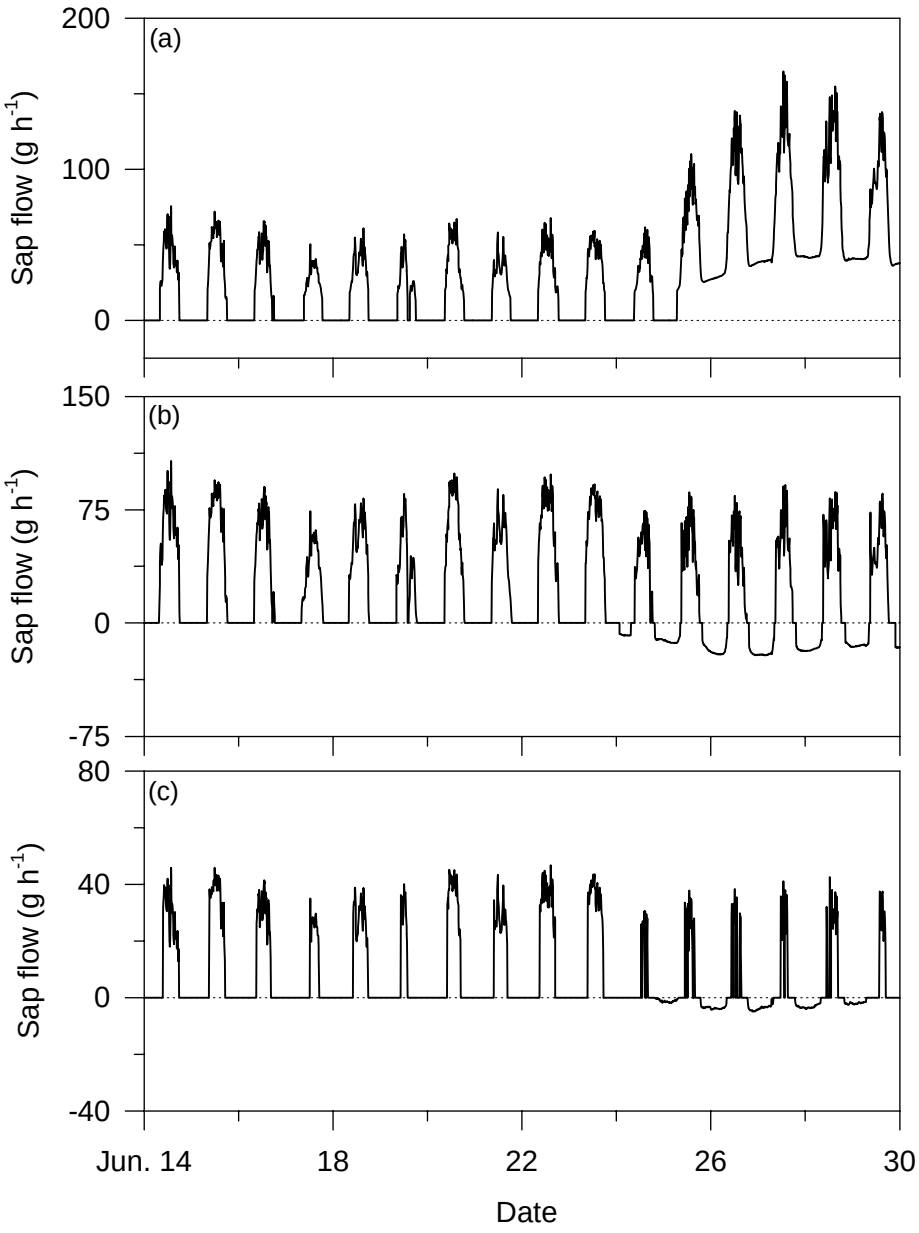

Figure 4.22: Sap flow in (a) an 18-mm diameter near-surface lateral, (b) a 29-mm diameter sub-surface lateral and (c) a 22-mm diameter vertical root of *G. robusta* during Installation 3; positive flow was towards the trunk.

Such estimates likely contain large uncertainties, however, because of variation in the lengths of each major root exposed to different water potentials in each soil layer. Thus, to properly quantify the influence of downward siphoning on soil water balances, sap flow must be measured in more roots of each tree than was possible in this study. The observed rates of downward flow in roots indicate, however, that downward siphoning may be a substantial component of the soil water balance where vertical gradients in soil water potential are large. Emerman & Dawson (1996) reached a similar conclusion for hydraulic lift, as they estimated that approximately 20 percent of daily uptake by an *Acer saccharum* tree was transferred to surface soil layers by reverse flow.

4.5.7 *Implications of downward siphoning for agroforestry*

Downward siphoning may have important consequences for interactions between trees and neighbouring crops. Emission of water into soil may result in the storage of water, if it can be re-extracted at a later time, below the maximum rooting depth of crops. Storage of water in this way would enhance the competitiveness of trees, by increasing their ability to capture water resources while reducing the availability of water to crops.

At sites in arid or semi-arid regions where deep-rooted trees or shrubs utilise groundwater, downward siphoning may enable roots to grow down through dry soil layers to the water table. Downward siphoning may therefore be an important adaptation allowing juvenile phreatophytic plants to make the transition from reliance on seasonal rainfall to exploitation of groundwater (Caldwell *et al*., 1998). Downward siphoning may contribute, consequently, to the success of agroforestry systems in which tree and crop water use is complementary because of use of groundwater by the trees (Smith *et al*., 1997).

Like downward siphoning, Caldwell *et al*. (1991) suggested that hydraulic lift enables plants to store water for later use, when transpirational demand cannot be met by the sparse root network in the subsoil. In contrast to downward siphoning, however, hydraulic lift also makes water available to shallow-rooted neighbours (Corak *et al*., 1987; Caldwell and Richards, 1989; Dawson, 1993), creating a form of parasitism in which water resources captured by one species are transferred to competitors (Caldwell *et al*., 1991). While downward siphoning may enhance the competitiveness of deep-rooted trees, therefore, the opposite process, hydraulic lift, may improve the competitive ability of neighbouring crops.

Downward siphoning should tend to reduce the extent to which the patterns of water uptake by crops and trees such as *G. robusta* are thought to be complementary (Lott *et al*., 1996; Howard *et al*., 1997), as it results in the transfer resources away from zones that are accessible to crops. The competitiveness of trees would, however, be reduced if the availability of water to crops was enhanced by hydraulic lift, (Emerman & Dawson, 1996). Thus, while hydraulic lift might allow a higher density of trees to be grown without deleterious effects on crops, it could be necessary, for example, to increase the spacing between trees in agroforestry in conditions where downward siphoning may be substantial.

4.5.8 *Competition and complementarity for water between* G. robusta *and crops*

When most water was available from near the soil surface, water used by *G. robusta* was taken up primarily by lateral roots (Figs. 4.17, 4.19 and 4.22), with some water diverted

by downward siphoning. Thus, *G. robusta* competes strongly with crops when the wettest part of the soil coincides with the rooting zone of the crop. When the distribution of water in the soil was more uniform, however, the degree of complementarity in water use by the trees and crop was enhanced because the trees then obtained some water from below the rooting zone of the crop (Fig. 4.22, prior to June 24). When the top of the profile was drier than underlying layers of soil, as it was prior to March 30 in Installation 2, uptake of water was dominated by the activity of vertical roots (Fig. 4.19); complementarity in water use by *G. robusta* and crops is maximised, therefore, when most water is available from below the rooting zone of the crop. Thus, the severity of competition, or the extent of complementarity, for water between *G. robusta* and adjacent crops is dependent on the distribution of soil water rather than the distribution of tree roots.

A dimorphic root system, one with both lateral and vertical roots, enables *G. robusta* to utilise water from below the rooting zone of crops, but it competes with crops if water is available from shallower depths. Lott *et al*. (1996) severed the lateral roots of a *G. robusta* tree and concluded that it was complementary with crops in use of water because uptake then continued through intact vertical roots. However, as water from near the soil surface was no longer available to the tree because the lateral roots had been severed, they demonstrated only that *G. robusta* has the capacity for complementarity in water use. Measurements of sap flow in roots made for this study demonstrate that this capacity is fulfilled by *G. robusta* only if the subsoil has a higher potential than soil near the surface. If most water is available from shallow soil depths, *G. robusta* competes with crops.

This conclusion is consistent with the idea that plants utilise water first from soil with the highest water potential, to ensure that they can maintain as high leaf water potentials as possible. This repudiates the notion that there are trees with dimorphic root systems that are ideally adapted to agroforestry because they are able to preferentially utilise water from below the rooting zone of the crop. Without evidence for a mechanism enabling trees to activate and de-activate portions of dimorphic root systems, such a notion is fanciful.

4.6 Hydraulic Conductivities of *Grevillea robusta* and Maize Roots

Hydraulic conductances for roots of *G. robusta* measured with the HPFM are plotted in Fig. 4.23(a) against the length of each root recovered by excavation, which was determined by digital image analysis. As lengths of individual roots determined in this way are inevitably underestimates of true root lengths, because much of each root remains in the soil, Fig. 4.23(a) does not give an accurate indication of the relationship between hydraulic conductance and root length.

Much better estimates of the true lengths of these roots were obtained using the fractal branching model, as described in Section 4.4, because the model was calibrated against the results of soil coring. Hydraulic conductances in Fig. 4.23(a) are re-plotted in Fig. 4.23(b), together with data from other roots which were not excavated, against root lengths estimated using the fractal method. These are root lengths for ordinary, non-proteoid roots. Correction of root lengths for errors caused by excavation reduces the slope of the relationship between conductance and root length. This slope is the hydraulic conductivity, κ_r, of roots of *G. robusta*; the mean value of κ_r for the data in Fig. 4.23(b) is given in Table 4.12.

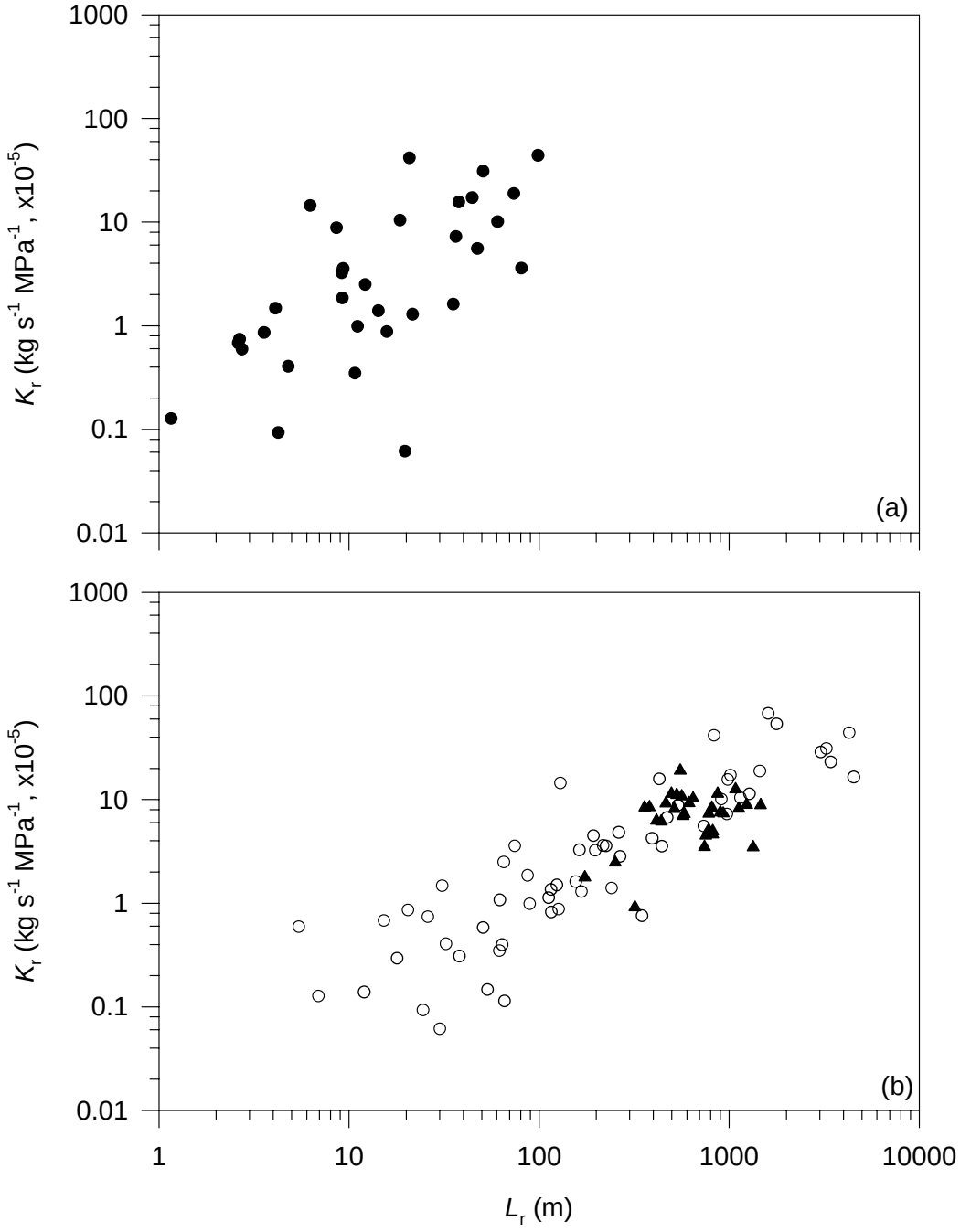

Figure 4.23: (a) Hydraulic conductances (K_r) for roots of *G. robusta* plotted against root length (L_r) recovered by excavation. (b) K_r for *G. robusta* roots plotted against L_r estimated from the recursive branching algorithm and the effective link length (○); K_r for maize root systems (▲).

Table 4.12: Mean values of the hydraulic conductivity (κ_r), on a root length basis, determined for *G. robusta* and maize.

Species	κ_r (kg s^{-1} MPa^{-1} m^{-1})	±se (kg s^{-1} MPa^{-1} m^{-1})
G. robusta	1.91×10^{-7}	0.27×10^{-7}
maize	1.24×10^{-7}	0.13×10^{-7}

Hydraulic conductances for maize roots measured using the HPFM are also plotted in Fig. 4.23(b). In the case of maize, root lengths were estimated by extrapolating from soil coring to root length per plant, as described in Section 3.3.3. The mean value of κ_r derived from these data is given in Table 4.12.

4.7 Performance of Model of Water Uptake in Agroforestry

4.7.1 *Parameterisation of the uptake model*

The data used to parameterise the model are given in Appendix B, together with a listing of the model code. Wherever possible values measured during the CIRUS experiment were used for input data.

4.7.2 *Model output*

The model calculates hourly leaf water potentials (ψ_l) and mean soil water potentials (ψ_s), weighted by root and soil resistances, for both trees and crop plants. Daily uptake by each species from each compartment of the flow domain of the model is also computed, which allows calculation of the ratio of uptake by the tree (q_r^t) to uptake by the crop (q_r^c), which can be called the 'uptake partitioning ratio'.

The model was run for three scenarios, each with a different distribution of soil water. These were: (i) initially uniform volumetric soil water content (θ_v) of 0.20 m^3 m^{-3}; (ii) initial θ_v of 0.20 m^3 m^{-3} for depths of 0-0.4 m and 0.15 m^3 m^{-3} for 0.4-1.6 m; and (iii) initial θ_v of 0.15 m^3 m^{-3} for 0-0.4 m and 0.20 m^3 m^{-3} for 0.4-1.6 m.. In each case, the soil profile was assumed to be composed of a single horizon with the moisture retention characteristics plotted in Fig. 4.24, which were measured for the sub-surface horizon at the CIRUS site. The distribution of tree and crop roots used is shown in Fig. 4.25; the root length densities are representative of those measured at the CIRUS site for *G. robusta* and a maize crop at anthesis in CT_d plots during a season with poor rains. Only ordinary, non-proteoid roots of *G. robusta* are considered. Any effects of proteoid rootlets on water uptake are thus assumed to be the same for all compartments of the flow domain and proportional to lengths of ordinary roots, a reasonable assumption as proteoid rootlets are thought to be important for the uptake of non-mobile nutrients such as phosphorus, rather than a mobile substance such as water (Skene *et al*., 1996). Values of E_v, the transpiration rate possible without limitation by leaf water potential, for the simulations were set at 2.0 mm d^{-1} for the trees and 1.5 mm d^{-1} for the crop, which are typical of rates of

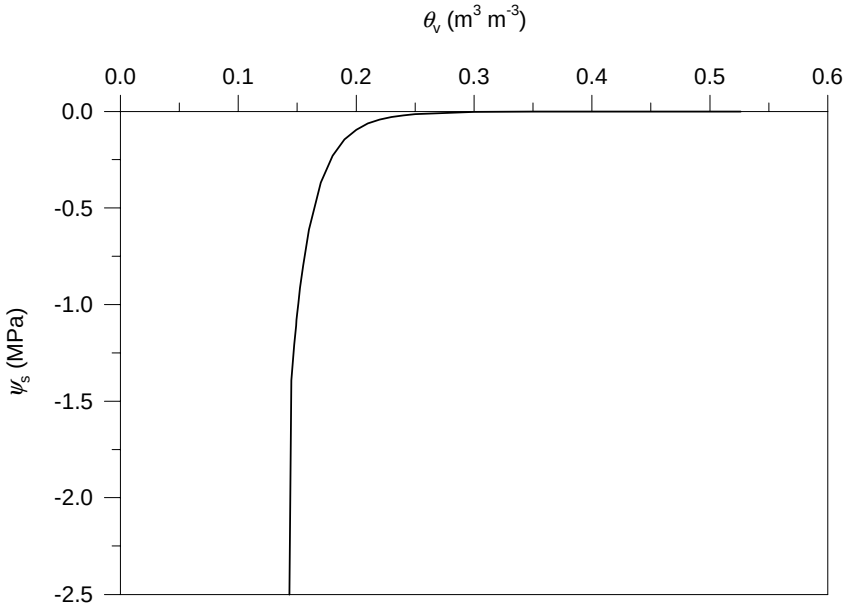

Figure 4.24: Moisture retention curve for the sub-surface horizon at the CIRUS site (see Wallace *et al.*, 1995)

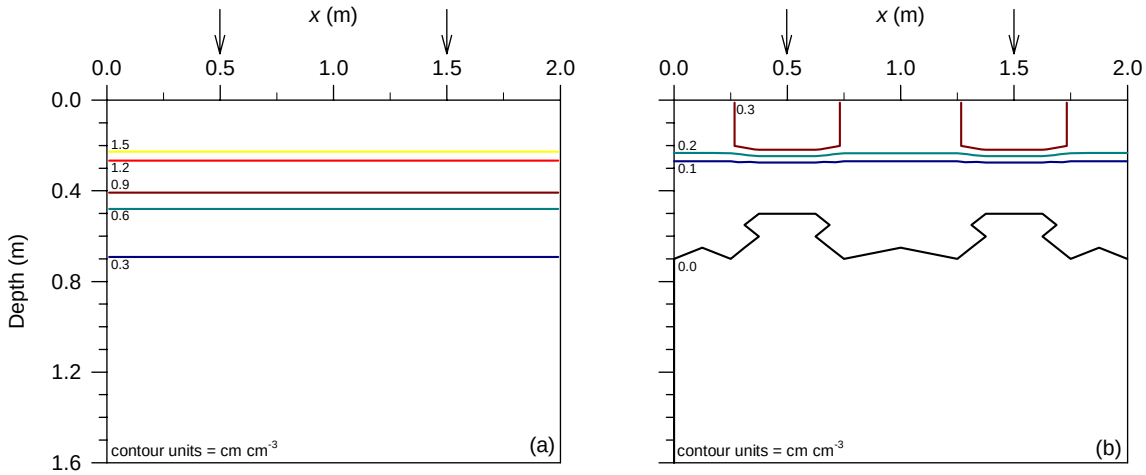

Figure 4.25: Contour plot of root length densities for (a) the tree and (b) the crop used in simulations of water uptake by roots in agroforestry. *x* is the distance from the base of the tree and the arrows mark the positions of crop plants. Values for the contours are labelled; the colours highlight the different lines.

transpiration measured at the site by Lott *et al*. (1997). Simulations of uptake under the three scenarios were made for periods of 14 days.

With initially uniform θ_v, there was a gradual decline in the midday minimum ψ_l for the crop that was eventually sufficient to limit transpiration (Fig. 4.26). The decline in ψ_l for the tree was not sufficient to limit transpiration. On the second day of the simulation, the highest rates of extraction by the crop occurred from near the soil surface, below the plant stems (Fig. 4.27(d)), where root length densities were highest. The tree extracted water more uniformly from the entire soil volume, although small negative values of uptake were computed for the top 0.1 m of the soil profile (Fig. 4.27(c)). Such negative values indicate reverse flow in roots; here, they are indicative of hydraulic lift resulting from a gradient in soil water potential created by faster drying of soil near the surface (Fig. 4.27(b)). Partitioning ratios (q_r^t/q_r^c) of between 0 and -0.5 occurred at the top of the profile (Fig. 4.27(e)), suggesting some facilitation of crop water use by hydraulic lift in the tree root system. Below the surface layer of soil, however, uptake was dominated by the trees (Fig. 4.27(e)).

With the top of the profile initially wetter than the subsoil, water available to the crop was quickly depleted, causing transpiration by the crop to decline rapidly (Fig. 4.28(a)). Values of ψ_l for the crop thus approached a minimum value (Fig. 4.28(b)). Transpiration by the tree also declined, but less rapidly (Fig. 4.28(a)), as water below the rooting zone of the crop was available to the tree. On the second day of the simulation, the pattern of uptake by the crop was similar to that computed for initially uniformly wet soil, with uptake highest where most roots were present (Fig. 4.29(d)). However, uptake by the tree was concentrated where most water was present, between depths of approximately 0.1 and 0.6 m (Fig. 4.29(c)). The ratio q_r^t/q_r^c was consequently >1 for almost the entire soil volume (Fig. 4.29(e)), indicating that the tree was more successful at capturing water resources. The rapid decline in crop transpiration, which would cause severely impaired growth and productivity of the crop, was therefore hastened by depletion of water resources by the tree. Thus, the model predicts that where most soil water is present near the surface, competition for water has a severe impact on the crop.

A further feature of the model output in Fig. 4.29(c), is that downward siphoning by the tree root system was simulated. Negative values of uptake were computed for the tree below ~0.8 m, indicating that where vertical gradients in soil water potential occur, water is transferred from a wetter surface layer to drier subsoil by root systems, a prediction supported by measurements of sap flow in roots under such conditions (Section 4.5).

In the final scenario, most soil water was present below 0.4 m. Crop transpiration was limited by ψ_l (Fig. 4.30) and uptake by the crop was from the surface layer of the soil (Fig. 4.31(d)). The model predicts, however, that under these conditions, water use by the crop is almost entirely facilitated by hydraulic lift by the tree root system, as uptake by the trees from the subsoil was computed together with high rates of emission of water into soil above depths of ~0.3 m (Fig. 4.31(c)). It is not possible to judge how realistic this simulation is for the system studied in the CIRUS trial, as conditions where the subsoil was at a much higher potential than the top of the profile were not encountered during the project. However, such conditions would likely occur frequently at semi-arid sites with groundwater accessible to tree roots and Dawson (1993) demonstrated that facilitation of

water use by shallow-rooted does occur in the field as a result of hydraulic lift by nearby,

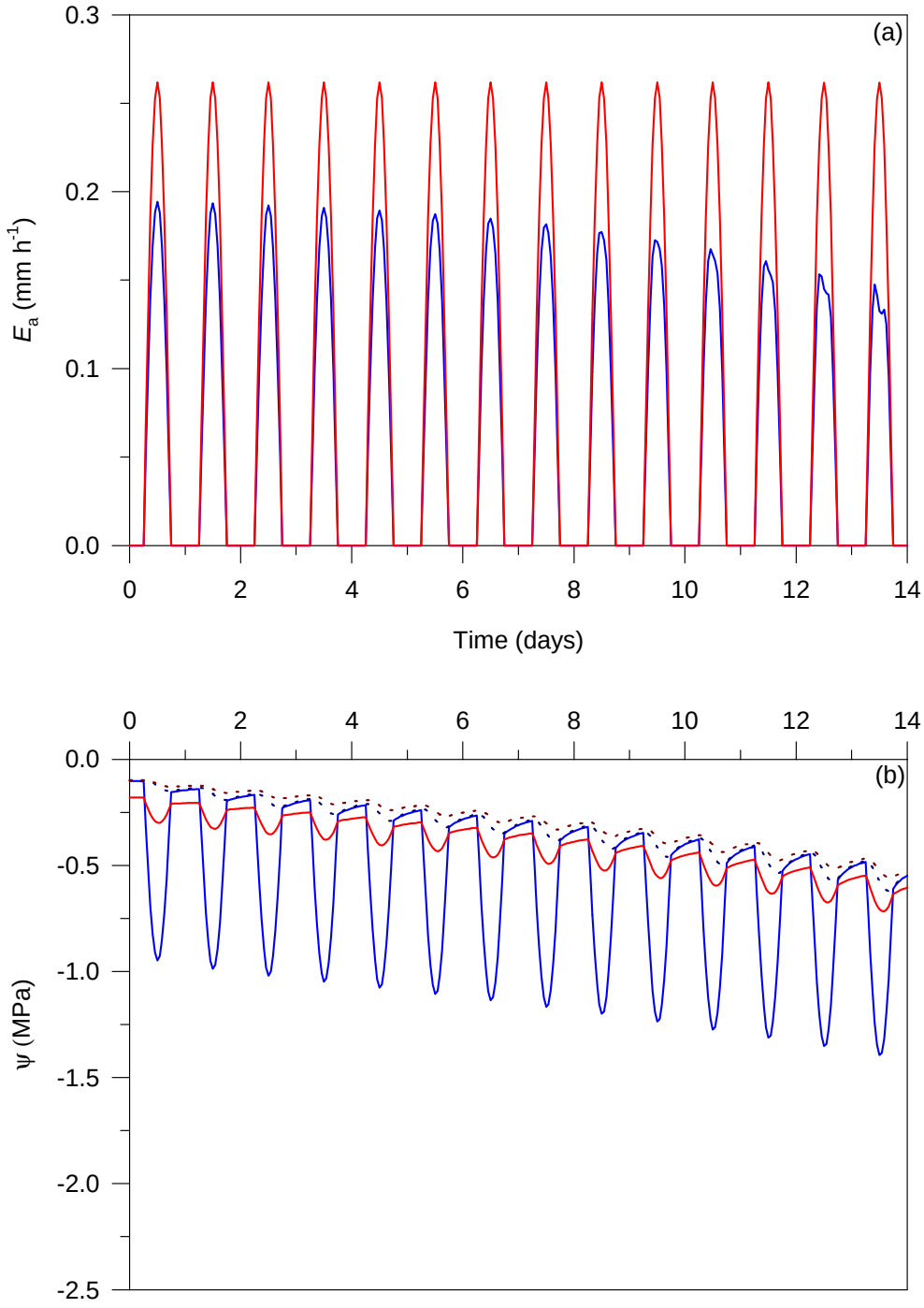

Figure 4.26: Output from the model of water uptake by trees and crops in agroforestry, for initially uniform soil water distribution: (a) simulated transpiration (E_a) by the tree (red line; maximum rate = 2.0 mm d^{-1}) and crop (blue line; maximum rate = 1.5 mm d^{-1}); (b) simulated water potentials (ψ) of leaves (solid lines) and soil (dashed lines) for the trees (red) and crop (blue). The soil water potentials are weighted means (see text).

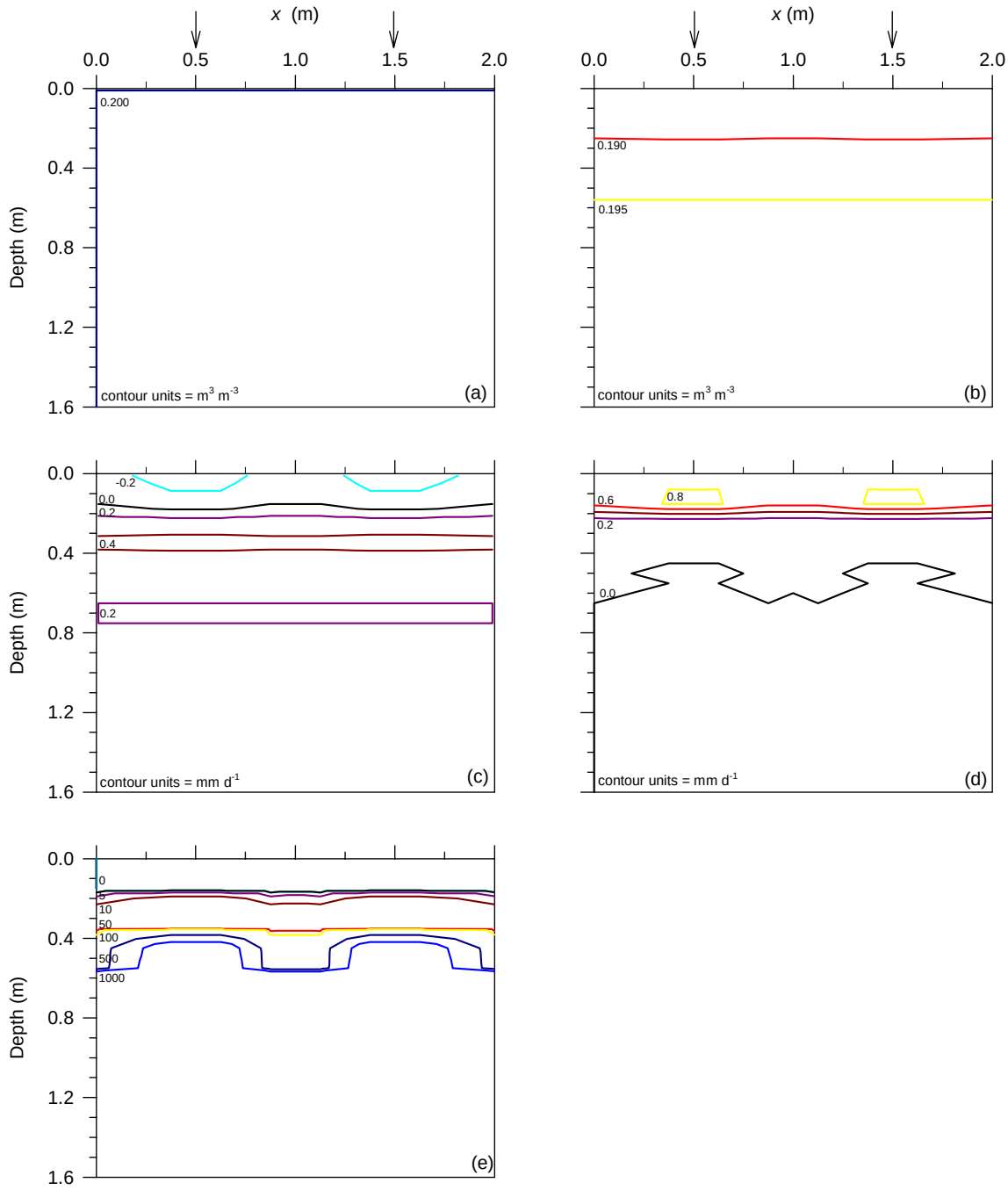

Figure 4.27: Contour plots from the simulation of water uptake by trees and crop plants from soil with an initially uniform distribution of water: (a) the initial volumetric soil water distribution; (b) soil water distribution after 2 d; (c) water uptake by trees roots on the second day (q_r^t); (d) water uptake by crop roots on the second day (q_r^c); and (e) the partitioning ratio (q_r^t/q_r^c). *x* is the distance from the base of the tree and the arrows mark the positions of crop plants. Values for the contours are labelled; the colours highlight the different lines.

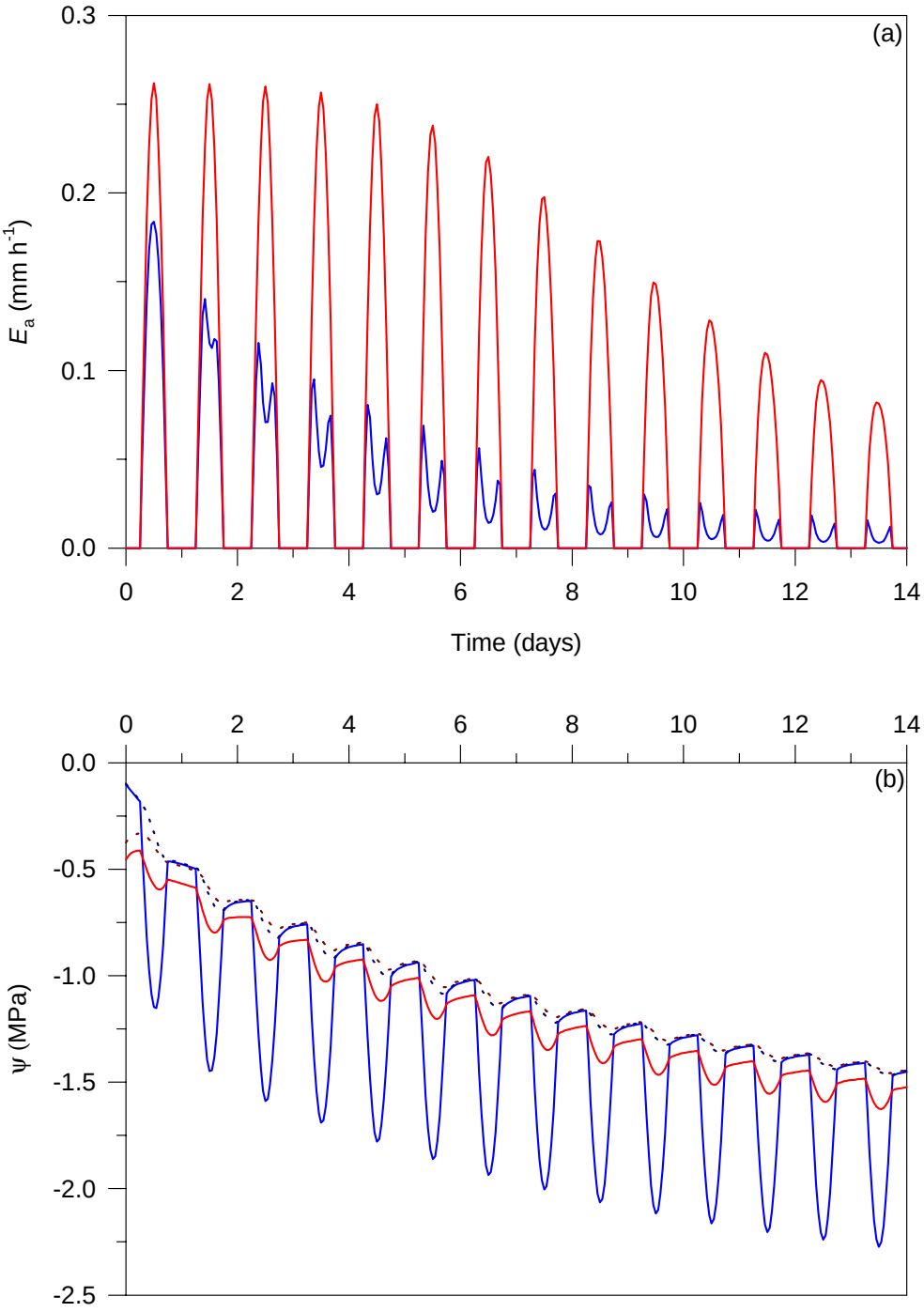

Figure 4.28: Output from the model of water uptake by trees and crops in agroforestry, for soil initially wettest above the depth of 0.4 m: (a) simulated transpiration (E_a) by the tree (red line; maximum rate = 2.0 mm d^{-1}) and crop (blue line; maximum rate = 1.5 mm d^{-1}); (b) simulated water potentials (ψ) of leaves (solid lines) and soil (dashed lines) for the trees (red) and crop (blue). The soil water potentials are weighted means (see text).

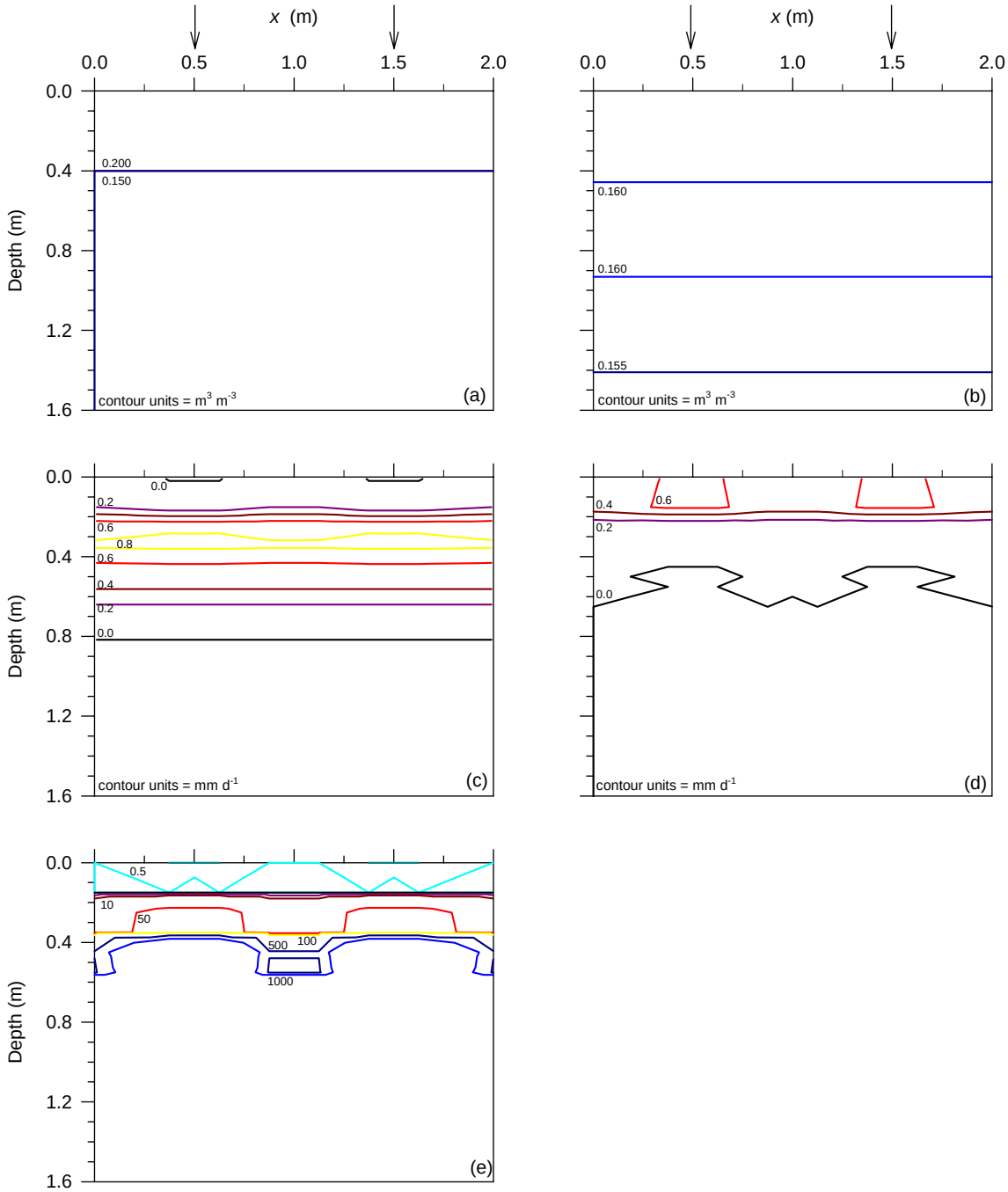

Figure 4.29: Contour plots from the simulation of water uptake by trees and crop plants from soil that was initially wettest above the depth of 0.4 m: (a) the initial volumetric soil water distribution; (b) soil water distribution after 2 d; (c) water uptake by trees roots on the second day (q_r^t); (d) water uptake by crop roots on the second day (q_r^c); and (e) the partitioning ratio (q_r^t/q_r^c). x is the distance from the base of the tree and the arrows mark the positions of crop plants. Values for the contours are labelled; the colours highlight the different lines.

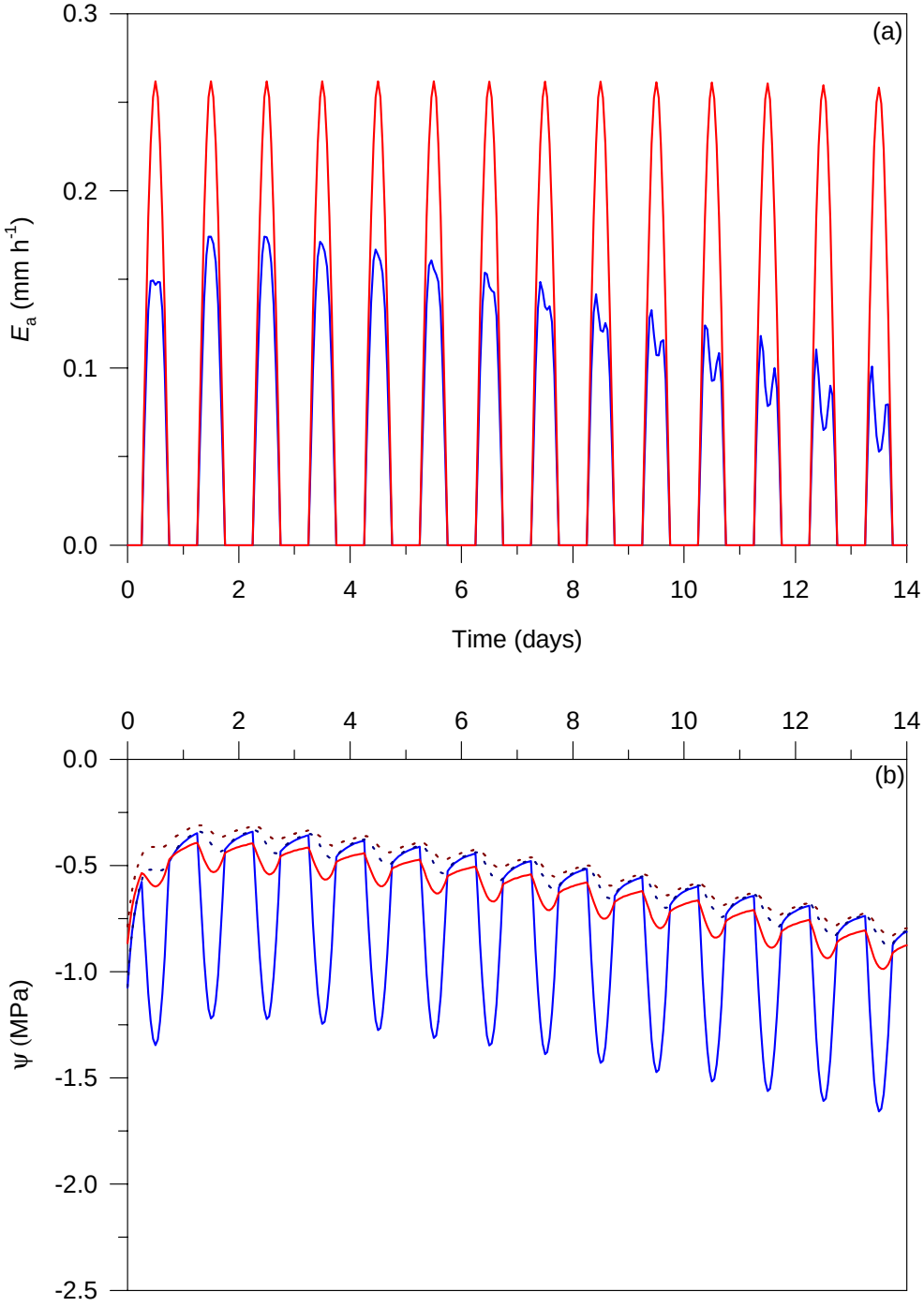

Figure 4.30: Output from the model of water uptake by trees and crops in agroforestry, for soil initially wettest below the depth of 0.4 m: (a) simulated transpiration (E_a) by the tree (red line; maximum rate = 2.0 mm d^{-1}) and crop (blue line; maximum rate = 1.5 mm d^{-1}); (b) simulated water potentials (ψ) of leaves (solid lines) and soil (dashed lines) for the trees (red) and crop (blue). The soil water potentials are weighted means (see text).

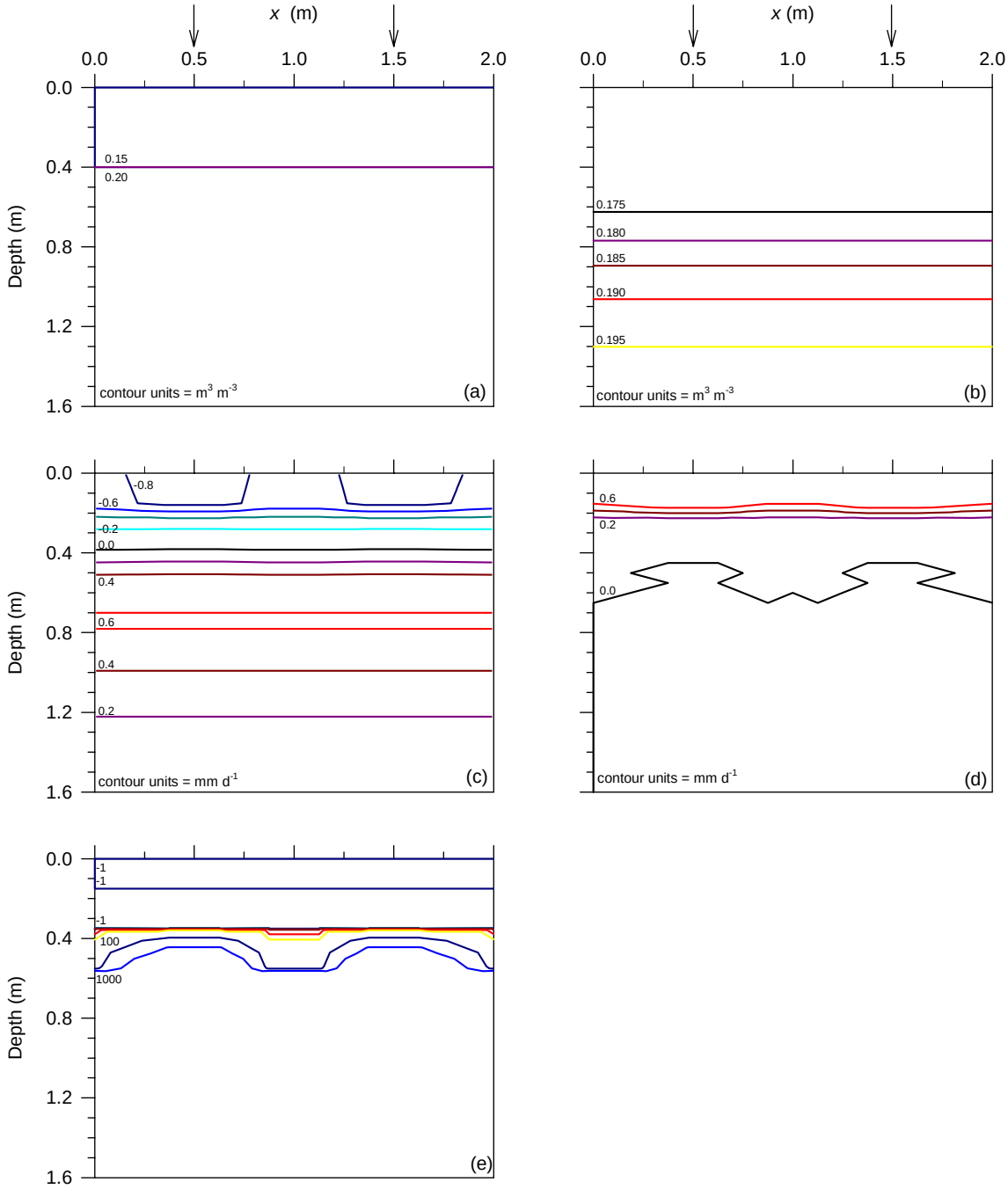

Figure 4.31: Contour plots from the simulation of water uptake by trees and crop plants from soil that was initially wettest below the depth of 0.4 m: (a) the initial volumetric soil water distribution; (b) soil water distribution after 2 d; (c) water uptake by trees roots on the second day (q_r^t); (d) water uptake by crop roots on the second day (q_r^c); and (e) the partitioning ratio (q_r^t/q_r^c). x is the distance from the base of the tree and the arrows mark the positions of crop plants. Values for the contours are labelled; the colours highlight the different lines.

deep-rooted trees. Thus, the role of hydraulic lift in tree-crop interactions in agroforestry is a subject that demands further research.

4.7.3 *Simulation of competition, complementarity and reverse flow phenomena*
A key feature of the model is that it is capable of predicting the spatial extent of competition or complementarity between trees and crops for water. Where the ratio q_r^t/q_r^c is >1 for all of the flow domain, competition between the tree and crop is severe, as water available to the crop is then depleted by the tree. Where there are distinct zones with $q_r^t/q_r^c>1$ and q_r^t/q_r^c of ~0, water use by the tree and crop are complementary.

A further feature of the model is its ability to predict downward siphoning and hydraulic lift, known in general terms as 'reverse flow phenomena'. No specific allowance was made in the design of the model for this; rather, by representing the root systems of the tree and crop as physically-realistic networks of resistances to flow, reverse flow results when gradients in water potential occur between soil regions interconnected by roots. However, as study of the water relations controlling reverse flow phenomena is only now becoming possible through the use of sap flow instrumentation on roots (Smith *et al*., 1998), it is not certain whether such a representation of root systems in models is sufficient where reverse flow occurs. In particular, it is possible that an additional resistance is encountered during reverse flow in roots, perhaps as a result of water crossing interstitial tissue between xylem vessels conducting water towards the stem and those conducting water towards the root tips. Additional research is required to resolve this question, as well as other issues causing uncertainty, such as the movement of water away from roots after emission into soil.

4.7.4 *Testing of the model*
The model has yet to be properly tested against measured data from the field. However, there are data available from this project and the study of the soil water balance (R6364) that will enable completion of this task. Total uptake of water from the different regions of the soil can be calculated from measurements of soil water content and the partitioning ratio estimated on the basis of measured leaf water potentials, root lengths and conductivities. These values can then be compared with output from the model.

4.7.5 *Assumptions and simplifications in the model*
The present version of the model of water uptake incorporates many simplifying assumptions. For example, there is no provision for water storage in either the tree or crop plants; stem resistance is constant and there is thus no representation of cavitation of xylem vessels when water potentials become very low; differences in atmospheric coupling between the tree and crop do not affect changes in transpiration resulting from stomatal responses to leaf water potential; and possible effects on stomatal behaviour of osmotic adjustment and chemical signalling from roots in response to soil drying are not included. Future versions of the model could include representations of these effects on uptake and partitioning.

Other processes associated with roots and uptake of water are also not included in the model. These have been excluded because there is not currently sufficient information available on how and when they operate, especially in the field. Of particular importance are osmotic effects on water uptake by roots and the dependency of the hydraulic conductivities of roots on fluxes when uptake is driven by a combination of osmotic and

hydrostatic gradients in potential (Steudle, 1994). In addition, the importance of an interfacial resistance to water movement at the point where soil and root make contact (Tinker, 1976; Stirzaker and Passioura, 1996) is under debate. However, as the model is based on physical principles, as more is learned about other important processes controlling uptake of water by roots, incorporation of them into the present model will be possible.

4.7.6 *Future development of the model*

Future versions of the model will be written to enable use of the model as the uptake component of larger models integrating other important processes in agroforestry, such as modification of the soil water balance and microclimate, and plant growth and development. As such models are being developed with increasing frequency using a modularised approach to programming, a version of the model should be developed in a modelling environment such as STELLA, which will enable it to be used easily as a module of larger models.

When incorporated into a more comprehensive model of tree-crop interactions in agroforestry, it will be possible to simulate the effects on competition and partitioning of water resources of, for example, changing weather patterns and climate, or growth and development of the trees and crop. It will also enable prediction of the effects of other components of the soil water balance, such as infiltration and soil evaporation, on tree and crop water use.

During incorporation of the uptake model into larger models, it may become necessary to make simplifications to the parameterisation of the processes controlling uptake and partitioning. However, by using the present, physically-based model as a starting point, it will be possible to assess the risks and importance of errors associated with such simplifications.

5. CONTRIBUTION OF OUTPUTS TO DEVELOPMENT

5.1 Progress Towards Development Goals

From its inception, this project was intended to address two objectives of DFID's Forestry Research Strategy. At the purpose level, it was conceived to improve knowledge of below-ground interactions between trees and crops in agroforestry and at the goal level, it was designed to promote the optimisation of the use of trees within farming systems in the semi-arid tropics. The following highlights from the project illustrate ways in which the project has contributed to the achievement of these objectives.

(i) *Maximum root length densities for* G. robusta *are found at the top of the soil profile and the population of roots in the soil is dominated by* G. robusta.

Results from the project thus support contentions by Jonsson *et al*. (1988) and Schroth (1995) that trees and crops used in agroforestry tend to have profiles of root length densities with similar shapes, most roots being found in the surface layer of the soil. As a consequence, competition between trees and crops for water is likely to occur at semi-arid locations, having a severe impact where tree roots are dominant and tree water use is high. Use of water by trees and crops will be complementary *only* where there is a spatially distinct source of water that is available to trees, but not the crop. To optimise the use of trees in farming systems in the semi-arid tropics, therefore, most effort should be given to characterising the availability of below-ground resources from different sources, rather than trying to identify tree species with root distributions that are complementary to those of crops.

As Smith *et al*. (1997) showed for windbreak systems in the Sahel, groundwater provides a spatially-distinct source of water that can result in complementary use of water by trees and crops when it is accessible to tree roots. Where groundwater is not present or not accessible to trees, complementarity between trees and crops for water is likely to occur only if the climate is wet enough for large amounts of water to drain beyond the rooting zone of the crop (van Noordwijk *et al*., 1996). However, McIntyre *et al*. (1997) contended that the latter is unlikely in semi-arid regions.

Where spatially-distinct sources of water are not present, management strategies that enable water use by the trees to be controlled must be used (Schroth, 1995; Smith *et al*., 1998). In designing such strategies, consideration must be given to pruning the canopies of trees and finding configurations and densities of trees that optimise the trade-off between tree-crop competition for water and the benefits of trees for soil conservation, microclimate modification and nutrient cycling. When selecting tree species for use in agroforestry at these sites, the amount of water required by different species should be a more important criterion than any perceived differences in root distribution.

(ii) *Water can be transported downwards, from a wet soil surface to dry subsoil, by tree roots, thus reducing the availability of water to crops.*

Measurement of sap flow in tree roots provided direct evidence, for the first time, of downward siphoning of water by tree roots. This process, like the inverse process of hydraulic lift, has fundamental implications for our understanding of tree-crop interactions in agroforestry. If sufficient quantities of water are transported, the

competitiveness of trees is likely to be strengthened by downward siphoning, but hydraulic lift may facilitate water use by crops. It is possible that these processes are common features of agroforestry in semi-arid regions, as sharp gradients in soil water potential between different soil layers occur frequently in such areas, either because of rainfall infiltrating into a dry soil profile or because of groundwater underlying dry soil. Developing knowledge of downward siphoning and hydraulic lift will consequently be a crucial step in progress towards achieving optimal use of trees on farms in the semi-arid tropics.

This project has provided the first advances necessary to understanding the role of downward siphoning and hydraulic lift in agroforestry. However, additional research must be undertaken to quantify their effects on partitioning of water resources and to determine how they are controlled by physiological and physical mechanisms in the plant and soil. The technical ability to make these determinations is available, as use of techniques for measuring sap flow in roots has shown.

(iii) *Modelling of uptake of water by trees and crops in mixed stands enables the spatial extent of complementarity for water to be assessed quantitatively.*

A physically-based model of partitioning of water between trees and crops was produced and used to simulate the spatial extent of competition or complementarity for water between trees and crops. Although additional testing of the model is required, simulated partitioning was similar to results from measurements of sap flow in roots, including the occurrence of reverse flow in roots. Once testing of the current version has been completed, a version of the model will be developed which can be used as a module of larger models of the soil water balance and growth and productivity in agroforestry. When used in conjunction with a growth model, the uptake model will also allow simulation of the extent of temporal complementarity. Use of the model will enable researchers to develop and test ideas about relationships between the availability of water resources, root distributions and resource partitioning in agroforestry. The model should therefore become a valuable tool in the design of management strategies for optimising the use of trees on farms.

5.2 Dissemination of Results and Plans for Dissemination

Dissemination of results from the project achieved to date are listed below.

5.2.1 *Publications*

Smith, D.M.; Jackson, N.A.; Roberts, J.M. (1997). A new direction in hydraulic lift: can tree roots siphon water downwards? Agroforestry Forum 8(1): 23-26.

Smith, D.M.; Jackson, N.A.; Roberts, J.M.; Ong, C.K. (1998). Reverse flow of sap in tree roots and downward siphoning of water by *Grevillea robusta*. Functional Ecology (*submitted*).

5.2.2 *Internal reports*

Smith, D.M.; Jackson, N.A.; Roberts, J.M.; Wallace, J.S. (1996). Root quantity, activity and below-ground competition in *Grevillea robusta* agroforestry systems: annual report 1995/96. Institute of Hydrology, Wallingford. 20 pp.

Smith, D.M.; Jackson, N.A.; Roberts, J.M. (1997). Root quantity, activity and below-ground competition in *Grevillea robusta* agroforestry systems: annual report 1996/97. Institute of Hydrology, Wallingford. 9 pp.

5.2.3 *Other dissemination of results*

Conference papers

Smith, D.M. (1998). Assessing root system properties. 4th International Workshop on Field Techniques for Environmental Physiology. Almeria, Spain, March 30-April 5, 1998.

Lectures

Smith, D.M. (1996). Site modification by agroforestry: physical interactions between trees and crops. Lecture to the summer course, Agroforestry: Tees in Support of Agriculture. Oxford Forestry Institute, August 15, 1996.

Smith, D.M. (1997) Site modification by agroforestry: physical interactions between trees and crops. Lecture to the summer course, Agroforestry: Trees in Support of Agriculture. Oxford Forestry Institute, July 24, 1997.

Smith, D.M. (1997) Plant water use and competition in agroforestry. Lecture to the course, Current Methods in Tropical Forestry. Oxford Forestry Institute, September 3, 1997.

Exhibit

Roberts, J.M. (1997). Agroforestry: making plants work together. Exhibit at The Royal Society "New Frontiers in Science" Exhibition 1997. 18-19 June, 1997, London.

Plans for further dissemination include publication of scientific papers on: (i) root length distributions in the *G. robusta* - maize mixture; (ii) testing and calibration of van Noordwijk's fractal method for estimating tree root lengths; (iii) measurement and analysis of hydraulic conductances of tree and crop roots in agroforestry; and (iv) construction and testing of the model of water uptake by roots in agroforestry. In addition, we will utilise results from the project in a short course in June 1998 for a group of technical staff and students from ICRAF and other CGIAR Centres that has been organised through the Agroforestry Modelling Project of the Forestry Research Programme. As further development of the model of uptake proceeds, existing links between the Institute of Hydrology and ICRAF will be used to ensure that ICRAF is able to utilise the model in their research programmes and by participants in the AFRENA network of national research programmes.

6. REFERENCES

Anderson LS & Sinclair FL. 1993. Ecological interactions in agroforestry systems. *Agroforestry Abstracts* 6: 57-91.

Baker JM & van Bavel CHM. 1987. An analysis of the steady-state heat balance method for measuring sap flow in plants. *Plant, Cell & Environment* 10: 777-782.

Böhm W. 1979. *Methods of studying root systems*. Berlin: Springer.

Brenner AJ, Jarvis PG & van den Beldt RJ. 1995. Tree-crop interactions in a Sahelian windbreak system.2. Growth response of millet in shelter. *Agricultural and Forest Meteorology* 75: 215-234.

Brown DA & Upchurch DR. 1987. Minirhizotrons: a summary of methods and instruments in current use. In: HM Taylor (Ed.), *Minirhizotron Observation Tubes: Methods and Applications for Measuring Rhizosphere Dynamics*. Madison WI: American Society of Agronomy. pp. 15-30.

Caldwell MM & Richards JH. 1989. Hydraulic lift: water efflux from upper roots improves effectiveness of water uptake by deep roots. *Oecologia* 79: 1-5.

Caldwell MM, Richards JH & Beyshlag W. 1991. Hydraulic lift: ecological implications of water efflux from roots. In: D Atkinson (Ed.), *Plant Root Growth: an Ecological Perspective*. Oxford: Blackwell. pp. 423-443.

Caldwell MM, Dawson TE & Richards JH. 1998. Hydraulic lift: consequences of water efflux from the roots of plants. *Oecologia* 113: 151-161.

Campbell GS. 1985. *Soil Physics with BASIC: Transport Models for Soil-Plant Systems*. Amsterdam: Elsevier.

Campbell GS. 1991. Simulation of water uptake by plant roots. In: J Hanks & JT Ritchie (Eds.), *Modelling Plant and Soil Systems*. Madison WI: American Society of Agronomy. pp. 273-285.

Cooper PJM, Leakey RRB, Rao MR & Reynolds L. 1996. Agroforestry and the mitigation of land degradation in the humid and sub-humid tropics of Africa. *Experimental Agriculture* 32: 235-290.

Corak SJ, Blevins DG & Pallardy SG. 1987. Water transfer in an alfalfa/maize association. *Plant Physiology* 84: 582-586.

Cunningham M, Adams MB, Luxmoore RJ, Post WM & DeAngelis DL. 1989. Quick estimates of root length using a video image analyzer. *Canadian Journal of Forest Research* 19: 335-340.

Dawson TE. 1993. Hydraulic lift and water use by plants: implications for water balance, performance and plant-plant interactions. *Oecologia* 95: 565-574.

Emerman SH & Dawson TE. 1996. Hydraulic lift and its influence on water content of the rhizosphere: an example from sugar maple, *Acer saccharum*. *Oecologia* 108: 273-278.

Fownes JH & Anderson DG. 1991. Changes in nodule and root biomass of *Sesbania sesban* and *Leucaena leucocephala* following coppicing. *Plant and Soil* 138: 9-16.

Gale MR & DF Grigal. 1987. Vertical root distributions of northern tree species in relation to successional status. *Canadian Journal of Forest Research* 17: 829-834.

Gardner WR. 1960. Dynamic aspects of water availability to plants. *Soil Science* 89: 63-73.

Gijsman AJ, Floris J, van Noordwijk M & Brouwer G. 1991. An inflatable minirhizotron system for root observations with improved soil/tube contact. *Plant and Soil* 134: 261-269.

Govindarajan M, Rao MR, Mathuva MN & Nair PKR. 1996. Soil-water and root dynamics under hedgerow intercropping in semiarid Kenya. *Agronomy Journal* 88: 513-520.

Green SR & Clothier BE. 1995. Root water uptake by kiwifruit vines following partial wetting of the root zone. *Plant and Soil* 173: 317-328.

Grime JP. 1979. *Plant Strategies and Vegetation Processes*. London: Wiley.

Howard SB, Ong CK, Black CR & Khan AAH. 1997. Using sap flow gauges to quantify water uptake by tree roots from beneath the crop rooting zone in agroforestry systems. *Agroforestry Systems* 35: 15-29.

Huang B & Nobel PS. 1994. Root hydraulic conductivity and its components, with emphasis on desert succulents. *Agronomy Journal* 86: 767-774.

Huxley PA, Pinney A, Akunda E & Muraya P. 1994. A tree/crop interface orientation experiment with a *Grevillea robusta* hedgerow and maize. *Agroforestry Systems* 26: 23-45.

Jonsson K, Fidjeland L, Maghembe JA & Högberg P. 1988. The vertical distribution of fine roots of five tree species and maize in Morogoro, Tanzania. *Agroforestry Systems* 6: 63-69.

Kaspar TC & Ewing RP. 1997. ROOTEDGE: software for measuring root length from desktop scanner images. *Agronomy Journal* 89: 932-940.

Lott JE, Khan AAH, Ong CK & Black CR. 1996. Sap flow measurements of lateral tree roots in agroforestry systems. *Tree Physiology* 16: 995-1001.

Lott JE, Black CR & Ong CK. 1997. *Resource Utilisation by Trees and Crops in Agroforestry Systems*. Final Technical Report to the Department for International Development, Forestry Research Programme, Research Contract R5810. 81 pp.

McIntyre BD, Riha SJ & Ong CK. 1997. Competition for water in a hedge-intercrop system. *Field Crops Research* 52: 151-160.

Nambiar EKS & Sands R. 1993. Competition for water and nutrients in forests. *Canadian Journal of Forest Research* 23: 1955-1968.

Ong CK & Black CR. 1994. Complementarity of resource use in intercropping and agroforestry systems. In: JL Monteith, RK Scott & MH Unsworth (Eds.), *Resource Capture by Crops*. Nottingham: Nottingham University Press. pp. 255-278.

Ong CK & Khan AAH. 1993. The direct measurement of water uptake by individual tree roots. *Agroforestry Today* 5: 2-5.

Ong CK, Black CR, Marshall FM & Corlett JE. 1996. Principles of resource capture and utilization of light and water. In: CK Ong & P Huxley (Eds.), *Tree-Crop Interactions: A Physiological Approach*. Wallingford: CAB International. pp. 73-158.

Onyewotu LOZ, Ogigirigi MA & Stigter CJ. 1994. A study of competitive effects between a *Eucalyptus camaldulensis* shelterbelt and an adjacent millet (*Pennisetum typhoides*) crop. *Agriculture, Ecosystems & Environment* 51: 281-286.

Ragab R, Feyen J & Hillel D. 1984. Simulating infiltration into sand from a trickle line source using the matric flux potential concept. *Soil Science* 137: 120-127.

Richards JH & Caldwell MM. 1987. Hydraulic lift: substantial nocturnal water transport between soil layers by *Artemisia tridentata* roots. *Oecologia* 73: 486-489.

Rowse HR, Mason WK & Taylor HM. 1983. A microcomputer simulation model of soil water extraction by soybeans. *Soil Science* 136: 218-225.

Sakuratani T. 1981. A heat balance method for measuring water flux in the stem of intact plants. *Journal of Agricultural Meteorology* 37: 9-17.

Schroth G. 1995. Tree root characteristics as criteria for species selection and systems design in agroforestry. *Agroforestry Systems* 30: 125-143.

Skene KR, Kierans M, Sprent JI & Raven JA. 1996. Structural aspects of cluster root development and their possible significance for nutrient acquisition in *Grevillea robusta* (Proteaceae). *Annals of Botany* 77: 443-451.

Smith DM & Allen SJ. 1996. Measurement of sap flow in plant stems. *Journal of Experimental Botany* 47: 1833-1844.

Smith DM, Jarvis PG & Odongo JCW. 1997. Sources of water used by trees and millet in Sahelian windbreak systems. *Journal of Hydrology* 198: 140-153.

Smith DM, Jarvis PG & Odongo JCW. 1998. Management of windbreaks in the Sahel: the strategic implications of tree water use. *Agroforestry Systems* (in press).

Smith DM, Jackson NA, Roberts JM & Ong CK. 1998. Reverse flow of sap in tree roots and downward siphoning of water by *Grevillea robusta*. submitted to *Functional Ecology*.

Spek LY & van Noordwijk M. 1994. Proximal root diameter as predictor of total root size for fractal branching models. II. Numerical model. *Plant and Soil* 164: 119-127.

Steudle E. 1994. Water transport across roots. *Plant and Soil* 167: 79-90.

Stirzaker RJ & Passioura JB. 1996. The water relations of the root-soil interface. *Plant, Cell & Environment* 19: 201-208.

Tinker PB. 1976. Transport of water to plant roots in soil. *Philosophical Transactions of the Royal Society of London* B. 273: 445-461.

Toky OP & Bisht RP. 1992. Observations on the rooting patterns of some agroforestry trees in an arid region of north-western India. *Agroforestry Systems* 18: 245-263.

Tyree MT, Patiño S, Bennink J & Alexander J. 1995. Dynamic measurement of root hydraulic conductance using a high-pressure flowmeter in the laboratory and field. *Journal of Experimental Botany* 46: 83-94.

van Noordwijk M & Purnomosidhi P. 1995. Root architecture in relation to tree-soil-crop interactions and shoot pruning in agroforestry. *Agroforestry Systems* 30: 161-173.

van Noordwijk M, Spek LY and de Willigen P. 1994. Proximal root diameter as predictor of total root size for fractal branching models. *Plant and Soil* 164: 107-117.

van Noordwijk M, Lawson G, Soumaré A, Groot JJR and Hairiah K. 1996. Root distribution of trees and crops: competition and/or complementarity. In: CK Ong & P Huxley (Eds.), *Tree-Crop Interactions: A Physiological Approach*. Wallingford: CAB International. pp. 319-364.

Wallace JS, Jackson NA & Ong CK. 1995. *Water Balance of Agroforestry Systems on Hillslopes*. Final Technical Report to the Overseas Development Administration, Forestry Research Programme. Research Contract R4853. 39 pp.

ACKNOWLEDGEMENTS

Many people have contributed to the work described in this report. Foremost of these are Mr. Elijah Kamalu and Mr. Patrick Angala, technicians at the Machakos Research Station, whose skilled dedication and commitment made possible much of the work undertaken in the field for this project, especially the large and long-running programme of soil coring and root length measurement. We are particularly grateful, also, to the many others who joined them in the task of washing and sorting root samples, all of whom brought patience and a careful eye - as well as, most importantly, good humour - to a very tedious endeavour.

We thank Mr. Peter Kurira, the farm manager of the Machakos Research Station, for his consistently helpful co-operation, and Mr. Ahmed Khan of ICRAF for sharing his ideas and for his and his team's expertise in helping us solve the inevitable problems with electronics. The co-operation of Jamie Lott, from Nottingham University, in helping to ensure the smooth running of the CIRUS site is acknowledged, especially for the good spirit he brought to finding solutions to the difficult question of deciding where it was possible to make holes in plots.

In the UK, Professor Peter Gregory of Reading University provided invaluable advice on how to organise a manageable programme of soil coring and root length measurement; he also provided, together with Professor Roger Mead of Reading University, guidance on statistical analysis of root length data, which we gratefully acknowledge.

The staff of the workshops at the Institute of Hydrology made a large and valuable contribution to the project, by designing and fabricating numerous parts for field equipment; we thank them especially for their assistance in developing and building the minirhizotrons and for machining over-sized compression fittings for the HPFM.

We are grateful also to Dr. Simon Allen for supporting the project with advice on the interpretation of data from sap flow gauges and Dr. Ragab Ragab for guidance on soil water modelling and for providing us with a copy of his model of soil water redistribution, which became the foundation for our model of uptake by roots.

APPENDIX A: CODING FOR RECURSIVE BRANCHING ALGORITHM

The basic program for the recursive branching algorithm used to estimate numbers of root links from the diameters of tree branches is listed below. For details on use of the program, see Sections 3.5 and 4.4. The program was developed from an original program provided by Dr. Meine van Noordwijk, of ICRAF-S.E. Asia, Bogor, Indonesia.

```
REM     This program generates data on root diameters and link connections
REM     based on simple branching rules (Spek and van Noordwijk, 1994)
REM
REM     Input parameters are: D(1), avga, avgq, ranga and rangq
        OPEN "c:\dms\ih-data\cirus\rootbran\fracmod\RBfrtst2.out" FOR OUTPUT AS #1

        PRINT #1, "Fractal test trees"

REM     $DYNAMIC
        DIM D(32500), conto(32500), ftroots(408, 4)


REM     These are data from the fractal test trees
REM     order: treeid, rootid, proximal root diameter

        DATA 1,20,1,34.3
        DATA 2,20,2,10.1
        DATA 3,20,3,3.5
        .
        .
        .
        DATA 407,226,35,26.2
        DATA 408,226,36,15.7



        FOR x = 1 TO 408
        FOR y = 1 TO 4
        READ ftroots(x, y)
        NEXT y
        NEXT x


        RANDOMIZE (12321)

REM
        nkeer = 100



REM     fracqhigh = fraction of q values in the 0.9 - 1.0 range
REM             the remainder is  in the 0.5 - 0.9 range
REM     D(1) = squared proximal root diameter; Dmin = squared min D
REM     ranga = relative range in which alpha varies
        PRINT #1, "Output file from RBfrtest.bas"

REM     RBfrtest runs with overall median alpha, overall fracqhigh and
REM     overall median alpha residuals for D<=5mm and D>5mm.


        avga = 1.0233
        fracqhigh = .7475
        Dmin = .01
        medresadlt5 = .1408
        medresadgt5 = .0384

        PRINT #1, "alpha", "fracqhigh", "a residuals (<5)", "a residuals (>5)", "N runs", "D min^2"
        PRINT #1, avga, fracqhigh, medresadlt5, medresadgt5, nkeer, Dmin
        PRINT #1, ""
        PRINT #1, "Tree id", "Root id", "Prox D", "avgnlink", "stdev", "c.v.", "maxn"
        PRINT #1, ""


        FOR id = 194 TO 408
        treeid = ftroots(id, 2)
        rootid = ftroots(id, 3)
        D(1) = (ftroots(id, 4)) ^ 2


        rangadlt5 = medresadlt5 * 4
        rangadgt5 = medresadgt5 * 4

        PRINT id, treeid, rootid, ftroots(id, 4), avga, rangadlt5, rangadgt5
        maxn = 0
        sum = 0
        sumsq = 0
        FOR keer = 1 TO nkeer STEP 1
        n = 1
        i = 0
        nbranch = 0
        conto(1) = 0
100     i = i + 1

        IF D(i) <= 5 THEN
```

```
        a = (1 + rangadlt5 * (RND - .5)) * avga
        ELSE
        a = (1 + rangadgt5 * (RND - .5)) * avga
        END IF

        IF RND > fracqhigh THEN
        q = .5 + .4 * RND
        ELSE
        q = .9 + .1 * RND
        END IF
        Dsub1 = q * D(i) / a
        Dsub2 = (1 - q) * D(i) / a
        IF Dsub1 > Dmin AND Dsub2 > Dmin THEN
           n = n + 1
           D(n) = Dsub1
           conto(n) = i
           n = n + 1
           D(n) = Dsub2
           conto(n) = i
           nbranch = nbranch + 1
        END IF
        IF i < n AND n < 32498 THEN GOTO 100
REM
REM     here starts the output section
REM
REM     PRINT "nlink = ", n, "nbranch = ", nbranch
REM     PRINT "link", "diamsq", "conto"
REM     FOR j = 1 TO n
REM             PRINT j, D(j), conto(j)
REM     NEXT j
        IF n > maxn THEN maxn = n
        sum = sum + n
        sumsq = sumsq + n ^ 2
        NEXT keer
        avglink = sum / nkeer
        stdev = ((nkeer * sumsq - sum ^ 2) / (nkeer * (nkeer - 1))) ^ .5
        coefvar = stdev / avglink
        PRINT avglink
        PRINT #1, treeid, rootid, ftroots(id, 4), avglink, stdev, coefvar, maxn
        NEXT id
```

APPENDIX B: INPUT DATA REQUIRED FOR USE OF WATER UPTAKE MODEL

B.1 Dimensional Parameters

Variable name	Description	Units in model	Value used in simulations	Notes
DELX	dimension of elements of flow domain in *x* direction	m	0.25	
DELZ	dimension in *z* direction	m	0.10	
DELY	dimension in *y* direction	m	3.0	
IMAX	number of elements in *z* dimension		16	
JMAX	number of elements in *x* dimension		8	

B.2 Soil Parameters

Variable name	Description	Units in model	Value used in simulations	Notes
CAPK	soil hydraulic conductivity; calculated using $CAPK=A\theta_v^B$	m h^{-1}	A=37.29 B=10.42	function fitted to $K(\theta)$ data (θ_v in $m^3\ m^{-3}$) measured for sub-surface horizon at CIRUS site using the 'hot air method' (see Ehlers, 1976)*
PSOIL	water retention function; calculated using $PSOIL=APS\theta_v^{BPS}$	m	APS=-1.43×10^{-5} BPS=-8.34	function fitted to $\psi(\theta)$ data measured for sub-surface horizon at CIRUS site.
MFLP	matrix flux potential function; calculated using $MFLP=AMFP(-PSOIL)^{BMFP}+CMFP$	$m^2\ h^{-1}$	AMFP=1.35×10^{-4} BMFP=-0.248 CMFP=-4.48×10^{-7}	function for sub-surface horizon at CIRUS site.

*Ehlers, W. 1979. Rapid determination of unsaturated hydraulic conductivity in tilled and untilled loess soil. Soil Sci. Soc. Am. J. 40: 837-840.

B.3 Tree Parameters

Variable name	Description	Units in model	Value used in simulations	Notes
TKROOT	hydraulic conductivity of tree roots	$m\ h^{-1}$	$6.7x10^{-9}$	value determined using methods described in Section 4.7; equivalent to $1.9x10^{-7}$ kg s^{-1} MPa^{-1} m^{-1}
TRSTEM	hydraulic resistance of stem and foliage of 1 tree	$h\ m^{-2}$	1650	estimated as equal to total resistance of root system.
TRRAD	radius of tree roots	m	0.0005	estimated
TEFIT	parameter *a* in Eq. 3.17		10	typical value; see Campbell (1991)
TPCONS	parameter c_ψ in Eq. 3.17	m	-150	typical value; see Campbell (1991). c_ψ is leaf water potential at which transpiration is 0.5 of potential
TBPRX	fitting parameter for cumulative root length function (Eq. 3.1)		0.97	measured value; see Section 5.2
RLPT	root length per tree	m	90000	measured value; see Section 5.2
APT	area per tree	m^2	12	value for CT_d plots in CIRUS trial
TH	tree height above soil	m	8	measured value

B.4 Crop Parameters

Variable name	Description	Units in model	Value used in simulations	Notes
CKROOT	hydraulic conductivity of maize roots	$m\ h^{-1}$	$4.4x10^{-9}$	value determined using methods described in Section 4.7; equivalent to $1.2x10^{-7}$ kg s^{-1} MPa^{-1} m^{-1}
CRSTEM	hydraulic resistance of stem and foliage of 1 maize plant	$h\ m^{-2}$	250000	measured with HPFM and assumed proportional to total hydraulic resistance of root system
CRRAD	radius of crop roots	m	0.0005	estimated
CEFIT	parameter *a* in Eq. 3.17		10	typical value; see Campbell (1991)
CPCONS	parameter c_ψ in Eq. 3.17	m	-150	typical value; see Campbell (1991). c_ψ is leaf water potential at which transpiration is 0.5 of potential
CBPRX	fitting parameter for cumulative root length function (Eq. 3.1)		0.81	measured value; see Section 5.2. CBPRX applies to half of area per plant closest to the plant. Value for CT_d maize in season with poor rains.
CBDST	fitting parameter for cumulative root length function (Eq. 3.1)		0.85	estimated from measured values discussed in Section 5.2. CBDST applies to half of area per plant furthest from the plant. Value for CT_d maize in season with poor rains.
RLPP	root length per maize plant	m	200	measured value; see Section 5.2. Value for CT_d maize in season with poor rains.
CRLRTO	ratio of root length per plant in closest and furthest half of APP		1.25	estimated from measured values discussed in Section 5.2
APP	area per maize plant	m^2	0.3	value for CIRUS trial
CH	crop height	m	0.5	measured value

B.5 Other Parameters

Variable name	Description	Units in model	Value used in simulations	Notes
TTDAY	E_v for tree; see Section 4.8.2	mm d^{-1}	2.0	estimated from Lott *et al*. (1997)
CTDAY	E_v for crop; see Section 4.8.2	mm d^{-1}	1.5	estimated from Lott *et al*. (1997)

APPENDIX C: CODING FOR MODEL OF WATER UPTAKE BY ROOTS IN AGROFORESTRY

A listing of the code for the model of water uptake by tree and crop roots in agroforestry is given below. The model is written in CSMP, a modelling language derived from FORTRAN that was designed for solving non-linear numerical problems.

```
************************************************************************
*****************ROOT WATER UPTAKE IN AGROFORESTRY**********************
*
*  ROOT UPTAKE COMPONENTS WRITTEN BY D.M. SMITH.  SOIL WATER FLOW
*  MODEL WRITTEN BY R. RAGAB (SEE RAGAB ET AL. (1984))
*
*     POSITIVE Z-AXIS IS DOWNWARDS
*     EACH COMPARTMENT IS 0.25 BY 0.10 M
*     UNIT TIME IS 1 HOUR
*
*     ALL UNITS BASED ON m AND h
*     UNITS OF SOIL HYDRAULIC CONDUCTIVITY ARE m h-1
*     UNITS OF MATRIC FLUX POTENTIAL ARE m2 h-1
*     UNITS OF RSOIL AND RROOT ARE h m-2
*     UNITS OF KROOT ARE m h-1
*
FIXED I,J,IMAX,JMAX,M,T,TEFIT,CEFIT,IDAY,IDCM,IODAY
*  DIMENSIONAL PARAMETERS
PARAMETER DELX=.25,DELZ=.10,DELY=3.,IMAX=16,JMAX=8
*  SOIL PARAMETERS
PARAMETER A=37.29,B=10.416,APS=-1.427E-05,BPS=-8.344
PARAMETER AMFP=1.3454E-04,BMFP=-0.2478,CMFP=-4.4756E-07
*  TREE PARAMETERS (TRSTEM IS FOR 1 TREE)
PARAMETER TRRAD=0.0005,TKROOT=6.7E-09,TEFIT=10,TPCONS=-150.,TRSTEM=1650
PARAMETER TBPRX=0.97,RLPT=90000,APT=12,TH=8
*  CROP PARAMETERS (CRSTEM IS FOR 1 PLANT)
PARAMETER CRRAD=0.0005,CKROOT=4.4E-09,CEFIT=10,CPCONS=-150.
PARAMETER CRSTEM=250000,CH=0.5
PARAMETER CBPRX=0.81,CBDST=0.85,CRLRTO=1.24,RLPP=200,APP=0.3
*  OTHER PARAMETERS
PARAMETER DELPR=5
* TREE AND CROP TRANSPIRATION RATE IN mm d-1
PARAMETER TTDAY=2.0,CTDAY=1.5
/    DIMENSION FLUXH(16,9),FLUXV(17,8),Z(16,8),DEPTH(16),DINDX(16)
/    DIMENSION DZDT(16,8),ZIC(16,8),MFLP(16,8),PSOIL(16,8)
/    DIMENSION TFLUXR(16,8),TRLD(16,8),TRROOT(16,8),TRSOIL(16,8)
/    DIMENSION CFLUXR(16,8),CRLD(16,8),CRROOT(16,8),CRSOIL(16,8)
/    DIMENSION CFRCRL(16,8),TFRCRL(16,8),TXCUM(16,8),CXCUM(16,8)
/    EQUIVALENCE (Z1(1),Z(1,1))
/    EQUIVALENCE (ZIC1(1),ZIC(1,1))
/    EQUIVALENCE (DZDT1(1),DZDT(1,1))
*
*  Dimension of ZZERO must be (IMAX*JMAX). Also see TABLE statement
STORAGE ZZERO(128)
TABLE ZZERO(1-128)=128*.20
TITLE ROOT WATER UPTAKE IN AGROFORESTRY
************************************************************************
INITIAL
NOSORT
     V=DELX*DELY*DELZ
*  CRSTEM FOR 3 X 4 M SOIL BLOCK CALCULATED BY TREATING AS 40 SINGLE
*  STEMS IN PARALLEL. IN UPTAKE SUBROUTINE, CRSTEM FOR WHOLE BLOCK
*  CONVERTED TO HALF BLOCK BASIS, AS DONE FOR TREE.
     CRSTEM=CRSTEM/40
*
     DO 4 I=1,IMAX
     DEPTH(I)=(I*DELZ)-(DELZ/2)
   4 CONTINUE
     DO 1 J=1,JMAX
     DO 1 I=1,IMAX
     M=(J-1)*IMAX+I
     ZIC(I,J)=ZZERO(M)
   1 CONTINUE
*  SET RLDs
     CALL DI(IMAX,DELZ,DINDX)
     TBDST=TBPRX
     CALL FRL(IMAX,DELZ,TBPRX,TBDST,DINDX,TFRCRL)
     CALL FRL(IMAX,DELZ,CBPRX,CBDST,DINDX,CFRCRL)
     CALL TRD(IMAX,JMAX,DELZ,RLPT,APT,TFRCRL,TRLD)
     CALL CRD(IMAX,JMAX,DELZ,RLPP,APP,CRLRTO,CFRCRL,CRLD)
* set SMC for top layer
     DO 3 J=1,JMAX
     DO 3 I=1,4
     ZIC(I,J)=0.15
   3 CONTINUE
     DO 5 I=1,IMAX
     FLUXH(I,1)=0.0
     FLUXH(I,JMAX+1)=0.0
   5 CONTINUE
     DO 6 J=1,JMAX
     FLUXV(1,J)=0.0
   6 FLUXV(IMAX+1,J)=0.0
*  ROOT RESISTANCE CALCULATED ONCE ONLY; THUS SUBROUTINE CALLED
*  IN INITIAL SEGMENT.  FIRST FOR TREE, THEN FOR CROP
```

```
      CALL RR(JMAX,IMAX,V,TKROOT,TRLD,TRROOT)
      CALL RR(JMAX,IMAX,V,CKROOT,CRLD,CRROOT)
      WRITE (6,90)
   90 FORMAT (5X,'TIME',3X,'PLF[m]',1X,'PSBAR[m]',1X,'EMAX[mm/h]',...
        1X,'EACT[mm/h]',1X,'SUMUT[mm/h]',1X,'TOTVOL[m3]')
*
*************************************************************************
DYNAMIC
      Z1=INTGRL(ZIC1,DZDT1,128)
PROCEDURE TOTVOL,DZDT1=INFILT(Z1,ZIC1,IMAX,JMAX,DELX,DELZ,...
          V,MF)
      TOTVOL=0.0
      DO 10 J=1,JMAX
      DO 10 I=1,IMAX
   10 TOTVOL=TOTVOL+Z(I,J)*V
*
*  DETERMINE EMAX FOR T AND C FROM DAILY MAXIMUM TR SUPPLIED
      CALL TRP(TIME,TTDAY,TTR)
      CALL TRP(TIME,CTDAY,CTR)
*  EMAX WITH UNITS OF m3 h-1
      TEMAX=(TTR/1000)*DELY*DELX*JMAX
      CEMAX=(CTR/1000)*DELY*DELX*JMAX
*
      DO 15 J=1,JMAX
      DO 15 I=1,IMAX
      PSOIL(I,J)=APS*(Z(I,J)**BPS)
   15 CONTINUE
      DO 35 J=1,JMAX
      DO 35 I=1,IMAX
   35 MFLP(I,J)=(AMFP*((-1*PSOIL(I,J))**BMFP))+CMFP
      DO 20 I=1,IMAX
      DO 20 J=2,JMAX
   20 FLUXH(I,J)=((MFLP(I,J-1)-MFLP(I,J))/DELX)*DELZ
      DO 30 J=1,JMAX
      DO 30 I=2,IMAX
      CAPKA=A*ABS(Z(I-1,J))**B
      CAPKM=A*ABS(Z(I,J))**B
      CAPKTM=(CAPKA*Z(I-1,J)+CAPKM*Z(I,J))/(Z(I-1,J)+Z(I,J))
   30 FLUXV(I,J)=(((MFLP(I-1,J)-MFLP(I,J))/DELZ)+CAPKTM)*DELX
   50 CONTINUE
*  SOIL RESISTANCE CALCULATED SEPARATELY FOR T AND C BECAUSE THEY
*  MAY HAVE DIFFERENT RADII, THOUGH BOTH ARE DEPENDENT ON TOTAL
*  RLD.
      CALL RS(JMAX,IMAX,V,A,B,TRRAD,Z,TRLD,CRLD,TRSOIL,GSOIL)
      CALL RS(JMAX,IMAX,V,A,B,CRRAD,Z,TRLD,CRLD,CRSOIL,GSOIL)
      CONTINUE
*  UPTAKE SUBROUTINE CALLED FIRST FOR TREES, THEN CROP.
      CALL RU(IMAX,JMAX,PSOIL,DEPTH,TH,TRSOIL,TRROOT,TRSTEM,...
        TPCONS,TEFIT,TEMAX,TPSBAR,TPLEAF,TEACT,TFLUXR,TSUMUT)
      CALL RU(IMAX,JMAX,PSOIL,DEPTH,CH,CRSOIL,CRROOT,CRSTEM,...
        CPCONS,CEFIT,CEMAX,CPSBAR,CPLEAF,CEACT,CFLUXR,CSUMUT)
      CONTINUE
      DO 60 J=1,JMAX
      DO 60 I=1,IMAX
      DZDT(I,J)=(FLUXH(I,J)-FLUXH(I,J+1)+FLUXV(I,J)-FLUXV(I+1,J))
   60 DZDT(I,J)=(DZDT(I,J)-TFLUXR(I,J)-CFLUXR(I,J))/V
*
*  DETERMINATION OF DAILY CUMULATIVE ROOT FLUXES, TXCUM AND CXCUM.
*  ARRAYS ARE RESET AT END OF DAILY OUTPUT SUBROUTINE.
      DO 65 J=1,JMAX
      DO 65 I=1,IMAX
      TXCUM(I,J)=TXCUM(I,J)+(TFLUXR(I,J)*(TIME-OLDT))
      CXCUM(I,J)=CXCUM(I,J)+(CFLUXR(I,J)*(TIME-OLDT))
   65 CONTINUE
      OLDT=TIME
ENDPRO
NOSORT
*  CONVERT TRANSPIRATION RATES TO mm/h FOR OUPUT
      TEMMM=(TEMAX/(JMAX*DELX*DELY))*1000
      TEAMM=(TEACT/(JMAX*DELX*DELY))*1000
      CEMMM=(CEMAX/(JMAX*DELX*DELY))*1000
      CEAMM=(CEACT/(JMAX*DELX*DELY))*1000
      TSUMMM=(TSUMUT/(JMAX*DELX*DELY))*1000
      CSUMMM=(CSUMUT/(JMAX*DELX*DELY))*1000
*  OUTPUT SECTION
      PR=IMPULS(0.0,PRDEL)
      IF (KEEP.EQ.0.0.OR.PR.EQ.0.0) GO TO 70
*
      WRITE (6,100) TIME,TPLEAF,TPSBAR,TEMMM,TEAMM,TSUMMM,TOTVOL
  100 FORMAT ('T',1X,F7.2,1X,F8.1,1X,F8.1,1X,F7.4,4X,F7.4,4X,F7.4,...
        5X,F8.4)
      WRITE (6,105) TIME,CPLEAF,CPSBAR,CEMMM,CEAMM,CSUMMM,TOTVOL
  105 FORMAT ('C',1X,F7.2,1X,F8.1,1X,F8.1,1X,F7.4,4X,F7.4,4X,F7.4,...
        5X,F8.4)
*
      ODAY=TIME/24
      IODAY=ODAY
      DUMT=ODAY-IODAY
      IF (DUMT.EQ.0.0) CALL OP(IMAX,JMAX,TIME,Z,TXCUM,CXCUM)
   70 CONTINUE
*************************************************************************
METHOD RKS
OUTPUT TOTVOL
TIMER FINTIM=336,DELT=1.0E-02,DELMIN=1.0E-04,PRDEL=1,OUTDEL=1,...
      DELMAX=1
END
STOP
*************************************************************************
```

```
*  THE FOLLOWING SUBROUTINE CALCULATES THE MAXIMUM TRANSPIRATION RATE
*  AT ALL TIMES OF DAY. THIS IS THE TRANSPIRATION RATE WHEN NOT LIMITED
*  BY LEAF WATER POTENTIAL.
*
      SUBROUTINE TRP(TIME,TDAY,TR)
      INTEGER IDAY
*
*  TDAY IS IN mm d-1. TNOON IS THE PEAK VALUE OF TR AT MIDDAY, IN mm h-1,
*  FROM THE INTEGRAL OF THE SIN FUNCTION GIVING TR OVER THE DAY.
      TNOON=(TDAY*3.14159)/24
*
*  TIME OF DAY REQUIRED ON 24 h CLOCK
      DAY=TIME/24
      IDAY=DAY
      HOUR=(DAY-IDAY)*24
*
*  TRANSPIRATION RATE TR CALCULATED FROM SIN FUNCTION OF TIME
      HX=((HOUR-6)*3.14159)/12
      TR=TNOON*SIN(HX)
      IF (HOUR.LT.6.0.OR.HOUR.GT.18.0) TR=0.0
      RETURN
      END
************************************************************************
*  THE FOLLOWING SUBROUTINE CALCULATES THE DEPTH INDEX FOR EACH I. THIS
*  IS USED WHEN FRACTION OF CUMULATIVE ROOT LENGTH IS CALCULATED.
*  VALUES ARE DETERMINED IN 20 cm STEPS.
*
      SUBROUTINE DI(IMAX,DELZ,DINDX)
      REAL DINDX(IMAX)
      INTEGER IDCM
*
      DO 510 I=1,IMAX
      DCM=I*DELZ*100
      DCM=DCM/20
      IDCM=DCM
      DUMMY=IDCM-DCM
      IF (DUMMY.NE.0.0) DINDX(I)=(IDCM*20)+20
      IF (DUMMY.EQ.0.0) DINDX(I)=(IDCM*20)
  510 CONTINUE
      RETURN
      END
************************************************************************
*  THE FOLLOWING SUBROUTINE CALCULATES THE FRACTION OF CUMULATIVE ROOT
*  LENGTH IN EACH SOIL COMPARTMENT.
*
      SUBROUTINE FRL(IMAX,DELZ,BPRX,BDST,DINDX,FRCRL)
      REAL DINDX(IMAX),FRCRL(IMAX,8)
      INTEGER ISUB,IINT,IREST
*
*  IINT IS THE NUMBER OF DEPTH INTERVALS TO BE TREATED AS A SINGLE
*  GROUP. IE. IF IINT=2 THEN PAIRS OF DEPTH INCREMENTS WILL HAVE THE
*  SAME RLD.  DEPENDS ON RESOLUTION OF ROOT DATA USED IN PARAMETERISATION.
      IINT=0.2/DELZ
      IREST=IINT+1
*
*  CALCULATIONS FIRST DONE FOR J=2,3,6,7. THESE ARE THE SOIL COMPARTMENTS
*  ADJACENT TO A MAIZE PLANT.
      DO 560 I=1,IINT
      FRCRL(I,2)=(1-(BPRX**DINDX(I)))
  560 CONTINUE
      DO 565 I=IREST,IMAX
      ISUB=I-IINT
      FRCA=(1-(BPRX**DINDX(I)))
      FRCB=(1-(BPRX**DINDX(ISUB)))
      FRCRL(I,2)=(FRCA-FRCB)
  565 CONTINUE
      DO 568 I=1,IMAX
      FRCRL(I,3)=FRCRL(I,2)
      FRCRL(I,6)=FRCRL(I,2)
      FRCRL(I,7)=FRCRL(I,2)
  568 CONTINUE
*
*  THEN DONE FOR J=1,4,5,8. THESE ARE NOT ADJACENT TO MAIZE PLANTS. IE
*  'DISTAL'.  FOR TREES, THESE ARE THE SAME AS ADJACENT, AS TBDST=TBPRX.
      DO 570 I=1,IINT
      FRCRL(I,1)=(1-(BDST**DINDX(I)))
  570 CONTINUE
      DO 575 I=IREST,IMAX
      ISUB=I-IINT
      FRCA=(1-(BDST**DINDX(I)))
      FRCB=(1-(BDST**DINDX(ISUB)))
      FRCRL(I,1)=(FRCA-FRCB)
  575 CONTINUE
      DO 578 I=1,IMAX
      FRCRL(I,4)=FRCRL(I,1)
      FRCRL(I,5)=FRCRL(I,1)
      FRCRL(I,8)=FRCRL(I,1)
  578 CONTINUE
      DO 580 J=1,8
      DO 580 I=1,IMAX
      FRCRL(I,J)=FRCRL(I,J)/IINT
  580 CONTINUE
      RETURN
      END
************************************************************************
*  THE FOLLOWING SUBROUTINE DETERMINES THE TREE ROOT LENGTH DENSITY
*  IN EACH SOIL COMPARTMENT.
*
```

```
      SUBROUTINE TRD(IMAX,JMAX,DELZ,RLPT,APT,TFRCRL,TRLD)
      REAL TFRCRL(IMAX,JMAX),TRLD(IMAX,JMAX)
*
      RLAT=RLPT/APT
      DO 610 J=1,JMAX
      DO 610 I=1,IMAX
      TRLD(I,J)=(TFRCRL(I,J)*RLAT)/DELZ
  610 CONTINUE
      RETURN
      END
************************************************************************
*  THE FOLLOWING SUBROUTINE DETERMINES CROP ROOT LENGTH DENSITY IN EACH
*  SOIL COMPARTMENT
*  CRLRTO IS THE RATIO OF ROOT LENGTHS IN COMPARTMENTS ADJACENT TO THE
*  CROP PLANT AND IN 'DISTAL' COMPARTMENTS.
*
      SUBROUTINE CRD(IMAX,JMAX,DELZ,RLPP,APP,CRLRTO,CFRCRL,CRLD)
      REAL CFRCRL(IMAX,JMAX),CRLD(IMAX,JMAX)
*
      RLAPRX=(RLPP*(CRLRTO/(1+CRLRTO)))/(APP/2)
      RLADST=(RLPP*(1/(1+CRLRTO)))/(APP/2)
*
*  FIRST FOR COMPARTMENTS ADJACENT TO PLANTS
      DO 650 I=1,IMAX
      CRLD(I,2)=(CFRCRL(I,2)*RLAPRX)/DELZ
      CRLD(I,3)=CRLD(I,2)
      CRLD(I,6)=CRLD(I,2)
      CRLD(I,7)=CRLD(I,2)
  650 CONTINUE
*
*  THEN FOR 'DISTAL' COMPARTMENTS
      DO 660 I=1,IMAX
      CRLD(I,1)=(CFRCRL(I,1)*RLADST)/DELZ
      CRLD(I,4)=CRLD(I,1)
      CRLD(I,5)=CRLD(I,1)
      CRLD(I,8)=CRLD(I,1)
  660 CONTINUE
      RETURN
      END
************************************************************************
*  THE FOLLOWING SUBROUTINE CALCULATES SOIL RESISTANCE
*
      SUBROUTINE RS(JMAX,IMAX,V,A,B,RRAD,Z,TRLD,CRLD,RSOIL,GSOIL)
      REAL Z(IMAX,JMAX),TRLD(IMAX,JMAX),CRLD(IMAX,JMAX),RSOIL(IMAX,JMAX)
      DO 210 J=1,JMAX
      DO 210 I=1,IMAX
*  SOIL RESISTANCE FOR BOTH T AND C DEPENDENT ON TOTAL RLD BECAUSE
*  EXTRACTION CYLINDER FOR ROOT OF SPECIES 1 LIMITED BY NEARBY ROOTS
*  OF SPECIES 1 AND SPECIES 2.
      RLD=TRLD(I,J)+CRLD(I,J)
*
*  CAPK IS SOIL HYDRAULIC CONDUCTIVITY
      CAPK=A*ABS(Z(I,J))**B
*
*  GSN AND GSD ARE THE NUMERATOR AND DENOMINATOR OF THE
*  EQUATION FOR SOIL CONDUCTANCE PER UNIT ROOT LENGTH, TAKEN
*  FROM ROWSE ET AL. (1983). GSOIL SET TO 0 IF THERE ARE NO
*  ROOTS.
      GSN=4*3.14159*CAPK
      GSD=-ALOG(RLD*3.14159*(RRAD**2))
      IF (RLD.GT.0) GSOIL=GSN/GSD
      IF (RLD.EQ.0) GSOIL=0
*
*  TOTAL CONDUCTANCE FOR SOIL COMPARTMENT CALCULATED FROM
*  CONDUCTANCE PER UNIT ROOT LENGTH.
      GSOIL=GSOIL*RLD*V
*
*  SOIL RESISTANCE CALCULATED AS INVERSE OF GSOIL.  RSOIL SET
*  TO HIGH VALUE WHEN THERE ARE NO ROOTS.
      IF (GSOIL.NE.0) RSOIL(I,J)=1/GSOIL
      IF (GSOIL.EQ.0) RSOIL(I,J)=1.0E20
  210 CONTINUE
      RETURN
      END
************************************************************************
*  THE FOLLOWING SUBROUTINE CALCULATES ROOT RESISTANCE
*
      SUBROUTINE RR(JMAX,IMAX,V,KROOT,RLD,RROOT)
      REAL KROOT,RLD(IMAX,JMAX),RROOT(IMAX,JMAX)
      DO 310 J=1,JMAX
      DO 310 I=1,IMAX
*
*  CONDUCTANCE PER UNIT LENGTH (KROOT) USED TO CALCULATE TOTAL
*  CONDUCTANCE FOR SOIL COMPARTMENT (GROOT).
      GROOT=KROOT*RLD(I,J)*V
*
*  ROOT RESISTANCE CALCULATED BY INVERTING GROOT. IF NO ROOTS
*  PRESENT, RROOT SET TO A HIGH VALUE.
      IF (GROOT.NE.0) RROOT(I,J)=1/GROOT
      IF (GROOT.EQ.0) RROOT(I,J)=1.0E20
  310 CONTINUE
      RETURN
      END
************************************************************************
*  THE FOLLOWING SUBROUTINE CALCULATES ROOT UPTAKE (FLUXR).
*  THE EQUATIONS FOLLOW CAMPBELL (1991).
*
      SUBROUTINE RU(IMAX,JMAX,PSOIL,DEPTH,HT,RSOIL,RROOT,RSTEM,
```

```
     4   PCONS,EFIT,EMAX,PSBAR,PLEAF,EACT,FLUXR,SUMUPT)
      REAL PSOIL(IMAX,JMAX),DEPTH(IMAX),RSOIL(IMAX,JMAX),
     4   RROOT(IMAX,JMAX),FLUXR(IMAX,JMAX)
      INTEGER EFIT
*
*  DETERMINATION OF WEIGHTED MEAN SOIL WATER POTENTIAL (PSBAR)
      PSBARN=0
      PSBARD=0
      DO 410 J=1,JMAX
      DO 410 I=1,IMAX
      PSBARN=PSBARN+((PSOIL(I,J)-DEPTH(I))/(RSOIL(I,J)+RROOT(I,J)))
      PSBARD=PSBARD+(1/(RSOIL(I,J)+RROOT(I,J)))
  410 CONTINUE
      PSBAR=PSBARN/PSBARD
  412 CONTINUE
*
*  DETERMINATION OF LEAF WATER POTENTIAL (PLEAF) BY NEWTON-RAPHSON
*  ITERATION.  RSR IS COMBINED SOIL-ROOT RESISTANCE FOR WHOLE SOIL
*  VOLUME. RSTEM IS DOUBLED TO GIVE RESISTANCE FOR HALF A TREE (THIS
*  CHECKED: GIVES SAME RESULT WITH HALF E AND HALF SOIL VOLUME).
      PLEAF=0
      RHSTEM=2*RSTEM
      RSR=1/PSBARD
      F=(PLEAF+HT)-PSBAR+((EMAX*(RSR+RHSTEM))/(1+((PLEAF/PCONS)**EFIT)))
      DO 420 I=1,100
*  (PCONS**EFIT) REPLACED BY CTE FOR BREVITY. FDERN AND FDERD, WHICH
*  ARE THE NUMERATOR AND DENOMINATOR IN THE FDER FUNCTION, ARE BOTH
*  MULTIPLIED THROUGH BY 1E-30 TO PREVENT OVERFLOW ERRORS CAUSED BY
*  NUMBERS BEING TOO LARGE.  THIS MAKES NO DIFFERENCE TO FDER.
      CTE=PCONS**EFIT
      FDERN=EFIT*CTE*(PLEAF**(EFIT-1))*1E-30
      FDERD=(CTE*CTE*1.0E-30)+(2*(PLEAF**EFIT)*CTE*1E-30)
     4 +((PLEAF**EFIT)*(PLEAF**EFIT)*1E-30)
      FDER=1-(EMAX*(RSR+RHSTEM)*(FDERN/FDERD))
      PLEAF=PLEAF-(F/FDER)
      F=(PLEAF+HT)-PSBAR+((EMAX*(RSR+RHSTEM))/(1+((PLEAF/PCONS)**EFIT)))
      IF (F.LT.1.0) GO TO 430
  420 CONTINUE
      IF (F.GE.1.0) PLEAF=999.
  430 CONTINUE
*
*  DETERMINATION OF ACTUAL E FROM PLEAF
      EACT=EMAX/(1+((PLEAF/PCONS)**EFIT))
*
*  DETERMINATION OF UPTAKE FROM EACH SOIL COMPARTMENT
      PBASE=PSBAR-(EACT*RSR)
      SUMUPT=0
      DO 440 J=1,JMAX
      DO 440 I=1,IMAX
      FLUXR(I,J)=(PSOIL(I,J)-DEPTH(I)-PBASE)/(RSOIL(I,J)+RROOT(I,J))
*  SUMUPT IS THE SUM OF UPTAKE FROM EACH SOIL COMPARTMENT.
*  SUMUPT AND EACT SHOULD BE EQUAL
      SUMUPT=SUMUPT+FLUXR(I,J)
  440 CONTINUE
      RETURN
      END
*************************************************************************
*  THE FOLLOWING SUBROUTINE OUTPUTS THE SMC, TREE ROOT FLUX AND CROP
*  ROOT FLUX ARRAYS WHEN CALLED (ONCE PER DAY, AT MIDNIGHT).
*
      SUBROUTINE OP(IMAX,JMAX,TIME,Z,TXCUM,CXCUM)
      REAL Z(IMAX,JMAX),TXCUM(IMAX,JMAX),CXCUM(IMAX,JMAX)
*
      WRITE (6,702)
  702 FORMAT (/)
      WRITE (6,705) TIME
  705 FORMAT ('TIME IS: ',F7.2,' HOURS')
      WRITE (6,710)
  710 FORMAT ('Z(I,J) ARRAY:')
      DO 730 I=1,IMAX
      WRITE (6,720) (Z(I,J),J=1,JMAX)
  720 FORMAT (15F6.4)
  730 CONTINUE
      WRITE (6,740)
  740 FORMAT (/)
      WRITE (6,750)
  750 FORMAT ('DAILY TFLUXR(I,J) ARRAY (m3):')
      DO 760 I=1,IMAX
      WRITE (6,755) (TXCUM(I,J),J=1,JMAX)
  755 FORMAT (20E9.2)
  760 CONTINUE
      WRITE (6,762)
  762 FORMAT (/)
      WRITE (6,770)
  770 FORMAT ('DAILY CFLUXR(I,J) ARRAY (m3):')
      DO 780 I=1,IMAX
      WRITE (6,775) (CXCUM(I,J),J=1,JMAX)
  775 FORMAT (20E9.2)
  780 CONTINUE
      TXDTOT=0
      CXDTOT=0
      DO 783 J=1,JMAX
      DO 783 I=1,IMAX
      TXDTOT=TXDTOT+TXCUM(I,J)
      CXDTOT=CXDTOT+CXCUM(I,J)
  783 CONTINUE
      WRITE (6,785) TXDTOT,CXDTOT
  785 FORMAT ('DAILY UPTAKE, TREE: ',E9.4,'  CROP: ',E9.4,/)
```

```
*  DAILY CUMULATIVE ROOT FLUX ARRAYS SET TO 0.
      DO 790 J=1,JMAX
      DO 790 I=1,IMAX
      TXCUM(I,J)=0
      CXCUM(I,J)=0
  790 CONTINUE
      RETURN
      END
ENDJOB
```